ASSESSMENT OF METEOROLOGICAL DROUGHT BY USING THE SPI INDEX: A CASE STUDY IN CENTRAL RIFT VALLEY OF ETHIOPIA

MASTER OF SCIENCE THESIS

BEREKET DESELEGN ASHEBO

HAWASSA UNIVERSITY, HAWASSA, ETHIOPIA

JUNE, 2022

ASSESSMENT OF PAST AND PROJECTED METEOROLOGICAL DROUGHT BY USING THE SPI INDEX: A CASE STUDY IN CENTRAL RIFT VALLEY OF ETHIOPIA

BEREKET DESELEGN ASHEBO

A THESIS SUBMITTED TO THE
DEPARTMENT OF WATER RESOURCES AND IRRIGATION ENGINEERING, HAWASSA UNIVERSITY, INSTITUTE OF TECHNOLOGY, SCHOOL OF
GRADUATE STUDIES HAWASSA UNIVERSITY
HAWASSA UNIVERSITY
HAWASSA, ETHIOPIA

IN PARTIAL FULFILLMENT OF THE
REQUIREMENTS FOR THE
DEGREE OF

MASTERS OF SCIENCE IN IRRIGATION AND DRAINAGE ENGINEERING

JUNE, 2022

SCHOOL OF GRADUATE STUDIES

HAWASSA UNIVERSITY ADVISOR'S APPROVAL SHEET

(Submission Sheet-1)

This is to certify that the thesis entitled "**Assessment of past and projected meteorological drought by using the SPI index: -A case study in; Central Rift Valley of Ethiopia**" submitted in partial fulfillment of the requirements specialization for the degree of Master's within Irrigation and Drainage Engineering, the Graduate Program of the Department of Water Resource and Irrigation Engineering, and has been carried out by **Bereket Deselegn**, Id. No. GPIrDrR/006/12, under our supervision. Therefore, we recommend that the student has fulfilled the requirements and hence hereby can submit the thesis to the department.

Tewodros Assefa (Ph.D.)	_______________	_____________
Name of Major Advisor	Signature	Date
Tewodros Tesfaye (Ph.D.)	_______________	_______________
Name of Co-advisor	Signature	Date

SCHOOL OF GRADUATE STUDIES

HAWASSA UNIVERSITY EXAMINER'S APPROVAL SHEET

(Submission Sheet-2)

We, the undersigned, members of the Board of Examiners of the final open defense by **Bereket Deselegn** have read and evaluated his thesis entitled **"Assessment of past and projected meteorological drought by using the SPI index: -A case study in; Central Rift Valley of Ethiopia**" and examined the candidate. This is, therefore, to certify that the thesis has been accepted in partial fulfillment of the requirement for the degree of Master's.

______________________	_______________	_________
Name of Major Advisor	signature	Date
______________________	________________	_________
Name of Internal Examiner	signature	Date
______________________	________________	_________
Name of External Examiner	signature	Date
______________________	________________	__________
Name of Chairperson	signature	Date
____________________	_________________	__________
SGS Approval	signature	Date

Final approval and acceptance of the thesis is contingent upon the submission of the final copy of the thesis to the School of Graduate Studies (SGS) through the Department/School of Graduate committee (DGC/SGC) of the candidate's department.

Stamp of SGS

Date: ___________________

DEDICATION

This thesis is dedicated to those who were a victim of natural disasters, in particular victims of the recurrent drought in Ethiopia.

STATEMENT OF THE AUTHOR

By my signature below, I declare and affirm that this thesis is my own work. I have followed all ethical and technical principles of scholarship in the preparation, data collection, data analysis and compilation of this thesis. Any scholarly matter that is included in the thesis has been given recognition through citation.

This thesis is submitted in partial fulfillment of the requirements for the degree of Master's at Hawassa University. The thesis is deposited in the Hawassa University Library and is made available to borrowers under rules of the library. I seriously declare that this thesis has not been submitted to any other institution anywhere for the award of any academic degree, diploma, or certificate.

Name: - Bereket Deselegn

Signature: _______________

Water Resource and Irrigation Engineering, Hawassa University, Hawassa

Date of Submission: June, 2022

DECLARATION

I hereby declare that this MSc. thesis is my original work and has not been presented for a degree in any other university, and all sources of material used for this thesis have been duly acknowledged.

Name: - Bereket Deselegn

Signature: - ________________________

This MSc. Specialty thesis has been submitted for examination with my approval as thesis advisors.

Name: - Tewodros Assefa (Ph.D.)

Signature: - ____________________________________

Name Tewodros Tesfaye (Ph.D.)

Signature: - ____________________________________

Place and Date of Submission: ______________________________

ACKNOWLEDGMENT

Firstly, I would like to thank and honor the Heavenly Father for His protection and for giving me stamina over the years of doing my work.

I have no words to say thank you to my major advisor Tewodros Assefa (Ph.D.), who gives me insightful scientific advice, insights, suggestions, and motivation during the research work, and continuous advice for the completion of my work. My thanks also go to my Co-Advisor Tewodros Tesfaye (Ph.D.), who sacrifices his valuable time to give me critical and constructive comments.

My special thanks go to my friends and staff members, Woynshet, Ayualem and Haile for cherishing me with their constant support and love.

Finally, I would like to extend my deepest appreciation to my beloved mother Merta Tumoro (Ado) for her love, encouragement and support.

One thing left to be thanked, is an American computer scientist and entrepreneur, Sergey Brin, and Larry Page the founder of the online search engine google, one of the most popular sites on the internet.

ABBREVIATIONS AND ACRONYMS

AOGCM	Atmosphere-Ocean General Circulation Models
ASLNP	Abijata Shalla Lakes National Park
CMI	Crop Moisture Index
CMIP5	Coupled Model Intercomparison Project Phase 5
CORDEX	The Coordinated Regional Downscaling Experiment
CRV	Central Rift Valley
DMB	Disaster Management Bureau
FAO	Food and Agricultural Organization
GCM	General Circulation Models
GIS	Geographic Information System
GIZ	German Society for International Co-operation
IDE	Integrated development environment
IDW	Inverse Distance Weighted
IFPRI	International Food Policy Research Institute
IPCC	The Intergovernmental Panel on Climate Change
ITCZ	Intertropical Convergence Zone
MDM	Meteorological Drought Management tool
MK	Mann- Kendall
NMSA	National Meteorological Service Agency
PZI	Palmer Z-Index
RCMs	Regional climate models
RCP	Representative concentration pathway
SD	Statistical Downscaling
SMI	Soil Moisture Index
SPEI	Standardized Precipitation and Evapotranspiration Index
SRTM	Shuttle Radar Topographic Mission
SPI	Standardized precipitation index
SSTs	Sea surface temperatures
SWSI	Surface Water Supply Index

TABLE OF CONTENTS

LIST OF TABLES

LIST OF FIGURES

LIST OF TABLES IN THE APPENDIX

LIST OF FIGURES IN THE APPENDIX

ABSTRACT

Drought is a complex and recurring phenomenon that has impacts on agriculture, water supply, and ecosystems. Even if its characteristics vary significantly from one region to another, and differs from aridity that is a permanent feature of climate restricted to low rainfall areas drought occurs in all climatic zones. Therefore, it is very important to increase the understandings of the concerned body and local community in the continent in general and in Ethiopia in particular for future most likely drought impacts. The objective of this study was to identify the past and projected meteorological drought by using the standardized precipitation index, in case of Central Rift Valley of Ethiopia. For this study 34 years historical precipitation data from (1985-2019) and (2020-2100) years projected climate data were used for analysis. RStudio software was used to calculate SPI at the nine major station to identify historical and future meteorological drought. The Mann-Kendall trend test and Sen's slope estimate were employed to find the nature of the drought, rainfall and temperature trend and significance level in the study area. Results showed that the study area was under drought condition in (1991-1992), (2015-2016), (2017-2018) and 2019 in historical period and for projected period in near future (2022, 2029 and 2046) in mid future (2058, 2065 and 2061,2068) in far future (2099, 2085 and 2099,2083) which were among the drought years for both RCP4.5 and RCP8.5 respectively. For historical data SPI-3 showed that 325 moderate, 141 severe and 87 extreme droughts events. Again, 3-month standardized precipitation index showed that 392 moderate, 171 severe and 95 extreme droughts events for RCP4.5 and 456 moderate, 142 severe and 80 extreme number of drought events occurred for RCP8.5. Statistical analysis for historical data showed increasing trends of drought at three-month timescale in Langano and Ziway station but decreasing tendencies in Tora, Kulmsa, Koshe, Degaga and Arsi Negele stations at significant level of ($p < 0.05$). RCP 8.5 shows significantly decreasing trend with the S-test of -158 and with the Z-value is $|Z| > 1.96$ at near future, (S-test= -122, Z=-2.3) at far future for 95% confidence level. But RCP4.5 shows decreasing trend at mid future (S-test=-106, Z= -1.67). Finally, from the result we conclude historical drought and projections indicated that its intensity, severity and duration is increase under past data as well as for both analyzed RCPs (RCP4.5 and RCP8.5).

Key words: - Meteorological drought, Mk test, trend, SPI

1. INTRODUCTION

1.1. Background

Drought is a complex and recurring phenomenon that has detrimental impacts on agriculture, economy, water supply, and ecosystems (Isabella et al., 2001). Due to its complexity, there is no single definition of drought, for example to meteorologist drought means below normal rainfall, to agrarian it means shortage of moisture in the root zone, to hydrologist it means below average water level in streams, lakes, reservoirs and the like, to the economist it means a water shortage that adversely affects the established economy (Bobadoye et al., 2019). Even if its characteristics vary significantly from one region to another, and differs from aridity that is a permanent feature of climate restricted to low rainfall areas drought occurs in all climatic zones.

Drought originates from a deficiency of precipitation (less than normal) over an extended period of time, usually a season or more (Wilhite and Glantz, 1985; Bordi and Sutera, 2007). According to Isabella et al. (2001), drought is one of climate extreme events which damage the economic and social value of one society. Ethiopia is one of the countries which highly affected by drought event. Drought occurs every 3-4 years in the northern and 6-8 years in other parts of Ethiopia (Haile, 1988). Drought can be categorized into four major categories (Wilhite and Glantz,2005) related to precipitation (meteorological), soil moisture (agricultural), stream flow (hydrological) and socioeconomic droughts. When meteorological drought appears in a region, agricultural and hydrological droughts follow.

Meteorological droughts are quite common, and they are primarily classified by the extent of dryness in a given location and the length of the dry period. Although agricultural drought is linked to a lack of water needed to support crops, the drought does not always coincide with meteorological drought. On the other hand, hydrological drought is limited to the level of streamflow that can meet the demand. A study by Wilhite and Glantz (2005) gives a detailed description of this specific drought phenomenon. In a recent study, (Adisa et al.,2019) noted that three-quarters of the total publications on drought over Africa between 1980 and 2020 focused on agricultural and hydrological droughts, while the remaining fraction was based on socio-economic and meteorological studies.

In this thesis, the studies and discussions are based on meteorological drought. This is because most agricultural activities that support over 80% of livelihoods across the African continent are regulated solely by weather and climate. Climate change can influence precipitation (meteorological) droughts through changes in atmospheric water-holding capacity, circulation patterns, and moisture supply (Ukkola et al.,2020).

Furthermore, changes in atmospheric dynamics and modes of variability such as the El Niño–Southern Oscillation (ENSO) can further influence regional precipitation patterns together with changes in evapotranspiration that show trends over lands and oceans (Roderick et al.,2014; Trenberth et al.,2014). Thus, meteorological droughts can result in negative anomalies in water supply, and changes leading to more drought occurrences at regional scales influenced by the complex interactions of the different processes. Meanwhile, in comparison between agricultural, hydrological, or socio-economic drought, meteorological drought is most prevalent and thus affects all sectors of the economy and ecosystem.

They are a number of methods to analyze drought in many parts of the world. Drought indices have been developed as a means to measure drought. There are several indices that measure how much precipitation for a given period of time has deviated from historically established norms. Some of the widely used drought indices include Palmer Drought Severity Index (PDSI), Crop Moisture Index (CMI), Standardized Precipitation Index (SPI), and Surface Water Supply Index (SWSI). The indices chosen are determined by the dataset available and the accuracy required.

The SPI and SPEI are similar to each other in calculation, but use two different inputs (precipitation versus precipitation and temperature) and can be calculated for any time scale of interest. The SPEI was proposed on the basis of the SPI by (Vicente Serrano et al., 2010). Based on the principle of water balance, the SPEI uses the difference between precipitation and potential evapotranspiration (PET) as the input condition to evaluate the dry and wet conditions of the area. Among them, both the SPI and SPEI have the characteristics of multiple timescales, which can represent various types of droughts and better reflect the variations in drought characteristics). Therefore, these indexes are widely used throughout the world (Haied et al., 2017).

The theories of the SPI and SPEI are similar, but there are obvious differences between the calculation parameters of the SPI and SPEI. The SPI only considers precipitation, which is easy to calculate, and it has strong adaptability in time and space (Bewket. ,2004). But the SPEI is calculated based on the accumulated difference between precipitation (P) and potential evapotranspiration (PET), which can comprehensively reflect the change in surface water balance (Zhang, 2015).

The Standardized Precipitation Index (SPI) is a drought index that was developed recently to improve the Palmer Drought Severity Index (PDSI) in the expression method of wetness and dryness, which is currently used in 40 countries for drought preparedness (Wambua, 2014). It was designed by (McKee, 2017) based on the idea that a reduction in precipitation with respect to the normal precipitation amount is the primary driver of drought, resulting in a successive shortage of water for different natural and human needs. The SPI, setting the time period on a monthly basis, typically 1, 3, 6, 9 or 12 months, calculates the shortage of precipitation and defines drought intensity based on SPI value (Mohammed et al., 2018). The SPI, as calculated for a different period of time, can be applied to various fields based on the length of the time units. The short accumulation period of SPI is used for agricultural purposes, while the SPI for relatively long accumulation periods is used for the supply and management of water resources. The calculated SPI enables the determination of precipitation probability necessary for resolving the current meteorological drought (Salehnia et al., 2017).

In addition, the SPI is still widely used around the world (Yacoub and Tayfur, 2017). So, the difference between the SPI and the SPEI in drought monitoring and their regional applicability with global climate change are still topics worthy of discussion.

Until recently, studies on the projections of extreme weather events, such as drought, have often been based upon a few general circulation models (GCMs), regional climate models (RCMs), and/or emission scenarios, partly due to availability. Only a few studies such as (Burke, 2011) have considered the changes in drought under a perturbed climate using a large ensemble of simulations. The different concepts and methods of representing drought events applied in different studies make inter-comparing results from different analyses challenging (IPCC, 2012). Existing studies have noted emerging issues related to possible changes in the drought situation over the East African region. Most studies show consistent results, with a likely increase in drought duration and moderate incidence, with fewer occurrences of extreme events across possible scenarios (i.e., RCP4.5 and 8.5) (Gidey et al.,2018; Haile et al., 2020). Examination of projected changes in drought frequency and severity depicts possible manifestations of severe to extreme drought occurrences that are expected to intensify during 2071–2100 (Haile et al.,2020a,2020b). For instance, using CMIP5 models, most studies projected an increase in drought episodes towards the end of the century by 16%, 36%, and54% under RCP 2.6, 4.5, and 8.5 scenarios, respectively (Haile et al.,2020a,2020b).

This study focused on assessment of past and projected meteorological drought by using the SPI index, which can be seen as a prolonged deficit in precipitation over a defined region and period of time as compared to average climatological values.

1.2. Statement of the Problem

According to certain study, in the CRV area there have been continual decreases in water resources; lakes levels have lowered and wetlands have deteriorated (Jansen et al., 2007; Temesgen et al., 2013; Abera, 2016; Gebretsadik & Mereke, 2017). The Central Rift Valley of Ethiopia is an area with diverse ecosystem services of socio-economic and ecological values. The ecosystems in the area are means of livelihood and income for many people via, for example, small-scale and large-scale irrigation farms, fishing and sources of fodder for livestock (Hengsdijk et al., 2010; Elias et al., 2019). The area is also the home of a wide variety of terrestrial and aquatic biodiversity including edible fish and varieties of bird species (Abera, 2016; Girmay et al., 2017).

Despite the enormous values, most of these resources are falling under threats and pressures due reduction of water. A study by (Elias et al. ,2019) revealed that the water bodies especially lakes and associated wetlands of the CRV area have decreased by 11.57% between the years 1985-2015; the highest turn down, which is 8.89%, was recorded in the years 1995-2015. The danger is highlighted for the wetlands of Lakes Ziway and Abijata where resource extraction related to human activities are being maximized beyond the resource’s capacity (Pascual-Ferrer et al., 2015; Bezabih & Mosissa, 2017).

Over the last decade the size and depth of Lake Abijata have shown a dramatic reduction which brings a great fear in the minds of people that it may dry up within a few years (Ewnetu et al., 2013; Temesgen et al., 2013).

So that decreasing in water resource or when an area or region experiences below-normal precipitation meteorological drought will occur. Drought is one of the most damaging natural hazards, and anthropogenic climate change will continue to impact drought sensitive sectors such as primary production, industrial and consumptive water users (Easterling, 2002).

Farmers inhabiting in the study area are exposed to the impact of agricultural drought that happen due to meteorological drought. This is due to the fact that most of farmer's cultivars (long duration crop variety) can no longer resist the exiting meteorological drought and intra seasonal dry spell. The main effect of meteorological droughts on agriculture is the reduction of available agricultural water resources, which causes crop water stress and decreases the yield. Like most parts of Ethiopia, food security situation of households in the CRV region of the country is greatly influenced by the performance of rain-fed cropping systems.

In the CRV, farmers also believe that a decrease in rainfall and a change in its distribution as the main cause of yield reduction (Kassie et al. 2013; Adimassu et al., 2014).

So that based on the above findings there are certainly condition of decreasing in water resource in the Central Rift Valley which is cause for drought.

1.3. Significance of the Study

About one-third of the global population is living under water stress at present which is projected to reach 52% by 2050 (Wang et al., 2016a). According to Elias et al. (2019) water bodies especially lakes and associated wetlands of the CRV area have decreased by 11.57% between the years 1985-2015; the highest turn down, which is 8.89%, was recorded in the years 1995-2015. Therefore, understanding possible future changes in the climate and their impacts on droughts is essential for adaptation and mitigation planning. Additionally, meteorological drought assessment aims to be useful in the decision-making process for drought monitoring and identifying appropriate site for specific adaptation and mitigation actions in order to prevent water stress.

1.4. Objectives

1.4.1. General objectives

The general objective of this study was to assess the past and projected meteorological drought by using standardized precipitation index (SPI) A case study in Central Rift Valley of Ethiopia.

1.4.2. Specific objectives

1) To determine frequency of meteorological drought using standardized precipitation index (SPI).
2) To test the trends of meteorological drought based on SPI3.
3) To identify the drought period
4) To determine the general severity of drought

1.5. Research Question

1) What is the frequency of drought?
2) Is there any trend in meteorological drought?
3) Which years in the future will be the drought period?
4)What is the general severity of drought for both past and future?

1.6. Scope of Study

The study is limited to only one meteorological variable which is rainfall. Study area was part of Ethiopian Central Rift Valley used to implement the methodological framework. Therefore, the historical droughts of Central rift valley are characterized, trend of drought was detected and possible projected drought was identified with associated framework developed in this study. Based on the availability of long-term data and representativeness for the study area, 34 years historical rainfall data and projected climate data were used for analysis. The results of non-parametric test (Mann-Kendall, Sen's slope estimator) were interpreted at a 95% confidence interval (at $\alpha = 0.05$ significance level).

2. LITERATURE REVIEW

2.1. Drought

The climate of Ethiopia is mainly controlled by the seasonal migration of the intertropical Convergence Zone (ITCZ), due to the complex topography of the country (NMSA, 2001). As (Arnell and Reynald, 2016) the main source of moist air is from the Atlantic Ocean, from the South-West, the eastern parts of the highlands are more or less rain shadowed. This combination results in a variety of climate types and climate conditions that may vary also within short space and time.

Drought occurs in virtually all climatic zones, but its characteristics vary significantly from one region to another and its definition varies from region to region and may depend upon the dominating perception, and the task for which it is defined.

Operational definitions identify the beginning, end, spatial extent and severity of a drought. In addition, drought over a geographic area represents a temporary condition of scarcity of water for an extended period of time caused by significantly low precipitation, high evapotranspiration and over-exploitation of water resources or a combination of all these (Guhathakurta, Pai and Rajeevan, 2017). It has been a part of the climate, and it has affected many countries in the world (Gutierrez et al., 2014). This included Ethiopia and the horn of Africa and many other Sub-Saharan countries as well as among the developed countries, Australia, Brazil, and California State in USA have the history of drought.

It is now fully recognized that drought is a global climatic phenomenon although the factors that causes it are not yet fully and convincingly explained. Conceptual definitions are normally formulated in general terms, do not provide quantitative answers to “when”, “how long” or “how severe” a drought is and are often used as a start-up in scientific papers and reports to help people understand the concept of drought.

Drought occurs when the seasonal precipitation drops below normal or long-term average (Wilhite et al., 2005). Some argue that it is difficult to give a universal definition for drought, because drought is a complex phenomenon (Van Lanen, 2015). However, several authors have given their version of the definition of drought or discussed its definitions in their articles

(Wilhite et al., 2007), Tallaksen and Van Lanen, 2015), Mishra and Singh, 2010) and Sheffield J. Wood, 2011). The simplest definition of drought from meteorological point of view is given as “a deficit of precipitation compared with normal conditions” (Sheffield J, Wood, 2011 edited in Van Lanen, 2015).

2.2. Past, Present and Future Pattern of Droughts

There are few studies available to date which offer possibility of comparing droughts observed during 1900–2013 (instrumental era) with those witnessed in the past centuries. This comparison is important as African climate displays high decadal and century scale variability. The work of (Touchen et al. 2008, 2011) provides a long-term perspective on droughts in eastern Africa (Burundi, Comoros, Djibouti, Ethiopia, Eritrea, Kenya, Rwanda). They used tree-ring records to construct the Palmer Drought Severity Index (PDSI) for the period of 1179–2002.

These studies reveal that the frequency of occurrence of a single drought event was 12–16 times per century before the 20th century, which was increased to 19 during the 20th century. The most severe multi-year drought occurred during 1999–2002, whereas 1847 and 2002 were identified as the driest single years with PDSI values of −3.74 and −3.90, respectively. The latter half of the 20th century is seen as the driest period in the last 9 centuries. This shift to drier conditions was attributed to anthropogenic climate change.

A number of researchers studied historic droughts in Africa based on lake sediment analyses. Evidence from the sediment analysis of the lake Bosumtwi, Ghana indicated several prolonged periods of drought during the last three millennia, most recent ones around 200–300 yr ago (Shanahan et al., 2009). Comparing 1970s droughts in Sahel with earlier drought episodes, they concluded that these droughts were not anomalous and monsoon had generated even more severe and prolonged droughts in the past. (Verschuren et al. 2000) investigated droughts over the period 900 to 2000 based on sediment analysis of Lake Naivasha Kenya in Equatorial East Africa. These drought episodes were more severe than recorded droughts in the 20th century. Shanahan et al. (2009) noted extreme droughts in Equatorial East Africa about 200 yr 10 ago based on the sediment analysis of three lakes (Chibwera and Kanya mukali in western Uganda, and Baringo in central Kenya). The authors, Verschuren et al.

(2000), Shanahan et al. (2009), compared their findings with the available evidence from the cultural history of east Africa and found consistency between two sets of observations.

The evidence presented in the previous section pointed out to the increased aridity and intensification of droughts, especially during the second half of the 20th century (e.g., Dai, 2011; Kasei et al., 2010; Touchan et al., 2008) predicted likelihood of increased droughts and aridity over central, eastern and southern Africa during the 21st century. Large uncertainties exist in these findings and thus require caution in making regional or continental conclusions. ((Masih *et al.*, 2014) reviewed studies which are based on the simulations of atmosphere-ocean global climate models on future climate of Sahel. Some studies predicted wetter conditions and some predicted more frequent droughts, thus, no consensus was observed. The large uncertainties and differences in these predictions were attributed to model limitations and complexity of many physical mechanisms governing the precipitation trends.

2.3. Causes of Droughts

Many studies attempted to investigate the natural and anthropogenic causes that could be associated with droughts in Africa (Dai, 2011, 2013; Dutra et al., 2013; Giannini et al., 2008; and Lebel et al., 2009; Richard et al., 2001). The review of these studies revealed that there is complex array of factors inter-playing in an intricate manner. There is no unique set of factors responsible for geospatial and temporal variation of droughts across the continent. The physical mechanisms causing droughts differ by region, although ENSO and SSTs are regarded major influencing factors across the continent.

Droughts in Southern Africa occur most of the time during the warm phase of ENSO (El Niño). However, this does not happen always as there are many other local and global factors influencing the drought phenomenon. For instance, Richard et al. (2001) examined droughts during 1950–1988 in Southern Africa. They found that droughts during 1970–1988 were intense and widespread compared to those during 1950– 1969. The El Niño was the main governing factor for droughts during 1970–1988. However, this observation require caution because droughts may not occur during El Niño periods, i.e., as happened during 1925–1926 and 1997–1998. For the droughts during 1950–1969, regional oceanic and atmospheric anomalies (e.g., southwest Indian Ocean SST) were named as the main causes. Contrary to

Southern Africa, East Africa region faces droughts during cold phase of ENSO (La Niña). For instance, Dutra et al. (2013) indicated that strong La Niña event was the main cause of 2010–2011 drought in the Horn of Africa. Giannini et al. (2008) argue that the low rainfall in this region occurs during fast westerlies which are usually accompanied by anomalously cold waters in the northwestern and warm anomalies in the southeastern extremity of the equatorial Indian Ocean Basin. This mechanism was found responsible for 2005 drought in the Horn of Africa.

The land-atmosphere feedbacks through natural vegetation and land cover change are also important factors. Anthropogenic contribution in land use change altering the land surface feedback mechanisms is also seen as a factor. Furthermore, human induced greenhouse gas emission is also considered as a contributory factor to oceans warming.

2.4. Drought Classifications

Drought definitions depend mainly on the types of droughts. But all have argued that the primary characteristic of drought is a reduction in precipitation (Agnew and Chappel, 1999). (Wilhite, 2005), (Paulo and Pereira, 2012), (Mishra and Singh, 2010) and (Dai, 2011) have comprehensively reviewed the concept of drought and drought classification, which can be defined and understood in many ways. Sections 2.4.1–2.4.4 are based on these and other studies.

Drought can be categorized into four major categories (Wilhite and Glantz 2005) related to precipitation (meteorological), soil moisture (agricultural), stream flow (hydrological) and socioeconomic droughts. Meteorological drought is a more common and natural event, whereas agricultural, hydrological and socio-economic droughts emphasis the human or social aspects (Van Loon, 2015). The sequence begins with meteorological drought; persistent dry conditions may induce agricultural, hydrological and water resources droughts (Vidal and Wade, 2009; Mishra and Singh ,2011).

2.4.1. Meteorological drought

Meteorological drought is defined usually on the basis of the degree of dryness (in comparison to some “normal” or average amount) and the duration of the dry period. It is based on solely on departures of rainfall from expected amounts. Thus, meteorological drought has been defined as a period of more than a particular number of days with precipitation less than some specified small amount (Wilhite and Glantz,2005). It is quite common and primarily classified by the extent of dryness in a given location and the length of the dry period.

Although agricultural drought is linked to a lack of water needed to support crops, the drought does not always coincide with meteorological drought. On the other hand, hydrological drought is limited to the level of streamflow that can meet the demand. A study by Wilhite and Glantz (2005) gives a detailed description of this specific drought phenomenon.

In a recent study, Adisa et al. (2019) noted that three-quarters of the total publications on drought over Africa between 1980 and 2020 focused on agricultural and hydrological droughts, while the remaining fraction was based on socio-economic and meteorological studies.

Climate change can influence precipitation (meteorological) droughts through changes in atmospheric water-holding capacity, circulation patterns, and moisture supply (Ukkola et al.,2020).

Furthermore, changes in atmospheric dynamics and modes of variability such as the El Niño–Southern Oscillation (ENSO) can further influence regional precipitation patterns together with changes in evapotranspiration that show trends over lands and oceans (Roderick et al.,2014; Trenberth et al.,2014).

Thus, meteorological droughts can result in negative anomalies in water supply, and changes leading to more drought occurrences at regional scales influenced by the complex interactions of the different processes. Meanwhile, in comparison between agricultural, hydrological, or socioeconomic drought, meteorological drought is most prevalent and thus affects all sectors of the economy and ecosystem.

2.4.2. Hydrologic drought

Hydrological drought refers to a lack of water in the hydrological system, manifesting itself in abnormally low streamflow in rivers and abnormally low levels in lakes, reservoirs, and groundwater (Van Loon, 2015). It is part of the bigger drought phenomenon that denotes a recurrent natural hazard (Wilhite DA and Glantz MH, 1995).

2.4.3. Agricultural drought

Agricultural drought occurs when soil moisture is depleted to the extent that crop and pasture yields are significantly affected. Agricultural drought definitions link various characteristics of meteorological drought to agricultural impacts, focusing, for example, on precipitation shortages, departures from normal, or numerous meteorological factors such as evapotranspiration (Wilhite and Glantz, 1985).

2.4.4. Socio-economic drought

Definitions which express features of the socioeconomic effects of drought can also incorporate features of meteorological, agricultural, and hydrological drought (Wilhite and Glantz, 1985). They are usually associated with the supply and demand of some economic good (Chopra, 2006) has suggested that the time and space processes of supply and demand are the two basic processes that should be considered for an objective definition of drought.

2.5. Drought Indices

According to the indicators of the given drought, severity and duration of the drought is represented by an index. An index assimilates different meteorological and hydrological parameters including precipitation, temperature, evapotranspiration, runoff and other water supply indicators into a single numerical value or formula and gives a comprehensive picture of decision making. Such an index is more readily useable and comprehensible than raw data and it is usually presented as a numerical value in order to create decision making power for planners and policy makers.

World meteorological organization in 1992 defined the drought index as ‘an index which is related to some of the cumulative effects of a prolonged and abnormal moisture deficiency’. Friedman identified four basic criteria that any drought index should meet (Hassanzad et al., 2011).

- The timescale (period) should be appropriate to the problem at hand (drought).

- The index should be a quantitative measure of large-scale, long-continuing drought conditions
- The index should be applicable to the problem being studied.
- Long accurate past record of the index should be available or computable.

Numerous indices have been developed for drought representation, while no one has inherent priority over others some of them have better performance in specific conditions. Some of the widely used drought indices include Palmer Drought Severity Index (PDSI), Crop Moisture Index (CMI), Standardized Precipitation Index (SPI), and Surface Water Supply Index (SWSI).

2.5.1. Palmer drought severity index (PDSI)

In 1965, Palmer developed an index to measure the departure of the moisture supply. The PDSI calculation is based on a simple supply-demand model of a water balance equation that builds on both the precipitation and temperature history for a location so that a calculated PDSI value represents a combination of the current conditions and previous PDSI values (Palmer, 1965).

Several parameters are used in the PDSI calculation, including precipitation, temperature, and soil properties (that is, available water-holding capacity). The index was specifically designed to treat the drought problem in semiarid and sub-humid climates; with palmer himself cautioning that extrapolation beyond these conditions may lead to unrealistic results. PDSI has been used in west Hungary as soil moisture indicator and has been widely used in United States for drought monitoring. It has been utilized as a tool to trigger actions associated with drought contingency plans.

Several researchers have given limitations of PDSI. The response of PDSI to an emerging drought event may lag by weeks or months compared to a quicker response index such as SPI (Hayes et al., 1999). Moreover, this index has many other problems related to calibration and spatial comparability (Guttman et al., 1992; Karl, 1983; Alley, 1984). McKee et al. suggested that PDSI is designed for agriculture but does not accurately represent the hydrological impacts resulting from longer droughts. Also, PDSI is applied within the United States and has less acceptance elsewhere (Mohammed *et al.*, 2018).

To solve these problems, (McKee et al.,1993) developed the Standardized Precipitation Index (SPI), which can be calculated at different time scales to monitor droughts in the different usable water resources.

2.5.2. Standardized precipitation index (SPI)

The Standardized Precipitation Index (SPI) is a tool developed in 1993 by Tom McKee, Nolan Doesken and John Kleist in Colorado Climate Centre with the main purpose to defining and monitoring drought (Komala Dhanapal, 2017). Compared with PDSI (Palmer drought severity index), SPI is a simpler tool because it just based on rainfall data and less calculation effort. It allows an analyst to determine the rarity of a drought at a given time scale (temporal resolution) of interest for any rainfall station with historic data.

It can also be used to determine periods of anomalously wet events. Mathematically, the SPI is based on the cumulative probability of a given rainfall event occurring at a station. The historic rainfall data of the station is fitted to a gamma distribution, as the gamma distribution has been found to fit the precipitation distribution quite well. This is done through a process of maximum likelihood estimation of the gamma distribution parameters, α and β. In simple terms, the process described above allows the rainfall distribution at the station to be effectively represented by a mathematical cumulative probability function.

Therefore, based on the historic rainfall data, an analyst can then tell what is the probability of the rainfall being less than or equal to a certain amount. Thus, the probability of rainfall being less than or equal to the average rainfall for that area will be about 0.5, while the probability of rainfall being less than or equal to an amount much smaller than the average will be also be lower (0.2, 0.1, 0.01 etc., depending on the amount) (Thomas B. McKee, 1993). Therefore, if a particular rainfall event gives a low probability on the cumulative probability function, then this is indicative of a likely drought event. Alternatively, a rainfall event which gives a high probability on the cumulative probability function is an anomalously wet event.
Gamma distribution is defined by its frequency or probability function as in Equation (3.3) Guttman (1999).

$$g(x)=\frac{x^{\alpha-1}\,e^{-\frac{x}{\beta}}}{\beta^{\alpha}\Gamma(\alpha)} \text{ for } x,\alpha,\beta>0 \text{---} 2.1.$$

Equations (3.4) and (3.5) are used to calculate the α and β parameters.

$$\alpha = \frac{1}{4A}\left\{1+\sqrt{1+\frac{4A}{3}}\right\}\text{--}2.2.$$

$$\beta = \frac{x}{a}\text{--}2.3.$$

$$A = \ln(x) - \sum\frac{\ln(x)}{n}\text{ --}2.4.$$

$$\Gamma(\alpha) = \int_0^{\alpha} x^{\alpha-1} e^{-y} dx\text{---}2.5.$$

The calculated values were in turn used to compute the cumulative probability for non-zero rainfall using Equations (3.8) and (3.9) respectively:

$$f(x,\alpha,\beta) = \int_0^{x} f(x,\alpha,\beta) = \frac{1}{\beta^{\alpha}\Gamma(\alpha)}\int_0^{\alpha} x^{\alpha-1} e^{-x/\beta} dx\text{---------------------------------}2.6.$$

The Equation (3.8) above was reduced to:

$$f(x,\alpha,\beta) = \int_0^{x} f(x,\alpha,\beta) = \frac{1}{\beta^{\alpha}\Gamma(\alpha)}\int_0^{\alpha} t^{\alpha-1} e^{-t} dt\text{------------------------------------}2.7.$$

for $t = \frac{x}{\beta}$

Where;

α = the shape parameter

β = scale parameters

x = mean rainfall (mm)

A = sample statistic

Γ (α) = gamma distribution function or the value taken by gamma function

t = the time period

The gamma function is not defined for x = 0, and the cumulative probability is calculated using Equation (3.7), since zero precipitation is the most common occurrence in terms of precipitation.

H(x) = q + (1 - q) G(x)---2.8.

Where;

H(x) = Cumulative probability

q = probability of zero rainfall

When *m* was taken as the number of zero entries in the time series rainfall data, then the *q* value was estimated by the ratio. n/m. The probability of zero precipitation is given as q, and G (x) is the gamma function's cumulative probability. The cumulative probability H (x) is then converted to the standard normal distribution (z) using the mean of zeros and the variance of one, and the result is SPI according to McKee (1993) then (Table 2.1) used to define drought. Based on the SPI methodology described above, SPI was calculated using RStudio software for all meteorological station of Central rift valley from 1985 to 2019. This step was carried out using approximate transformation functions adapted from(Mishra and Desai, 2006). These functions given in Equations (3.8) and (3.9) are expressed as:

$$SPI = -\left(K-\frac{C_O+C_1K+C_2K^2}{1+d_1K+d_2K^2+d_3K^3}\right) \text{ for } 0<H(x)\leq 0.5\text{-----------------------}2.9.$$

$$SPI = +\left(K-\frac{C_O+C_1K+C_2K^2}{1+d_1K+d_2K^2+d_3K^3}\right) \text{ for } 0<H(x)\leq 1\text{-------------------------}2.10.$$

Where; C_0, C_1, C_2, d_1, d_2 and d_3 parameters used to compute the SPI were adapted from (Cassiamani *et al*. ,2007) consideration constants. The value of *k* in Equations (3.11) and (3.12) was determined from the functions given as:

$$K=\sqrt{\ln\left(\frac{1}{H(x)^2}\right)} \text{ for } 0<H(x)\leq 0.5\text{--}2.11.$$

$$K=\sqrt{\ln\left(\frac{1}{1-H(x)^2}\right)} \text{ for } 0.5<H(x)\leq 1\text{---}2.12.$$

Table 2.1. Categories of dryness/wetness conditions evaluated by SPI assuming the classification by McKee et al. (1993)

SPI Value	Class
2.0 and more	Extremely wet
1.5 to 1.99	Very wet
1.0 to 1.49	Moderately wet
-0.99 to 0.99	Near normal
-1.0 to -1.49	Moderately dry
-1.5 to -1.99	Severely dry
-2.0 and less	Extremely dry

Positive SPI values indicate the rainfall is greater than median rainfall and negative values indicate less than median rainfall. In dry condition monitoring, the drought part of the SPI range is divided into near normal conditions (0.99 < SPI <-0.99), moderately dry (-1.0 < SPI < -1.49), severely dry (-1.5 < SPI <-1.99) and extremely dry (SPI < -2.0). A drought event starts when SPI value reaches -1.0 and ends when SPI becomes positive again. For several purposes, McKee design SPI for 3, 6, 12, 24, and 48-month time scales and then classified the drought class as shown in Table 2.1.

- 1-month SPI

A 1-month SPI map is very similar to a map displaying the percentage of normal precipitation for a 30-day period. In fact, the derived SPI is a more accurate representation of monthly precipitation because the distribution has been normalized. For example, a 1-month SPI at the end of November compares the 1-month precipitation total for November in that particular year with the November precipitation totals of all the years on record. Because the 1-month SPI reflects short-term conditions, its application can be related closely to meteorological types of droughts along with short-term soil moisture and crop stress, especially during the growing season(Mark Svoboda ; Michael Hayes ; Deborah A. Wood, 1987).

- 3-month SPI

The 3-month SPI provides a comparison of the precipitation over a specific 3-month period with the precipitation totals from the same 3-month period for all the years included in the historical record. In other words, a 3-month SPI at the end of February compares the December–January–February precipitation total in that particular year with the December–February precipitation totals of all the years on record for that location. Each year data is added, another year is added to the period of record, and thus the values from all years are used again. The values can and will change as the current year is compared historically and statistically to all prior years in the record of observation. A 3-month SPI reflects short and medium-term moisture conditions and provides a seasonal estimation of precipitation (Mark Svoboda; Michael Hayes; Deborah A. Wood, 1987).

- 6-month SPI

The 6-month SPI compares the precipitation for that period with the same 6-month period over the historical record. For example, a 6-month SPI at the end of September compares the precipitation total for the April–September period with all the past totals for that same period.

The 6-month SPI indicates seasonal to medium-term trends in precipitation and is still considered to be more sensitive to conditions at this scale than the Palmer Index. A 6-month SPI can be very effective in showing the precipitation over distinct seasons. For example, a 6-month SPI at the end of March would give a very good indication of the amount of precipitation that has fallen during the very important wet season period from October through March for certain Mediterranean locales. Information from a 6-month SPI may also begin to be associated with anomalous stream flows and reservoir levels, depending on the region and time of year (World Meteorological Organization, 1987).

- 9-month SPI

The 9-month SPI provides an indication of inter-seasonal precipitation patterns over medium timescale duration. Droughts usually take a season or more to develop. SPI values below -1.5 for these timescales are usually a good indication that dryness is having a significant impact on agriculture and may be affecting other sectors as well. Some regions may find that the pattern displayed by the map of the Palmer Index is closely related the 9-month SPI maps. For other areas, the Palmer Index is more closely related to the 12-month SPI. This time period begins to bridge a short-term seasonal drought to those longer-term droughts that may become hydrological, or multi-year, in nature (World Meteorological Organization, 1987).

2.5.3. Crop moisture index (CMI)

The Crop Moisture Index (CMI) developed by Palmer (1965), is a complement to the PDSI. It measures the degree to which crop moisture requirements are met, is more responsive to short-term changes in moisture conditions and is not intended to assess long-term droughts. It depends on the drought severity at the beginning of the week and the evapotranspiration, soil deficit or soil moisture recharge during the week (Heim, 2000). It measures both evapotranspiration deficits (drought) and excessive wetness (more than enough precipitation to meet evapotranspiration demand and recharge the soil).

CMI is designed to monitor short-term moisture conditions affecting a developing crop; therefore, CMI is not a good long-term drought-monitoring tool. The CMI’s rapid response to changing short-term conditions may provide misleading information about long-term conditions.

2.6. Non-parametric Trend Analysis

There are many studies over the world that investigated anthropogenic changes in the form of gradual trends or abrupt changes in the meteorological time series dataset (Kisi and Murat, 2014); (Totaro et al., 2020) and (Yue and Wang, 2004).

Statistical hypothesis tests including deterministic hydrological models, climate models, and expert opinion are undoubtedly indispensable tools for trend detection as chaos theory states that even deterministic systems may perform unpredictably rank-based non-parametric Mann-Kendall statistical test (Mann, 1945); (Kendall, 1975) has been widely used for detecting trends in meteorological time series such as precipitation and temperature. As compared to parametric methods (Linear regression and Multiple regression), a non-parametric test (Mann-Kendall, Modified Mann-Kendall, Spearman rho Correlation test, Sen's slope estimator, and innovative trend analysis) have no requirement for homoscedasticity or assumptions on the distribution of data sample to be normal distribution and are less sensitive to outliers (Hamed and Rao, 1997); (Teega varapu, 2018).

Moreover, the Mann-Kendall test is relatively effective and robust and has a basic requirement that the data should be independent. The test is not robust against serial correlation, which may be statistically significant in the hydrological and climate time series dataset. A positive serial correlation that exists in the dataset will result in overestimation and rejection of the null hypothesis of no monotonic trend (Hirsch and Slack, 1984).

Two approaches are proposed to eliminate the influence of serial correlation in the time series dataset. The first one is the application of pretreatment to the data and the second one is using the Modified Mann Kendall test to account for serial correlation.

Statistical analysis techniques have been widely studied in the Central Rift Valley to assess climatic trends and Spatial-temporal variability (Chimdesa, 2016) applied non-parametric test, Mann-Kendall, and standard Precipitation index to assess the trend of precipitation. The Sen's estimator is another non-parametric method used for the trend analysis of hydroclimate data set. It is also used to identify the trend magnitude. Hence, this test computes the linear rate of change (slope) and the intercept as shown in Sen's method (Sen 1968).

2.7. Innovative Trend Analysis (ITA)

Sen's ITA comprises a graphical tool and a formal hypothesis test (Sen, 2017c). The same material with minor changes has then been collected in a book (Sen, 2017b) and directly applied by other authors without any independent assessment of its rationale and mathematical formulation e.g. (Cui et al., 2017).

One of the added values of the innovative trend analysis method is that it is not affected by the restriction requirements for the Mann-Kendall application (Şen, 2017) such as serial autocorrelation and outliers. According to Sen (2017), ITA should be unaffected by serial correlation. However, Sen (2017b, pp. 194–196) shows that the shift of the ITA patterns from the 1:1 line increases as the correlation increases for fixed (linear) trend values. Sen (2017b, p. 196) also provides a table showing the values of the shift corresponding to a set of linear trend slopes β and lag -1 autocorrelation q_1, claiming that such a table can be used to determine the magnitude of monotonic trend in any time series provided that the serial correlation coefficient and the slope on the square area template are determined.

2.8. General Circulation Models (GCMs)

General Circulation Models or GCMs are Numerical models, representing physical processes in the atmosphere, ocean, cry sphere and land surface, are the most advanced tools currently available for simulating the response of the global climate system to increasing greenhouse gas concentrations. While simpler models have also been used to provide globally- or regionally-averaged estimates of the climate response, only GCMs, possibly in conjunction with nested regional models, have the potential to provide geographically and physically consistent estimates of regional climate change which are required in impact analysis (Intergovernmental Panel on Climate Change (IPCC),2012).

GCMs and global climate models are used for weather forecasting, understanding the climate and forecasting climate change. GCMs depict the climate using a three-dimensional grid over the globe, typically having a horizontal resolution of between 250 and 600 km, 10 to 20 vertical layers in the atmosphere and sometimes as many as 30 layers in the oceans(Komala Dhanapal Sagadevan, 2017). Their resolution is thus quite coarse relative to the scale of exposure units in most impact assessments.

Others relate to the simulation of various feedback mechanisms in models concerning, for example, water vapor and warming, clouds and radiation, ocean circulation and ice and snow albedo. For this reason, GCMs may simulate quite different responses to the same forcing; simply because of the way certain processes and feedbacks are modelled.

Coupled Model Intercomparison Project Phase 5 provides nearly 64 models (for temperature and precipitation) contributed by ~ 20 countries around the world (Taylor, 2012). These models are at a coarse resolution ranging from 0.9 (90 km) to 3.625 (362 km).

The historical simulations start from 1950-2005 while the scenarios from 2006 to 2100. The evaluation of future drought patterns should be generally handled with care due to the various sources of uncertainties (Burke and Brown, 2008). Moreover, many physical processes, such as those related to clouds, also occur at smaller scales and cannot be properly modelled. This is one source of uncertainty in GCM-based simulations of future climate.

2.9.Representative Concentration Pathways (RCPs)

The impacts of climate change on the environment and society will depend not only on the response of the Earth system but also on how humankind responds through changes in technology, economy, lifestyle and policy. These responses are uncertain, so future scenarios are used to explore the consequences of different options. The scenarios provide a range of options for the world’s governments and other institutions for decision making. The Intergovernmental Panel on Climate Change (IPCC) Fifth Assessment Report (AR5) has introduced a new way of developing scenarios. These scenarios span the range of plausible radiative forcing scenarios, and are called representative concentration pathways (RCPs)(Jubb, Canadell and Dix, 2013). They are prescribed pathways for greenhouse gas and aerosol concentrations, together with land use change, that are consistent with a set of broad climate outcomes used by the climate modelling community.

The pathways are characterized by the radiative forcing produced by the end of the 21st century. Radiative forcing is the extra heat the lower atmosphere will retain as a result of additional greenhouse gases, measured in Watts per square meter (W/m^2). The complexity of humanity’s possible future emissions has been reduced to just four representative pathways. Each of the RCPs represents a larger set of scenarios in the scientific literature.

The full range of emissions scenarios, with and without climate policy, is included within the range of the RCPs. They include one mitigation scenario leading to a very low forcing level (RCP2.6), two medium stabilization scenarios (RCP4.5 and RCP6) and one very high baseline emission scenario (RCP8.5). The 8.5 pathway arises from little effort to reduce emissions and represents a failure to curb warming by 2100. It is similar to the highest-emission scenario (A1FI) in the IPCC Fourth Assessment Report (AR4). The 6.0 pathway stabilizes total radiative forcing shortly after 2100 by the application of a range of technologies and strategies for reducing greenhouse gas emissions. RCP4.5 is similar to the lowest-emission scenario (B1) assessed in the IPCC AR4. RCP 2.6 is the most ambitious pathway.

It sees emissions peak early, then fall due to active removal of atmospheric carbon dioxide. This pathway is also referred to as RCP3PD (representing the mid-century peak radiative forcing of ~3W/ m² followed by a decline).

Table 2.2. Four global radiative forcing pathways from greenhouse gas emissions

Radioactive forcing	Atmospheric CO_2 equivalent (Parts per million)	When
8.5	>1370	By 2100 but rising
6	850	Stabilization after 2100
4.5	650	Stabilization after 2100
2.6	490	Peak before 2100 then decline

Source IGBP. http://www.igbp.net/download/18.1b8ae20512db692f2a680007120/NL75_one-planet.pdf.

2.10. Drought Impacts

Drought impacts affect almost all parts of the environment and communities. Unlike other natural hazard such as floods, earthquakes or hurricanes that result in clear damages, droughts develop slowly, and drought conditions often remain unnoticed until water shortages become severe and serious impacts begin to occur. The slow nature and long duration of drought typically makes the task of quantifying drought impacts difficult (Wilhite, 2005).

On the other hand, of all extreme weather types, droughts have one of the largest impacts on society. Impacts of natural hazards can be classified as direct or indirect (Montz and Tobin, 2011). Examples of direct impacts are the physical destruction of buildings, infrastructures, crops or other natural resources. In this context, drought can cause loss of life, reduce crop yields and limit public water supply (Liverman, 1990). Indirect impacts are related to the indirect consequences of the destruction of natural resources. These include temporary rural unemployment or business interruption. In extreme cases, droughts may result in malnutrition, starvation and disease in the more vulnerable countries (Greene, 1974; Prospero and Nees, 1986; Hillier and Dempsey, 2012). Because of their very nature, most of the drought impacts are indirect due to the dependence of many industrial sectors on water for production and the importance of water for providing services and recreation. These indirect damages can propagate quickly through the economic system, affecting regions far from the origin (Wilhite, 2002).

By the year 2011, Global Facility for Disaster Reduction and Recovery reported that, drought impacts include pasture shortages, overgrazing, land degradation, decreased water availability, and livestock diseases. All of these impacts lead to decreased livestock productivity, crop failure in agro-pastoral areas, food insecurity, and increased conflicts over scarce resources. Droughts not only bring loss of life, famine, and hardship to today's inhabitants (during the 2006 droughts, 25-60% of livestock were killed in some areas), but they also threaten the country's future, as children aged five or less are 36 and 50% (respectively) more likely to be malnourished if they were born during a drought (Amsalu, 2019).

3. MATERIALS AND METHODS

3.1. Description of the Study Area

3.1.1 Location

The study area lies between 7°10' to 8^{0}30'N and 38^{0}15' to 39^{0}25'E, about 200 Kilometer south of Addis Ababa, the capital city of Ethiopia with an area coverage of about one million hectares.

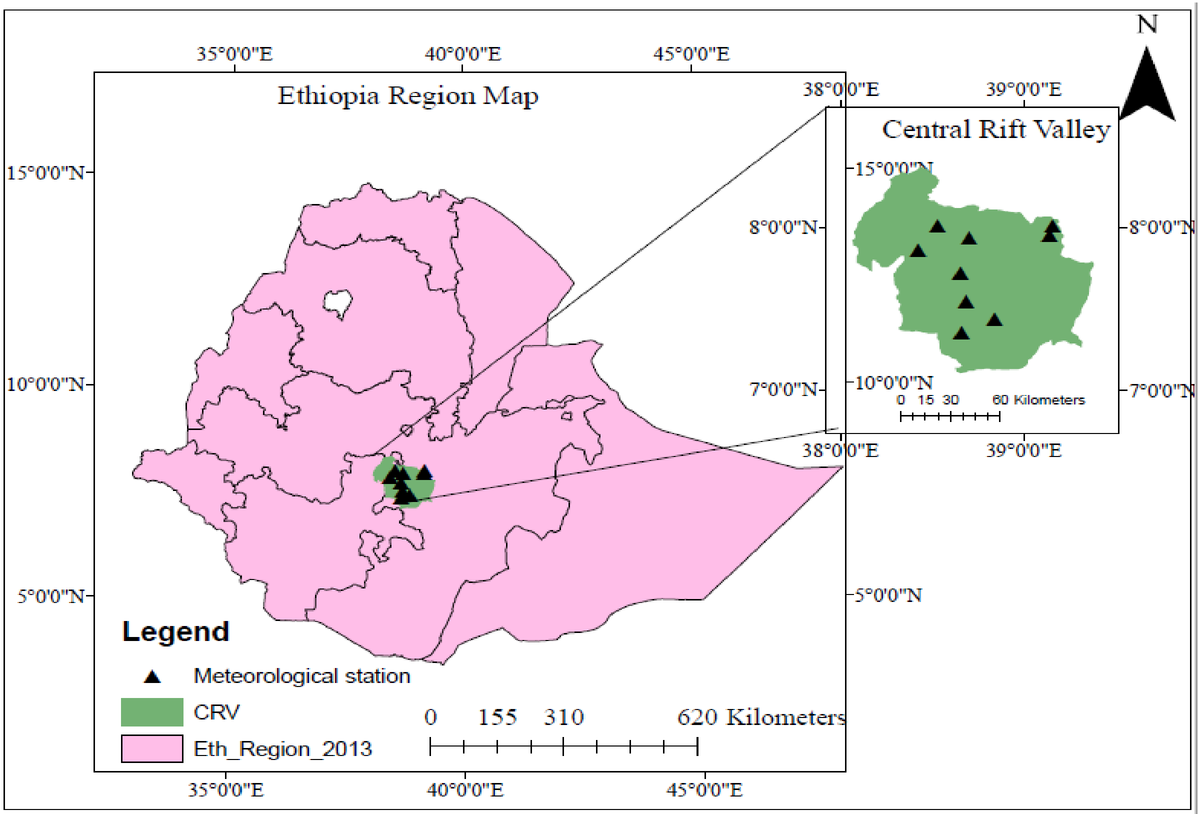

Figure 3. 1. Location map of the study area

3.1.1. Geology and hydrology

The CRV is a sub-basin of the Ethiopian Rift Valley system which is part of the Great African Rift Valley system or the Afro-Arabian rift system, bounded by the Arabian plate in the north and the African plate in the west and east. The CRV has three physiographic regions: the rift, escarpment and highland.

The lithology of the area is dominated by basalt, ignimbrite, lava, gneiss, lapilli tuff, volcanic ash and pumice as well as riverine and lacustrine alluvium (Fitsum-, 2020). The geological setting of the CRV involves volcanism, rifting, fluctuation of Quaternary Lake levels, and deposition of fluvial and volcano-lacustrine sediments (Ayenew & GebreEgziabher, 2015). Bordered by high altitude plateau to the east and west, the altitude of the CRV area ranging from 1539 m.a.s.l. in the lowest part of the rift to about 2434 m.a.s.l. in the largest part of the rift valley on the eastern side of the Ziway-Shala Lake basin (Ayenew, 2002; Ayenew, 2004; Pascual-Ferrer et al., 2014).

With unique hydrology and ecological characteristics CRV consists of a chain of lakes, rivers and associated wetlands. Being aclosed basin it consists of four lakes namely Ziway, Abijata, Langano and Shalla; and four rivers: Meki, Katar, Bulbula and Horakelo. Lake Ziway has two major sources of inflow, the Ketar River from east and the Meki River from west. Lake Langano receives its inflow merely from the eastern escarpment through the Teji-Gedemso streams. Lake Ziway, Lake Langano and Lake Abijata are hydrologically connected by rivers, i.e., Lake Abijata is connected to Lake Ziway and Lake Langano via Bulbula and Horakello Rivers respectively, whereas Lake Shalla has a closed catchment with no surface water connection to other lakes (Ayenew, 2002). Lake Shalla receives its water from River Dijo. It is the deepest lake in Ethiopia (with a depth of 266m); and there is unconfirmed hypothesis that the position and depth of the lake allows the infiltration of water from Lake Abijata (Muzein, 2006).

3.1.2. Climate

The climate of CRV area varies significantly along an altitudinal gradient, but generally arid and semi-arid climate characterizes the sub-basin with mean annual rainfall of 900 mm (Mengesha et al., 2012). The area mostly experiences bimodal rainfall: with most of the rain (about 70%) occurring during the three summer months (June to August and sometimes up to September), while very short and unreliable rain occurs during the months of April to May.

The temperature of the area is relatively high with mean monthly maximum and monthly minimum of 30.5^0C and 7.5^0C (Temesgen et al., 2013).

3.1.3. Soils

Apparently, the soil types of an area are closely related to the underlying rock or parent material. In most parts of the CRV area the soils observed are commonly derived from volcanic ash. Mostly the ash has been reworked and occurs as lacustrine sediment (Temesgen et al., 2013).

Andosols are coarse textured (loamy sand to fine sand), highly alkaline (PH of 7.6 -8.2) soils (Temesgen et al., 2013).

Generally, soils in the lake's areas tend to have high PH. High PH mean more nitrification, and thus it is expensive to maintain these soils, through fertilization, for agriculture. Generally, the soils have low fertility and organic matter with moderate nutrient retention capacity. Their low bulk density and hence weaker structure exposed the soils to wind and water erosion. Loss of soil through erosion, particularly via wind, is an increasing problem, which prevent regeneration and rehabilitation, as the vegetation around the lake is removed or degraded (Muzein, 2006; Temesgen et al., 2013; Mesfin, 2018).

3.1.4. Biodiversity (fauna and flora)

The CRV particularly the lakes support important biodiversity that have global significance. This sub-basin contains unique fauna and flora species of which a significant number are endemic. It is an important breeding and feeding area for some rare species of resident and migratory birds. A good example is Lakes Abijata and Shalla which together form the Abijata Shalla Lakes National Park (ASLNP), which has been recommended as a candidate site by the Ethiopian Government to the Ramsar convention on wetlands (Elias et al., 2019). ASLNP supports the highest bird life form among the six protected areas designated for conservation of wildlife in the Ethiopian Rift Valley (Muzein, 2006).

The phytogeography (distribution of plants) of the CRV is highly influenced by elevation, which also dictates the rainfall amount and pattern. In general, the climate of the area, particularly in the floor permits semi-climax perennials that are adapted to dry conditions or wet season vegetation that perish during dry spell (Muzein, 2006). Umbrella shaped woodland, classified as Acacia-Balanites woodland and savannas usually dominate the natural vegetation of the CRV and most often deciduous forest occupy the ridges and slopes (Temesgen et al., 2013). Along the rift floor the most common tree species belong to the
deciduous Acacia, whereas the cooler escarpments on both sides support a wide diversity of both broadleaves and conifers. The low altitudinal deciduous vegetation type is dominated by Tedecha Dere (Acacia tortilis), Kessele (Acacia etbaica), Wacho (Acacia seyal) and Jemo (Balanites aegyptiaca) with sparsely scattered Kbkib (Maytenus senegalensis) bushes.

Figure 3.2. Bird’s eye view of the surrounding study area. (Source: Google Earth)

3.2. Data Collection and Analyses

The overall study was done with the framework shown under the following section.

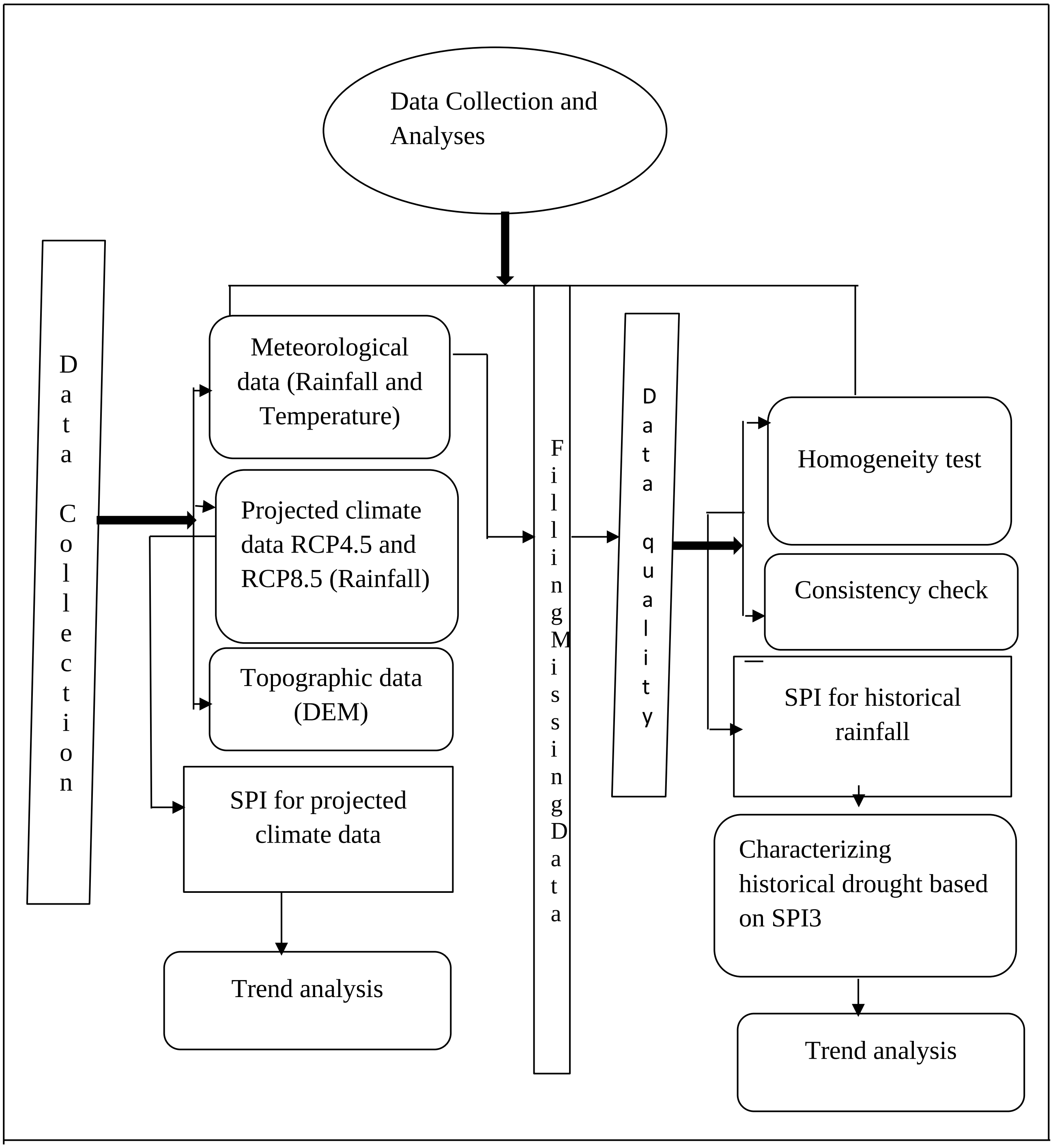

Figure 3.3. General framework of the study

Table 3.1. List of Software used for the study

Software used	Purpose	Source
ArcGIS	Study area delineation and to interpolate SPI	From USGS website and RStudio result
R	Explore and manipulate data	http://cran.r-project.org/
RStudio	For data analysis, statistical visualization, and time-series plot	https://www.r-project.org/
Mendeley desktop	To organize journals and other material for citation	https://www.mendeley.com/

3.2.1. Historical and Projected rainfall data

Monthly rainfall was obtained from Ethiopian National Meteorological Agency (NMA) for the period of (1985-2019) and used as an input variable to calculate Standardized precipitation index (SPI) and to detect climate change. This consists climatic elements record for 34 years. The available data was on monthly time step also had to be re-organized into yearly average time scales for needed variables to match with the data requirements.

Table 3.2. Meteorological station

S. N	Station name	Longitude	Latitude	Elevation	10% of ARD
1	Arsi Negele	38.66	7.35	1913	71.71
2	Assela	39.17	7.96	2413	66.8
3	Bulbula	38.65	7.72	1606	78
4	Degaga	38.84	7.43	2014	79.3
5	Koshe	38.53	8.01	2004	80
6	Kulamsa	39.16	8.01	2211	75
7	Langano	38.68	7.54	1539	108
8	Tora	38.42	7.86	2001	105
9	Ziway	38.70	7.93	1640	82

ARD = annual rainfall deference for each station.

3.2.2 Areal rainfall of Central Rift Valley

As the rainfall over a large area is not uniform, the mean depth of RF over the study area is determined by Thiessen polygon method. This method attempts to allow for non-uniform distribution of gages by providing a weighting factor for each nine gages in GIS 10.5 window. According to the Thiessen polygon analysis of nine RF gage stations; used for the study. So, for the study all RF analysis accomplished according to Thiessen polygon method.

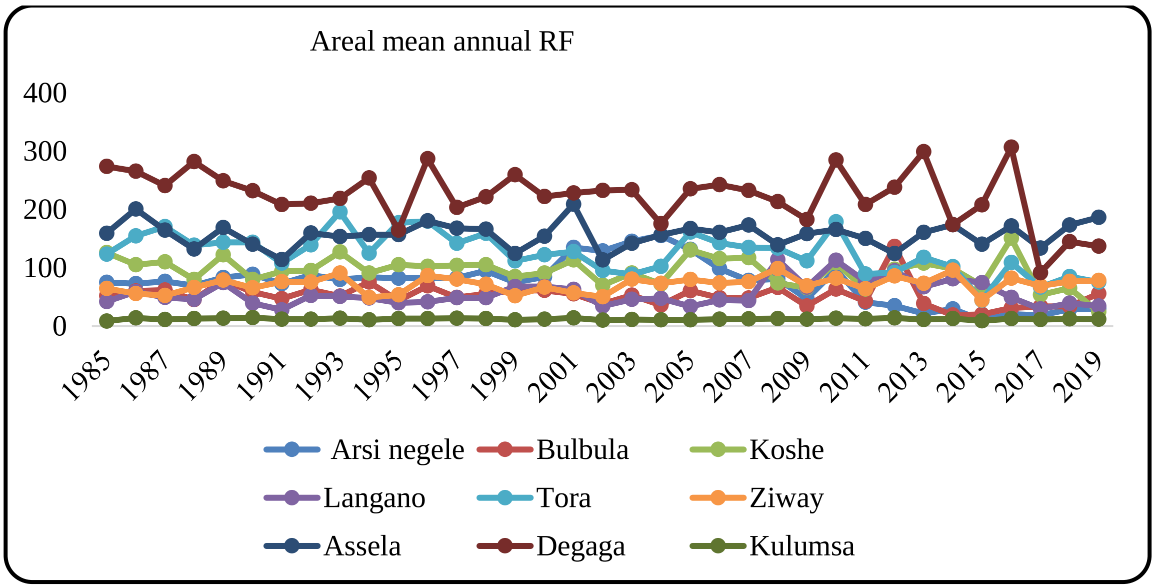

Figure 3.4 Historical areal mean annual rainfall characteristic

Table 3.3 Annual average areal precipitation (mm) using Thiessen polygon method

Sr.N	Station Name	Longitude	Latitude	Mean annual Perecipitation	Area of polygone	Weighted area	Weighted perecipitation
		x	y	prcp	Ai	Wi=Ai/A	Wi*Prcp
		Decimal degree	Decimal degree	mm	Km2	Unitless	mm
1	Arsi negele	38.6578	7.35212	717.0743304	1249	0.104571333	74.9854185
2	Bulbula	38.6525	7.72	668.4036607	945	0.079119223	52.88357831
3	Koshe	38.5253	8.0065	780.6853125	1448	0.121232418	94.64436809
4	Langano	38.68383	7.5405	793.5780357	843	0.07057937	56.01023812
5	Tora	38.420667	7.855	808.2010714	1856	0.155391829	125.5878423
6	Ziway	38.7	7.9333	752.0453571	1134	0.094943068	71.40149322
7	Assela	39.1383	7.9557	1081.442589	1736	0.145344943	157.1822116
8	Degaga	38.8375	7.4337	1050.051205	2556	0.21399866	224.7095513
9	Kulumsa	39.1553	8.0097	824.1621429	177	0.014819156	12.21338742
					A = 11944		

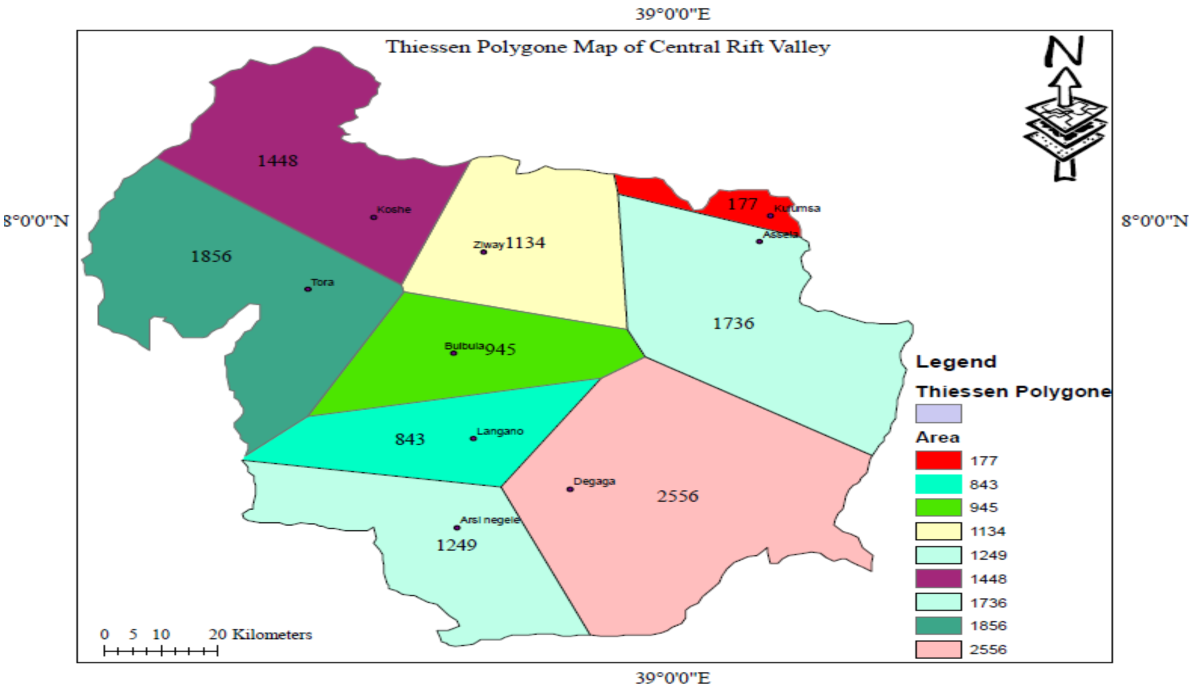

Figure 3.5 Thiessen polygon used to estimate ama RF

Statistically downscaled daily base rainfall climate data for the period 2020-2100 obtained from HadGEM2-ES United Kingdom Met Office Hadley Center (Collins et al., 2011) climate model of Coordinated Regional Climate Downscaling Experiment (CORDEX) under Africa database of CMIP5 used to derive indicators related to future change in climate. CORDEX is responsible to advance and coordinate the science and application of regional climate downscaling models through global partnerships.

An ensemble of historical and future climate projections generated by the coordinated regional downscaling experiment (CORDEX) is available from the World climate research program (Giorgietal.,2009). CORDEX Africa (http://cordex.org/domains/region-5-africa/) provides regionally-downscaled climate data for the continent at a spatial resolution of 0.44° × 0.44°.

Generally, simulate the future climate characteristic of the study area, data for baseline and future projection periods (from 2020-2100) under representative concentration pathway (RCP4.5 anRCP8.5) scenario climate data was used.

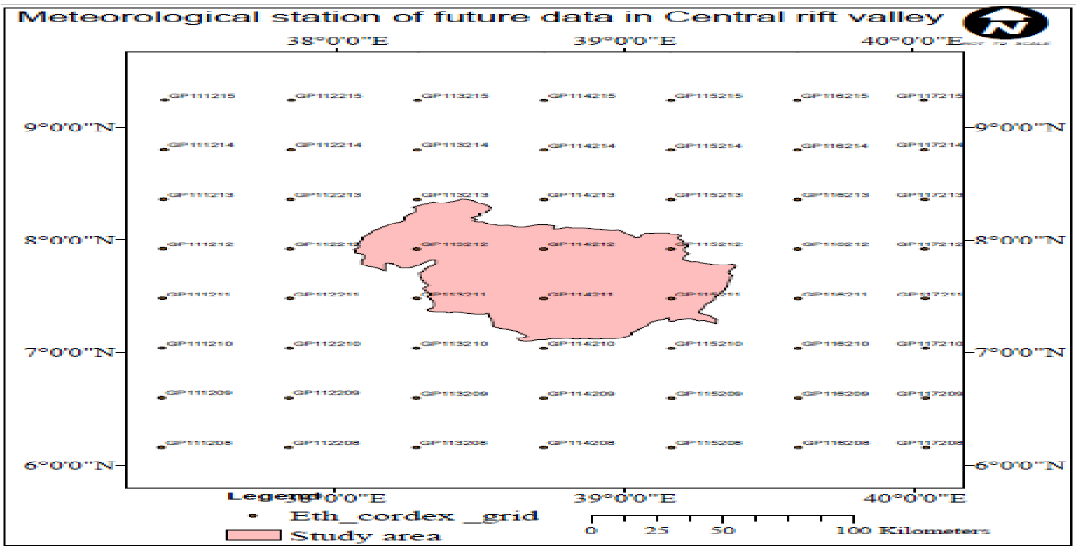

Figure 3.6. Distributions of meteorological stations of future data in Central rift valley

Table 3.4. Meteorological stations for future data (grid points)

code	station	Latitude	Longitude	Elevation
115211	GP115211	7.48	39.16	2522.94
115212	GP115212	7.92	39.16	2281.25
113212	GP113212	7.92	38.28	2187.19
114211	GP114211	7.48	38.72	2093.38
114212	GP114212	7.92	38.72	1986.89

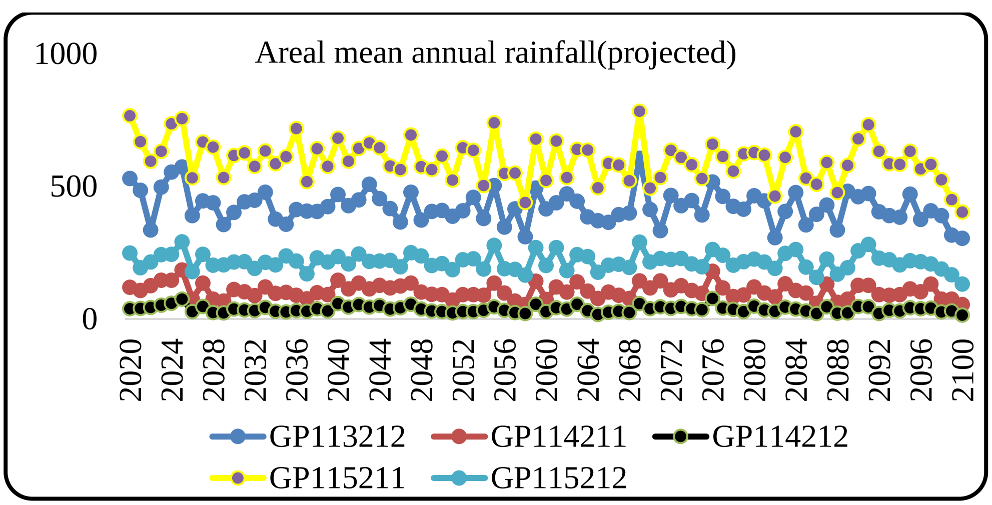

Figure 3.7 Projected areal mean annual rainfall characteristic.

Table 3.5 Annual average areal precipitation (mm) using Thiessen polygon method

Sr.N	Station Name	Longitude	Latitude	Mean annual Perecipitation	Area of polygone	Weighted area	Weighted perecipitation
		x	y	prcp	Ai	Wi=Ai/A	Wi*Prcp
		Decimal degree	Decimal degree	mm	Km2	Unitless	mm
1	115211	39.16	7.48	3397.039554	2110	0.176672528	600.1635652
2	115212	39.16	7.92	1915.308841	1353	0.113288119	216.981735
3	113212	38.28	7.92	1822.092405	2774	0.232269949	423.2173098
4	114211	38.72	7.48	368.0794815	3431	0.287281253	105.7423345
5	114212	38.72	7.92	196.6569296	2275	0.190488152	37.46081511
					A = 11943		

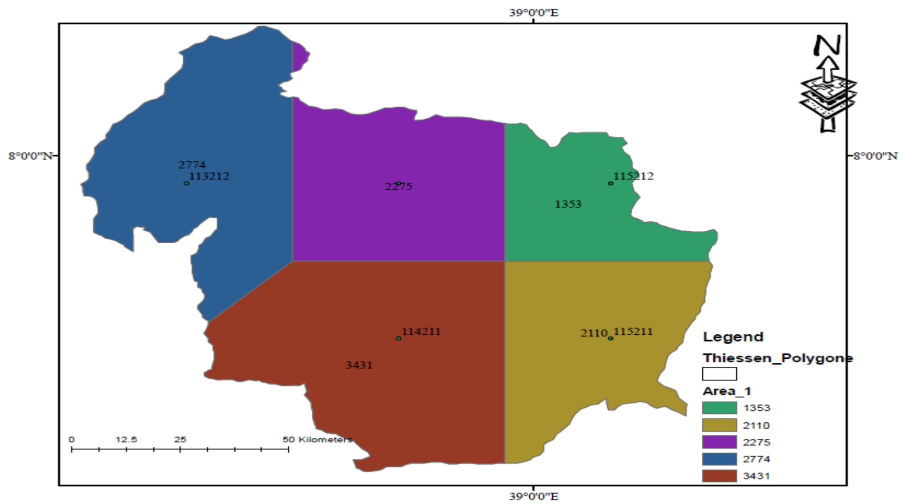

Figure 3.8 Thiessen polygon used to estimate annual mean average rainfall for grid points

3.2.2. Filling missing rainfall data

Rainfall data in the study area may have missed information in their records. Thus, it is necessary to estimate the missing rainfall to keep the continuous time series of the data. There are different methods to fill the data gap such as invers distance square method, stations average method, normal ratio method, quadrant method and so on, When the total annual rainfall at any of the "n" gauges differ from annual rainfall at the point of interest more than 10%, normal ratio method was recommended (Sajikumar and Pulikkottil 2013). In this thesis normal ratio method was used to fill missing rainfall data cause of 10% the total annual rainfall difference in each gauging stations. The general formula is given by: -

$$Px=1/n\sum_{i=1}^{n}\left(\frac{Nx}{Ni}\right)Pi \quad (3.1)$$

Where Px is the missing precipitation for any storm at the interpolation station 'x', Pi is the precipitation for the same period for the same storm at the "i^{th}" station of a group of index stations, Nx the normal annual precipitation value for the 'x' station and Ni the normal annual precipitation value for 'i^{th}' station.

3.2.3. Consistency checking of meteorological data

After all the missed rainfall data was filled, their consistency is checked by double mass curve and the homogeneity is also by Pettitt's test in XL-STAT software based on the P-value of the two hypotheses at 95% confidence interval (Pettitt's,1979).

As the computed p-value is greater than the significance level alpha=0.05 at 95% confidence interval, one cannot reject the null hypothesis H0. The measured homogeneity assures that the observations are from the same population and homogeneous (Table 3.). The use of the double-mass curve for checking the consistency of precipitation records is done by using the annual records of nine precipitation stations, designated*, Arsi Negele, Bulbula, Koshe, Langano, Tora, Ziway, Assela, Degaga and Kulamsa*.

First the annual precipitation data for each year are tabulated and then cumulated in chronological order and then plotted as showed in (Fig.3.7). The consistency of meteorological time series data was conducted to detect for any possible errors resulting from the data measurements. When the double-mass curve of precipitation data from a particular station indicates a break in slope and the reason for the break is determined, the record for one set of conditions may be adjusted to what it would have been if it had been collected under the other set of conditions.

Any sudden change in the gradient of the double-mass curve was considered to indicate inconsistency in the data. Although there were some changes at some points on the curves for some stations, it was considered insignificant for the present study.

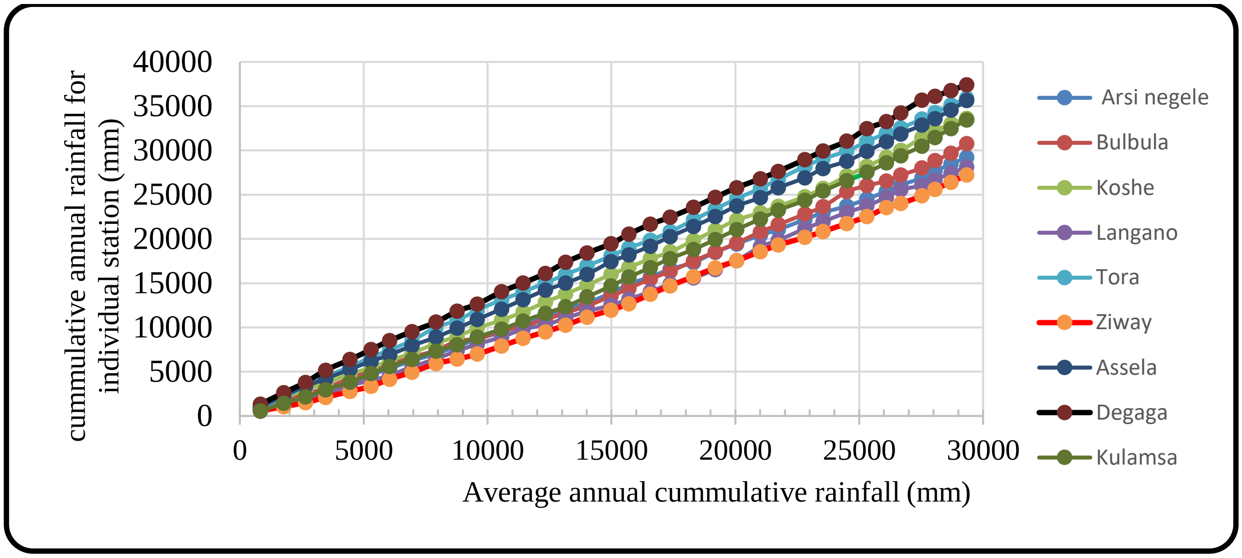

Figure 3.9. Double mass curve to check consistency for precipitation data for all meteorological station.

Table 3.6. Pettitt tests result of mean annual rainfall

S. N	Station name	K	t	p-value	alpha	Statics
1	Arsi Negele	45	18	0.842	0.05	Significant
2	Bulbula	42	19	0.763	0.05	Significant
3	Koshe	86	16	0.123	0.05	Significant
4	Langano	80	15	0.952	0.05	Significant
5	Tora	76	10	0.186	0.05	Significant
6	Ziway	61	9	0.235	0.05	Significant
7	Assela	102	10	0.874	0.05	Significant
8	Degaga	56	7	0.240	0.05	Significant
9	Kulamsa	57	8	0.681	0.05	Significant

The observed data for 1985-2019 are adjusted by multiplying observed data by the ratio of the slope of the double-mass curve for point of sudden change in the gradient of the double-mass curve to other end of graph for each station.

$P_a = \frac{b_a}{b_o} P_o$---3.2.

Were

P_a= adjusted precipitation

P_o=observed precipitation

b_a = slope of graph to which records are adjusted

b_o slope of graph at time *Po* was observed

3.3.Historical Meteorological Drought Determination Using Standardized Precipitation Index (SPI)

Globally, two indicators were most frequently applied: the Palmer Drought Severity Index (PDSI: Palmer, 1965) and the Standardized Precipitation Index (SPI: McKee et al., 1993). We selected the SPI, for it requires only precipitation data as input. The commonly used probability density functions for calculation of SPI are log-logistic, Gamma and Pearson Type 3. Long-term precipitation data is fitted to a probability distribution, which is then transformed into a normal distribution so that the mean SPI for the location and desired period is zero (Edwards and McKee, 1997) as cited (World Meteorological Organization, 1987). Positive SPI values indicate greater than median precipitation, and negative values indicate less than median precipitation. Drought, according to the SPI, starts when the SPI value is equal or below -1.0 and ends when the value becomes positive. Gamma distribution is defined by its frequency or probability function as in Guttman (1999).

H(x) = q + (1 - q) G(x)---3.3.

Where;

H(x) = Cumulative probability

q = probability of zero rainfall

When *m* was taken as the number of zero entries in the time series rainfall data, then the *q* value was estimated by the ratio. n/m. The probability of zero precipitation is given as q, and G (x) is the gamma function's cumulative probability. The cumulative probability H (x) is then converted to the standard normal distribution (z) using the mean of zeros and the variance of one, and the result is SPI according to McKee (1993) then (Table 2.1) used to define drought. Based on the SPI methodology described above, SPI was calculated using RStudio software for all meteorological station of Central rift valley from 1985 to 2019. This step was carried out using approximate transformation functions adapted from(Mishra and Desai, 2006). These functions given in Equations (3.4) and (3.5) are expressed as:

$$SPI = -\left(K - \frac{C_O + C_1K + C_2K^2}{1 + d_1K + d_2K^2 + d_3K^3}\right) \text{ for } 0 < H(x) \leq 0.5 \text{-----------------------} 3.4.$$

$$SPI = +\left(K - \frac{C_O + C_1K + C_2K^2}{1 + d_1K + d_2K^2 + d_3K^3}\right) \text{ for } 0 < H(x) \leq 1 \text{-------------------------} 3.5.$$

In this study, SPI values were produced for each month of the year as well as to SPI3, SPI6, and SPI12 using Rstudio software. The calculation of SPI index in RStudio Program requires input data, as can be seen in (Table 3.) bellow. Data can be imported directly from MS Excel files, manually or automatically.

Table 3.7. Sample of input data format for RStudio software (for Arsi Negele station)

Year	Month	Rainfall(mm)
1985	1	10.92
1985	2	46.9
1985	3	69.1
.	.	71.6
.	.	92.1
1985	12	89.8
1986	1	66.5
1986	2	81.0
1986	3	75.7
. . . 2019	. . . 12	. . . The last data

After determining all values of SPI according to (McKee et al., 1993) drought events classified in seven magnitude classes, i.e., if SPI ranges between 1.5 and 1.99, it is very wet; 1.00 and 1.49, it is moderate wet; -0.99 and 0.99, it is near normal; -1.00 and -1.49, it is moderately dry; -1.5 and -1.99 severely dry and extreme drought if SPI is -2.00 or less as well as extremely wet if SPI greater than 2 according to McKee (1993). To assess the spatial extent of droughts in the study area, SPI3 time series values of each meteorological station have been interpolated by inverse distance weighted (IDW) method using the Spatial Analyst tool of ArcGIS. The interpolated maps are reclassified into different drought severity classes.

3.3.1. Characterizing SPI in terms of drought duration, severity and intensity

A drought index is main variable in order to assess the effect of a drought and to determine various drought characteristics, such as duration, intensity and severity(Thomas B. McKee, 1993). In this research, used meteorological drought indicator is SPI and calculated for the different time scale, 3-month, 6 month and 12 months. Fig. 3.7, (for Arsi Negele station) is used to define drought characteristics. The negative and positive values of SPI are considered as the drought and non-drought event. As drought is defined when the values of SPI fall below zero, a drought event is considered a period with negative SPI values. In order to measure length of drought duration and magnitude of drought severity, a threshold value must be defined. The drought duration (D) is the period length in which the SPI is continuous negative, started from the SPI values is equal to -1 and ends when the SPI values turn out to be positive. Severity score is computed as the sum of the differences, in absolute values, between the indicator values and the threshold (if the value is above the threshold but below the mean it is not counted). The drought severity (S) of any drought period starting at the ith month is defined as (Aksoy *et al.*, 2018): $S = \sum_{i=1}^{D} |-SPIi|$ and intensity of drought is the ratio of severity of drought to its duration.

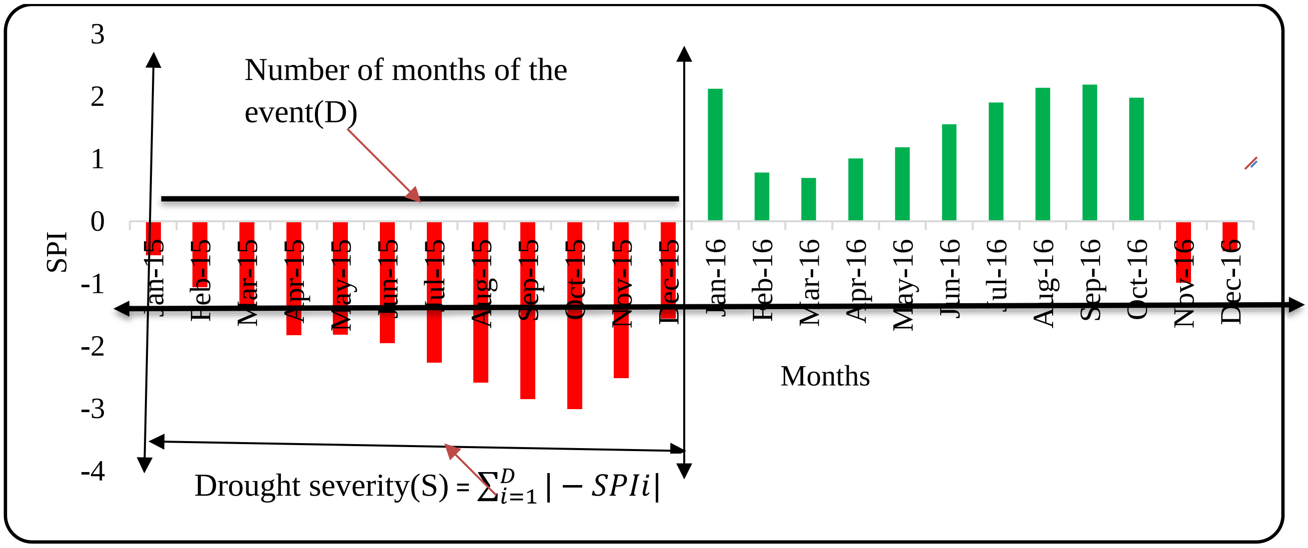

Figure 3.10. Severity S and duration D of a drought event quantified with drought index SPI

Drought durations are selected from 3,6 and 12 months in severity calculation. For each drought duration severities are determined. As expected, drought may not be observed for the selected drought periods for any year which means severity value is zero for selected duration in that year.

3.4. Non-parametric Trend Analysis of Historical Meteorological Drought

The Mann–Kendall (MK) (non-parametric) test is usually used to detect an upward trend or downward (i.e., monotonic trends) in a series of hydrological data (climate data) and environmental data. The null hypothesis for this test indicates no trend, whereas the alternative hypothesis indicates a trend in the two-sided test or a one-sided test as an upward trend or downward trend (Pohlert, 2020). Non-parametric statistics are usually much less affected by the presence of outliers and other forms of non-normality (Yadav *et al.*, 2014) and represent a measure of monotonic linear dependence according to (Davis 1986; Rossi et al., 1992) as cited by (Yadav et al., 2014).

The most frequently used non-parametric test for identifying trends in hydrologic variables is the Mann Kendall (MK) test. The statistical significance trend detected using a non-parametric model such as the Mann-Kendall (MK) test can be complemented with Sen's slope estimation to determine the magnitude of the trend. Mann Kendall program used to test current and future drought trend at annual, seasonal and monthly time scales as well as to detect climate change for Arsi Negele, Degaga, Bulbula, Koshe, Ziway, Assela, Tora, Langano and Kulamsa stations which are located in the study area. The first step is to determine the sign of the difference between consecutive sample results. Sgn (Xj - Xk) is an indicator function that results in the values 1, 0, or –1 according to the sign of (Xj – Xk) where j > k, the function is calculated as:

$$S = \sum_{i=0}^{n} * \sum_{j=k+1}^{n} sgn(Xj - Xk) \text{---------------------------------------} 3.6.$$

$$sgn(Xj\text{-}Xk) = \begin{cases} +1, \text{if}(Xj\text{-}Xk)>0 \\ 0, \text{ if } (Xj\text{-}Xk) = 0 \\ -1, \text{ if } (Xj\text{-}Xk) < 0 \end{cases} \text{---} 3.7.$$

Where Xj and Xk are the sequential precipitation or temperature values in months j and k (j > k) respectively whereas; A positive value is an indicator of increasing(upward) trend and a negative value is an indicator of decreasing (downward) trend. The slope of a linear trend is estimated with the nonparametric Sen's slope estimator's method according to (Gilbert, 1987) as cited by (Gemechu *et al.*, 2015). It is the best method to detect trend because it is not affected by outliers and missing data according to (Stern et al., 2006) as cited by (Gemechu *et al.*, 2015). The slope of n pairs of data points was estimated using the Sen's estimator is calculated as:

$$Qi = \frac{Xj-Xk}{j-k} for\ i = 1 \ldots. N \text{--}3.8.$$

Where, Xj and Xk are data values at times j and k, (j>k) respectively. The median of these N values of Q_i is Sen's estimator of slope. The positive slope Qi obtained shows an increasing/upward trend whereas the negative slope Qi obtained shows a decreasing/downward trend. But, if the slope is zero there is no trend other than things remain the same(Alemu and Dioha, 2020) . The presence of a statistically significant trend is evaluated using the Z value. To decide whether the null hypothesis is to be accepted or rejected, a test statistic is computed and compared with a critical value obtained from a set of statistical tables. Ho is rejected if the absolute value of Z is greater than Z1- α/2 and then the trend is considered as significant, where Z_1- α/2 is obtained from the standard normal distribution (Agbo and Ekpo, 2021). The standardized test static for the Mann–Kendall test (Z) can be calculated, as

$$Z=\begin{cases} \frac{S-1}{\sqrt{Var(S)}}\ when\ S > 0 \\ 0\ \ when\ S = 0 \\ \frac{S+1}{Var(S)}\ when\ S < 0 \end{cases} \text{---}3.9.$$

We need to calculate the variance of S „VAR (S) (Yadav *et al.*, 2014)

$$VAR(S) = 1/18\left[n(n-1)(2n+5) - \sum_{p=1}^{g} tp(tp-1)(2tp+5)\right] \text{----------------------}3.10.$$

The equation takes into account the several tied values (equal values); n is the number of data values, g here is representing the number of these equal trend values or groups, t_p represents the number of data values in the P^{th} group(Alemu and Dioha, 2020).The sign of Z indicates the direction of the trend(Abdourahamane and Acar, 2018). The negative value of Z indicates a decreasing trend and vice versa. At the 5% significance level, the null hypothesis of no trend is rejected if the absolute value of Z is higher than 1.645.

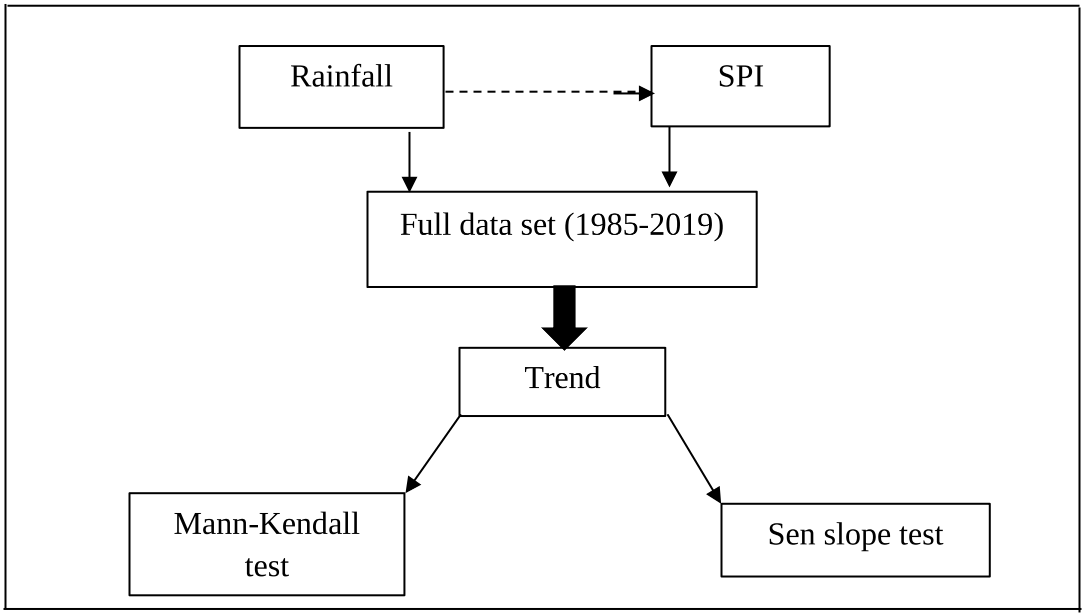

Figure 3.11. Drought trend analysis framework

3.4.1. Innovative trend analysis (ITA) of historical meteorological drought

The concept of ITA was initially proposed by ¸Sen (Ali et al., 2019) for the detection of trends in time series. In this method, data are equally divided into two segments between first dates to the last date. Both segments are arranged in ascending order and presented in the X and Y-axis The first segment (Xi: i =1, 2, 3…, n/2 is presented in the horizontal axis while the second segment (Xj: j = n/2 + 1, n/2 + 2 …, n) is presented in vertical axis in the Cartesian coordinate system. A bisector line at 1:1 (45°) divides the diagram into two equal triangles (Figure 3.9). The upper triangle represents an increasing trend, while a lower one indicates a decreasing trend. For the estimation of the trend, the SITA statistic is computed as follows according to (Khan et al.,2018) as cited by (Ali et al., 2019).

$$SITA = \frac{2(\mathrm{Xmi} - \mathrm{Xmj})}{\mathrm{n}} \ldots\ldots\ldots\ldots\ldots\ldots\ldots\ldots\ldots\ldots\ldots\ldots\ldots\ldots\ldots\ldots\ldots\ldots\ldots\ldots\ldots\ldots\ldots\ldots\ldots\ldots 3.11$$

Where SITA is the slope base on the ITA method, n is the sample size, Xmi and Xmj are the mean value of the first and second half of the series respectively.

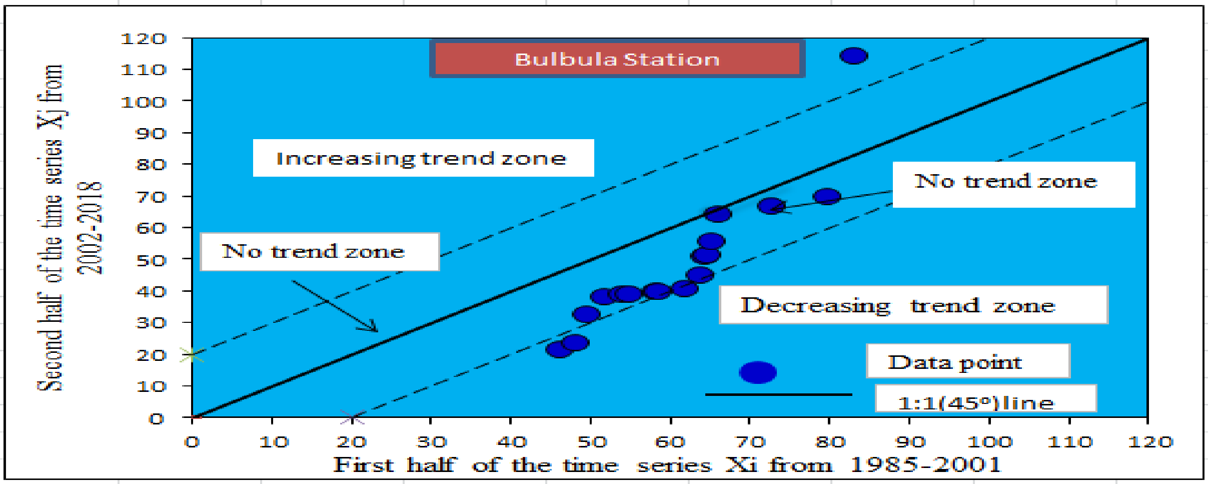

Figure 3.12. Innovative trend analysis method (Bulbula Station)

3.5. Projected Meteorological Drought Determination Using Standardized Precipitation Index (SPI) by Using Projected Climate Data Under Representative Concentration Pathway (RCP4.5 and RCP8.5) Scenario

Statistically downscaled daily base rainfall climate data for the period 2020-2100 obtained from HadGEM2-ES United Kingdom Met office Hadley center (Collins et al., 2011) climate model of coordinated regional climate downscaling Experiment (CORDEX) under Africa database of CMIP5 used to derive indicators related to future change in climate.

After obtaining future climatic data bias correction were done to minimize the discrepancy between observed and simulated climate variables on a daily time step (Fig. 3.10). Bias correction procedures are used to minimize the discrepancy between observed and simulated climate variables on a daily time step. CMhyd (Climate Model data for hydrologic modeling) is a tool that can be used to extract and bias-correct data obtained from global and regional climate models.

Numerous parameters are available for analyzing, the only parameter considered for analyzing the meteorological drought in the case of this thesis is precipitation data. The projected variables formed the basis to compute the SPI (at 3, 6 and 12-month accumulation scales) over the period 2020-2100 by using RStudio software. SPI calculation begins by selecting a suitable probability density function to describe the precipitation data (Cacciamani et al., 2007). The cumulative probability of an observed precipitation amount is computed after an appropriate density function is chosen. The inverse normal (Gaussian) function is then applied to the probability(Belayneh *et al.*, 2014).

The approach focuses on the estimating future meteorological drought projected to change in the near future period (2020-2049), mid future (2050-2079) and in the far future (2080-2100) according to Komala Dhanapal Sagadevan Eng and Tech, (2017) and (Kwak *et al.*, 2016).

This thesis done based on representative concentration pathway of (RCP4.5) and (RCP8.5) scenario. After determining all values of SPI, according to (McKee et al., 1993) drought events classified in seven magnitude classes, i.e., if SPI ranges between 1.5 and 1.99, it is very wet; 1.00 and 1.49, it is moderate wet; -0.99 and 0.99, it is near normal; -1.00 and -1.49, it is moderately dry; -1.5 and -1.99 severely dry and extreme drought if SPI is -2.00 or less as well as extremely wet if SPI greater than two.

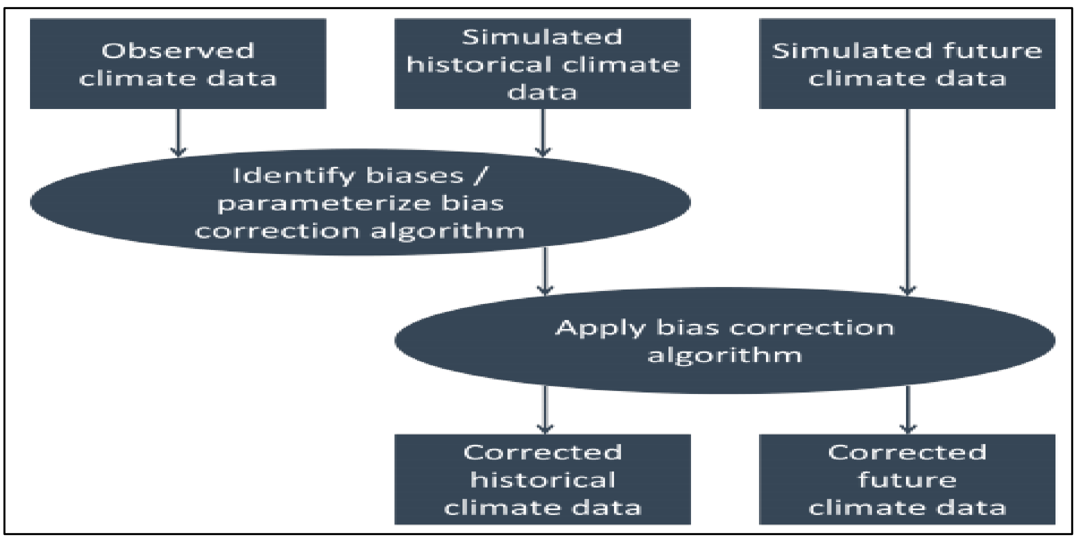

Figure 3.13. Bias correction frameworks

4. RESULTS AND DISCUSSION

4.1. Historical Meteorological Drought Using Standardized Precipitation Index (SPI)

Drought was measured by the SPI, which involves relatively simple calculations and data requirements. Drought was defined as SPI≤−1.0 detailed in section 3.3. In the present study, SPI and trend analysis of meteorological data in CRV presented individually for each selected station. The SPI1 and SPI3 for all meteorological station is shown in the following panels.

1) Arsi Negele station SPI1, SPI3 and areal SPI

Drought index SPI was applied to all 9 meteorological stations and areal rainfall of Central Rift Valley covering 1- month and 3-month, time scales. In this study the historical period climatic condition is analyzed based on meteorological station records (1985-2019) of the study area. All results of standard precipitation indexes (SPI1 and SPI3) for wettest and driest periods to all meteorological station were tabulated in Appendix 1 section. The below panels depict the drought events for 3-month time scales and monthly time scale results.

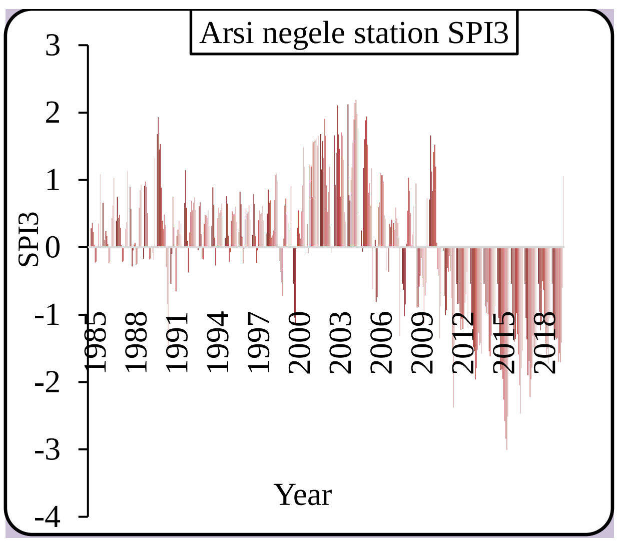

a).

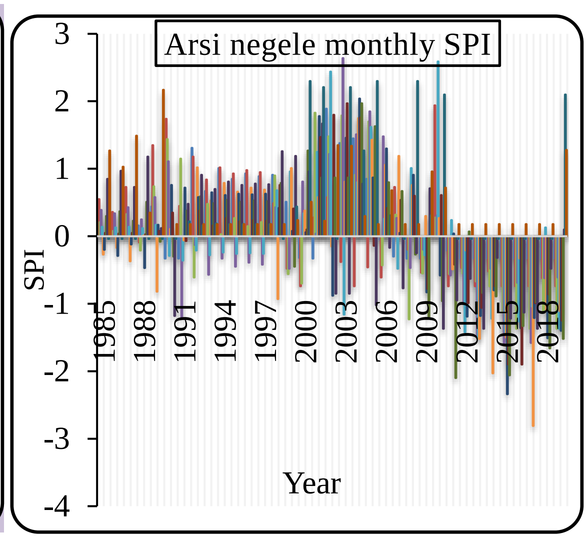

b).

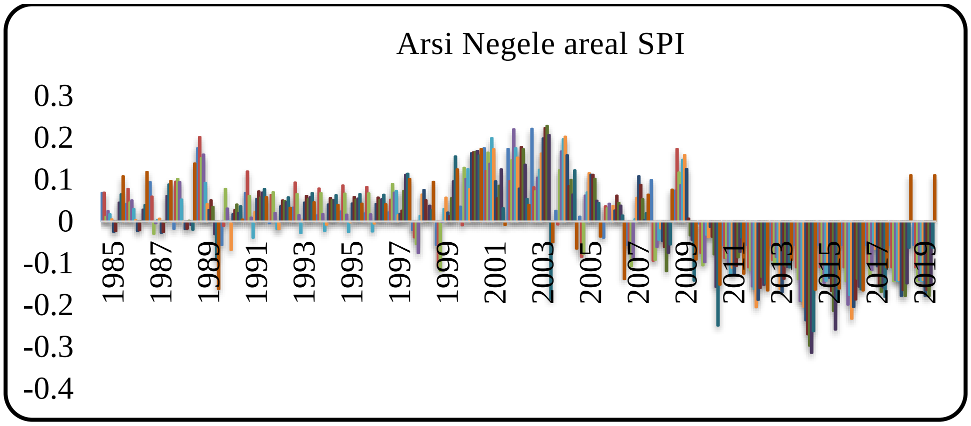

c)

Figure 4.1. Drought events identified using SPI for Arsi negele meteorological station with (a) 3-month time scale (b) monthly time scale and (c) areal SPI.

As indicated in fig. 4.1 the SPI value obtained in Arsi Negele showed an extreme drought during 2015, 2017 in October, and Jun months for SPI3, and SPI1 value respectively which where, -3.01 and -2.81 according to McKee (1993) drought classification. Also, there were notable, SPI value was obtained in 2013 and 1991, which were -1.79 and -1.73 considered to be severely dry condition. Also, there were also the condition of moderately dry and near normal condition was also identified for long period of time.

2) Assela station SPI1, SPI13 and areal SPI results

The SPI value obtained in Assela meteorological station showed maximum drought during 1991 and 1991 in November and September months for SPI3 and monthly SPI value respectively were -3.32 and -3.13 which were considered to be a situation of extreme drought. Additionally severe drought condition was observed in (2017 = -1.69 and (2012 = -1.83) for SPI3 and SPI1 respectively.

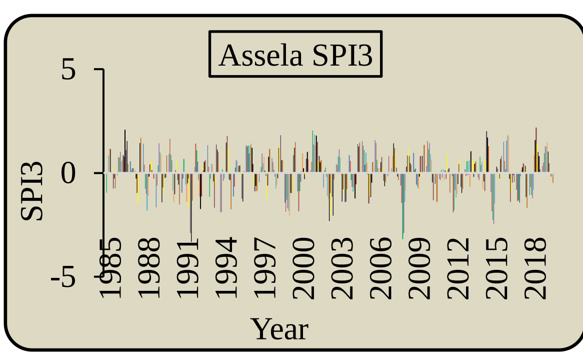

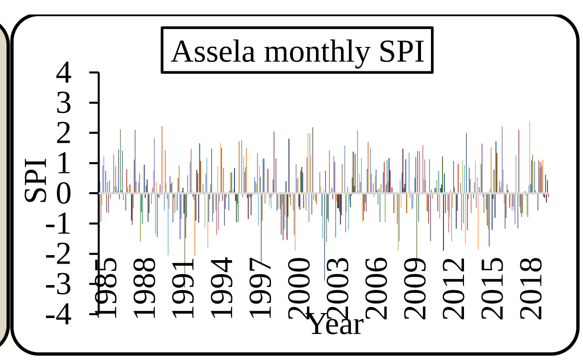

a). b).

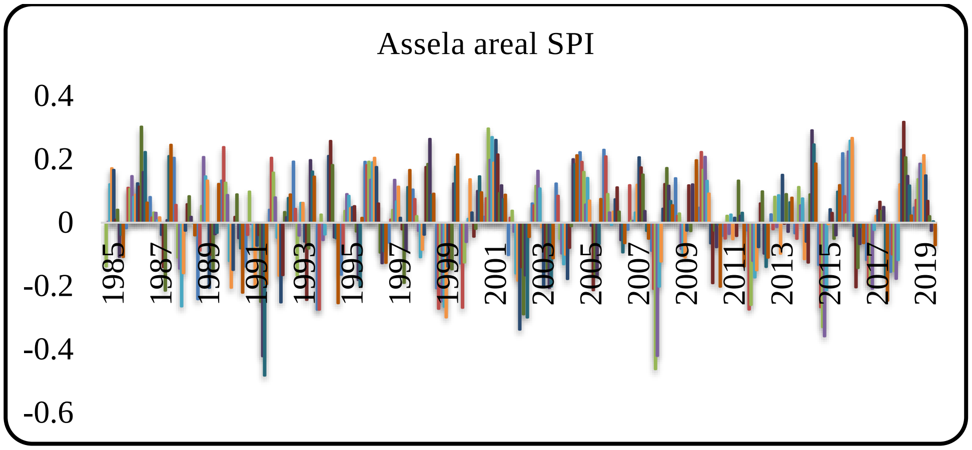

c)

Figure 4.2. Drought events identified using SPI for Assela meteorological station with (a) 3-month time scale, (b) monthly time scale (c) areal SPI.

3) Bulbula station SPI1, SPI3 and areal SPI results

Standardized precipitation index values during 2014 and 2016 at July and August months for SPI3 and monthly SPI value respectively were -3.42 and -2.73 which were considered to be a situation of extreme drought. Bulbula station in bellow panel of Fig. 4.3 the SPI1 in (April, August, July May and September in 2009, 1991, 1985, 2004 and 20016 respectively) showed that, there were severely dry. Also results indicate sever and moderate drought for SPI3 in (Jan/1994), (Apr/2008), (Nov/2016) and (Oct/1991), (Jul/1999 and 2004).

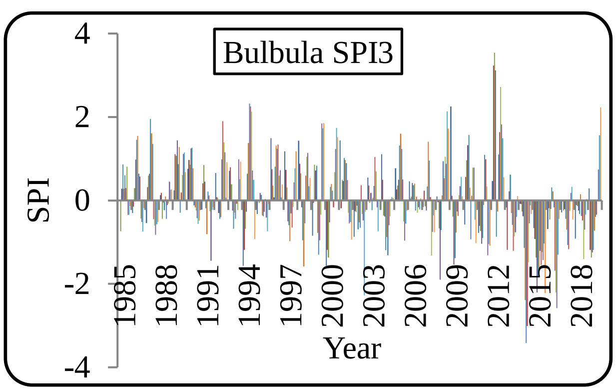

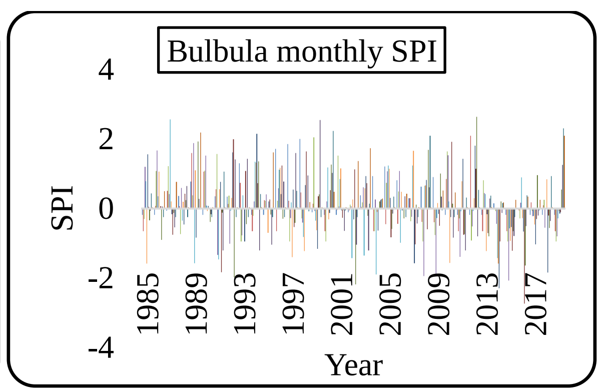

a). b).

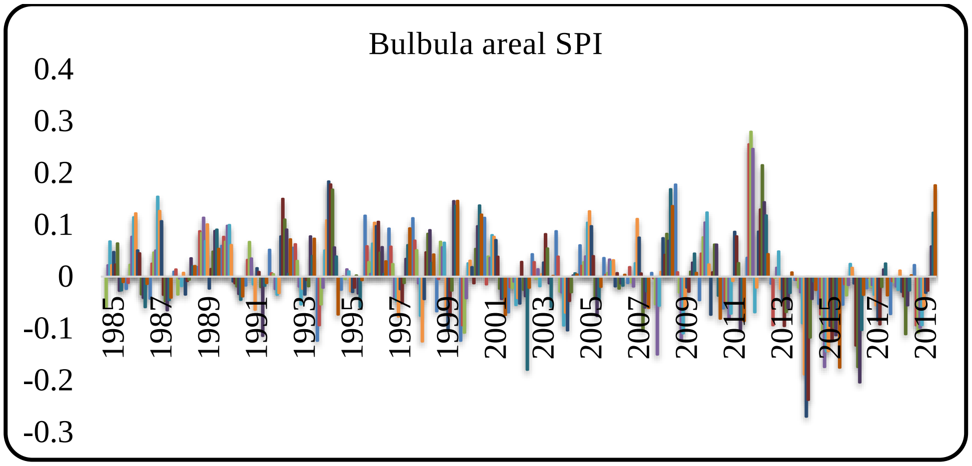

c)

Figure 4.3. Drought events identified using SPI for Bulbula meteorological station with (a) 3-month time scale, (b) monthly and (c) areal SPI time scale.

4) Degaga station SPI1, SPI3 and areal SPI results

The SPI value greater than negative two meaning that, very or extremely dry years in 2018,2017,2018 and 2019 at September, December, march and September months for SPI3, SPI6, SPI12 and monthly SPI value respectively which had -3.33, -3.3, -4.42 and -2.56 index value.

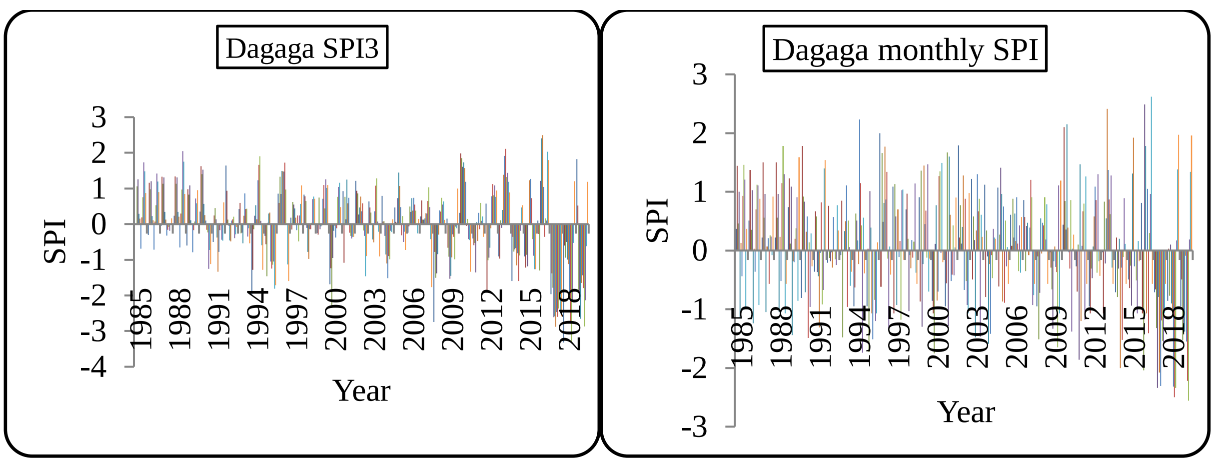

a). b).

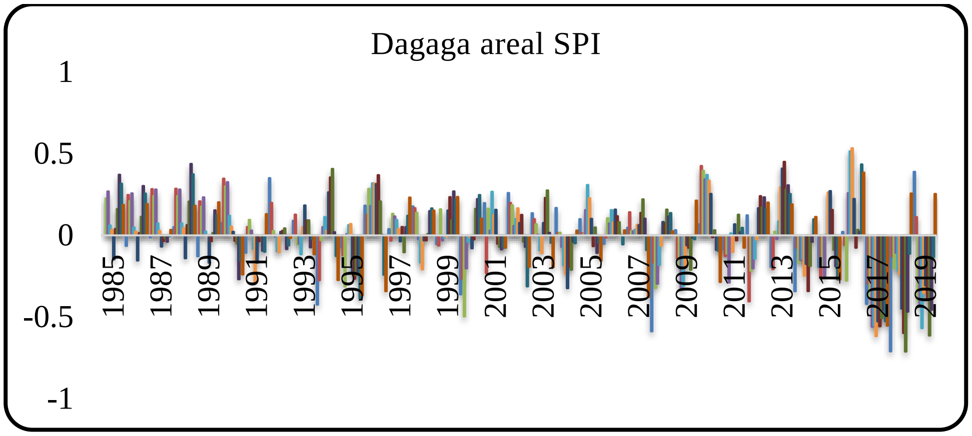

Figure 4.4. Drought events identified using SPI for Dagaga meteorological station with (a) 3-month time scale ,(b) monthly time scale and (c)areal SPI.

5) Koshe station SPI1, SPI3 and areal SPI results

For Koshe meteorological station as indicated in fig. 4.5 the maximum drought obtained in year 2019 for all time scale in July, November, December and July months for SPI3 and monthly SPI value respectively were -3.7 and -3.25 which were considered to be a situation of extreme.

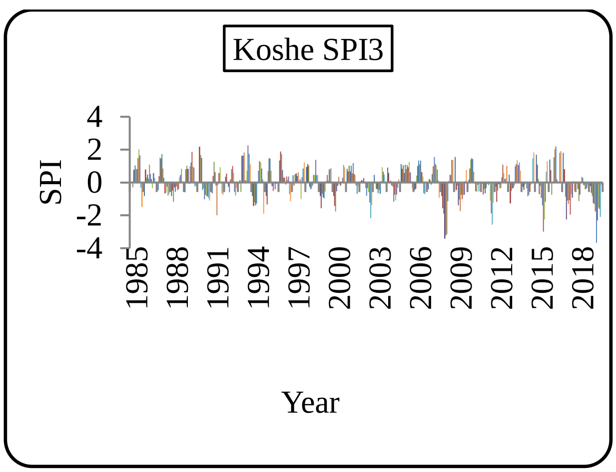

a).

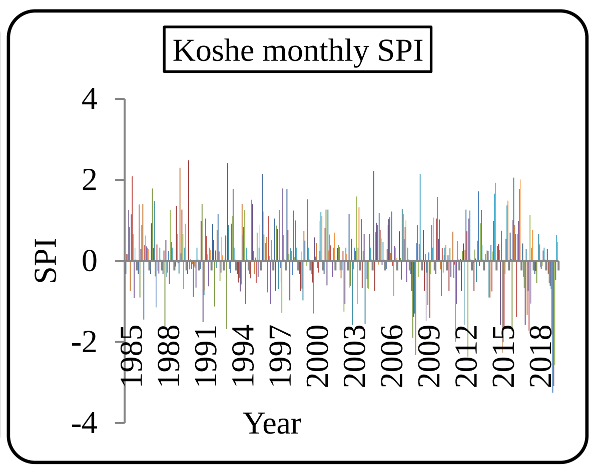

b).

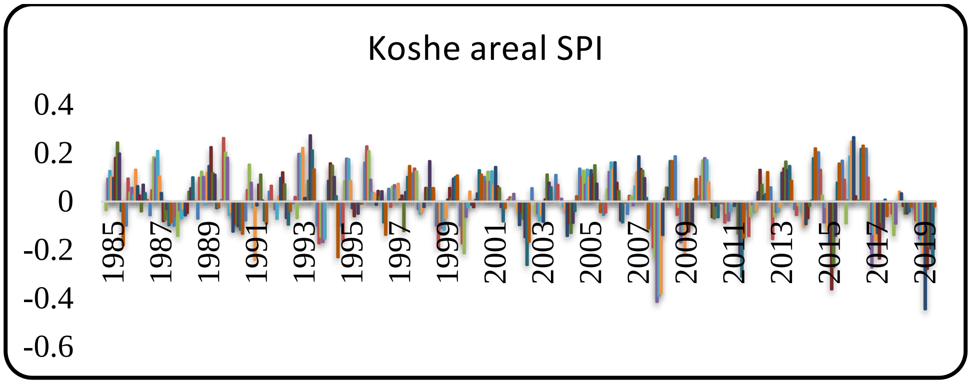

c)

Figure 4.5. Drought events identified using SPI for Koshe meteorological station with (a) 3-month time scale , (b) monthly time scale and (c) areal SPI.

6) Kulmsa station SPI1, SPI3 and areal SPI results

For Kulumsa meteorological station as indicated in fig. 4.6 the maximum drought obtained in year 2000 and 2008 for all time scale in march and march months for SPI3 and monthly SPI value respectively were -4.83 and -2.96 which were considered to be a situation of extreme drought.

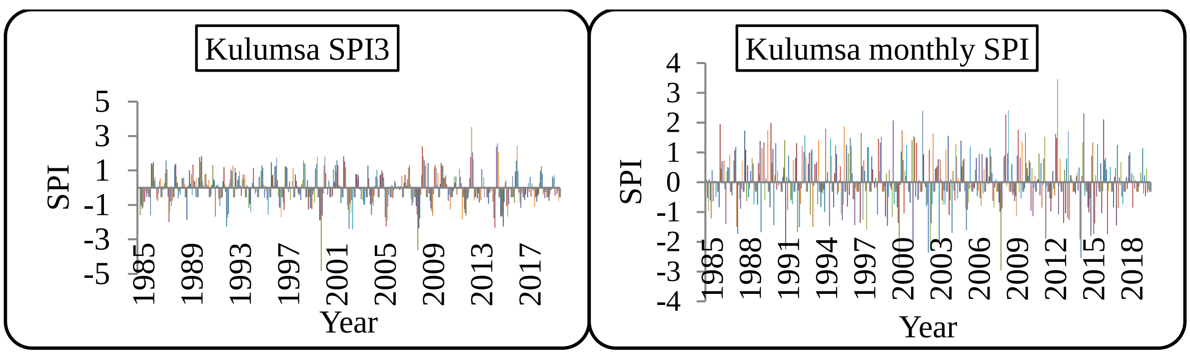

a). b).

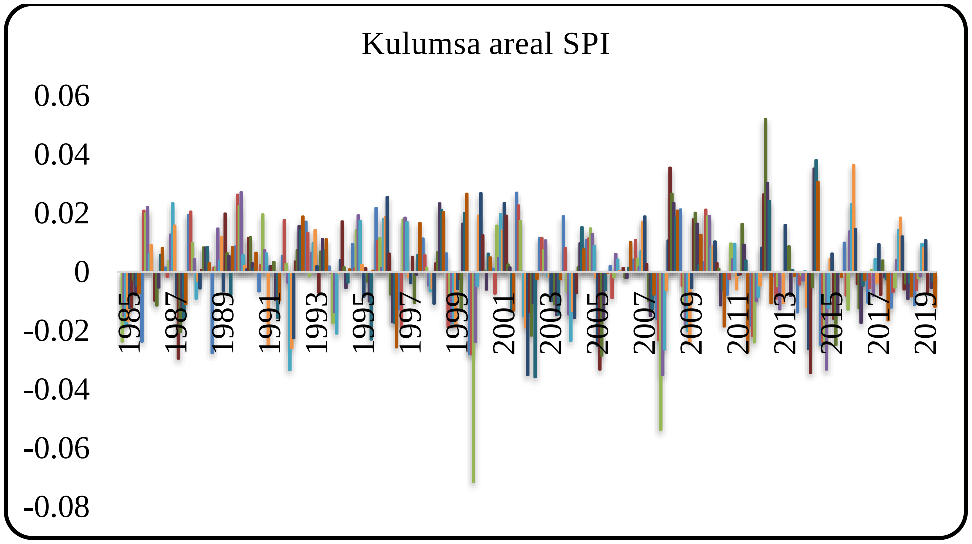

c)

Figure 4.6. Drought events identified using SPI for Kulumsa meteorological station with (a) 3-month time scale , (b) monthly time scale and areal SPI.

7) Langano station SPI1, SPI3 and (c) areal SPI results

For Langano meteorological station as indicated in fig. 4.7 the maximum drought obtained in year 1991 and 1991 at Jun and April months for SPI3 and monthly SPI. SPI values were -3.43, and -3.15 respectively, which were considered to be a situation of extreme based on table 2.1 drought classification.

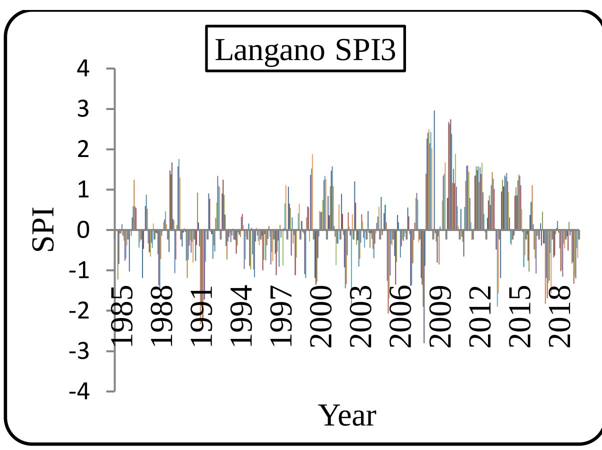

a).

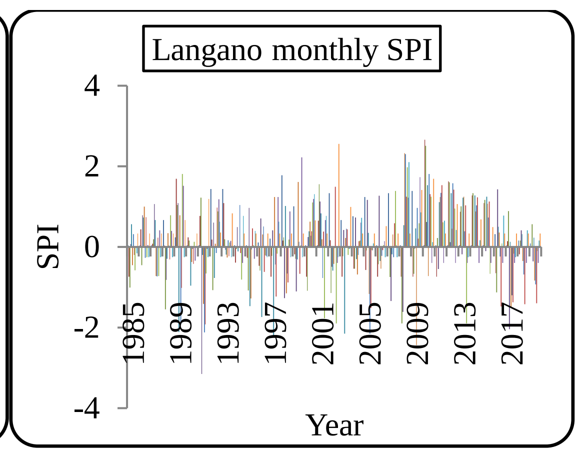

b).

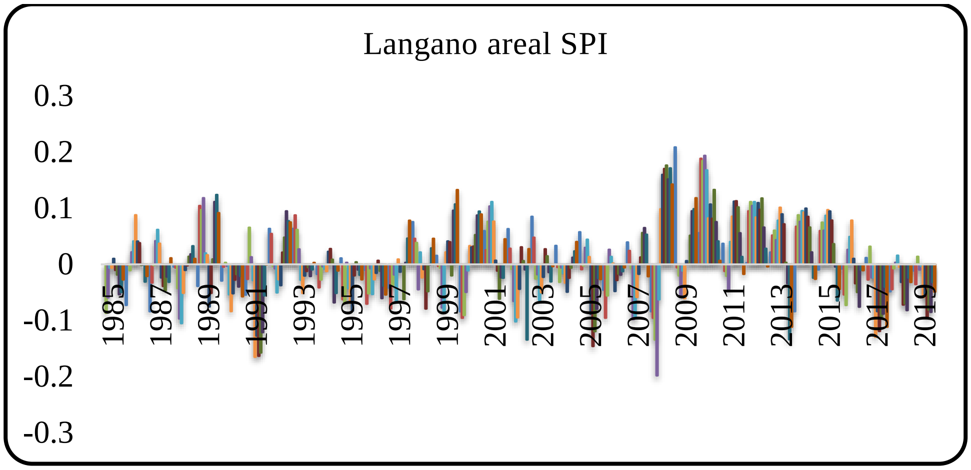

c)

Figure 4.7. Drought events identified using SPI for Langano meteorological station with (a) 3-month time scale (b) monthly time scale and (c) areal SPI

8) Tora station SPI1, SPI3 and areal SPI results

The maximum drought obtained in year 2000 and 2000 at march and march months for SPI3, and monthly SPI. SPI values for all listed time series were -4.5 and -2.83 respectively, which were considered to be a situation of extreme drought at this year.

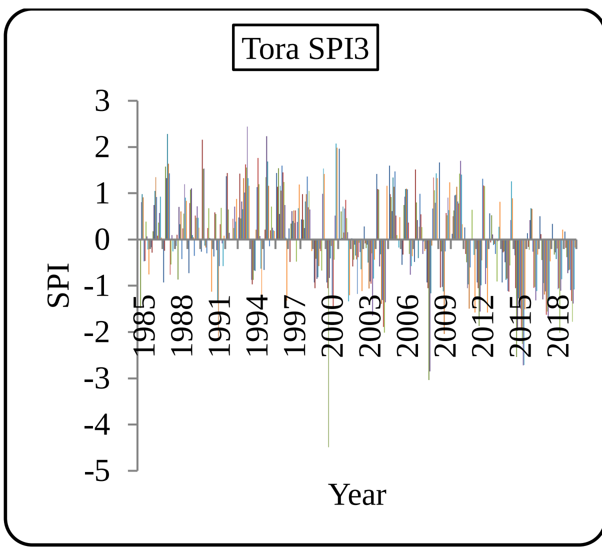

a).

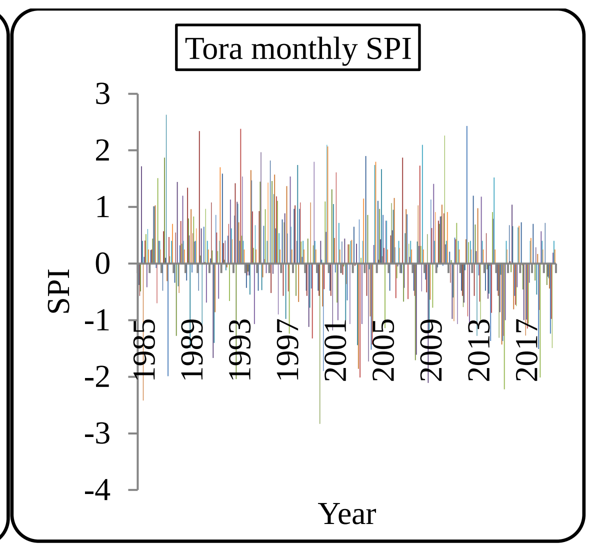

b).

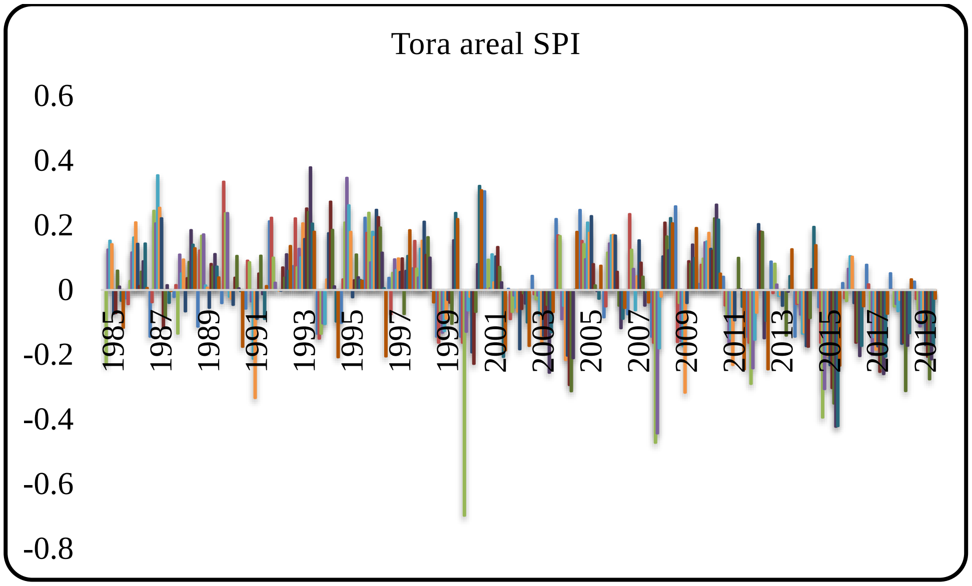

c)

Figure 4.8. Drought events identified using SPI for Tora meteorological station with (a) 3-month time scale, (b) monthly time scale and (c) areal SPI.

9) Ziway station SPI1, SPI13 and areal SPI results

For Ziway meteorological station as indicated in fig. 4.9 the maximum drought obtained in year 1989 and 2017 at July and September months for SPI3 and monthly SPI value respectively were -3.47 and -3.53 which were considered to be a situation of extreme drought. Also results indicate that severely, moderately and near normal drought condition according to McK., (1993).

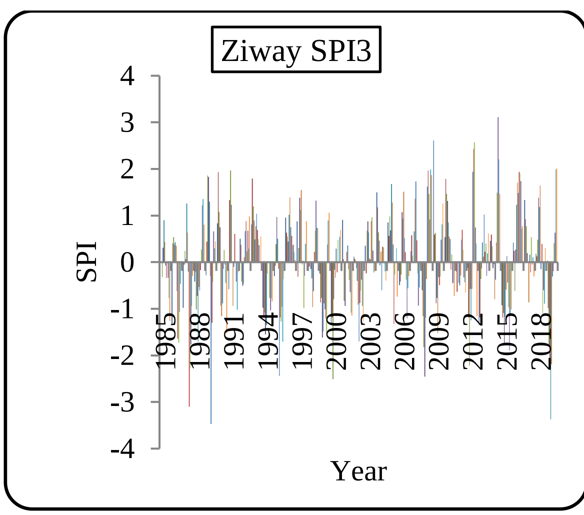

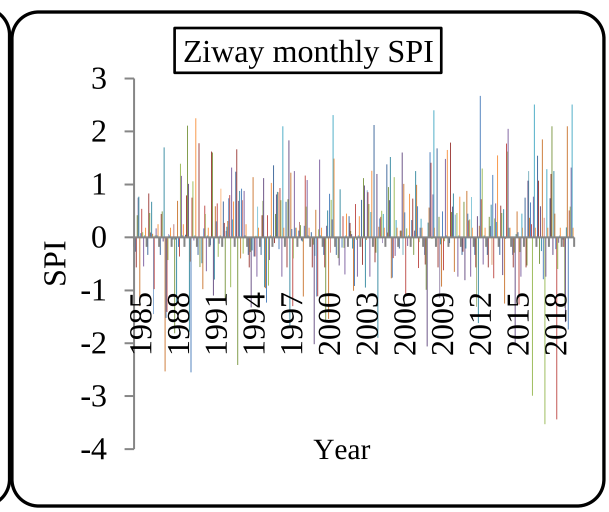

a). b).

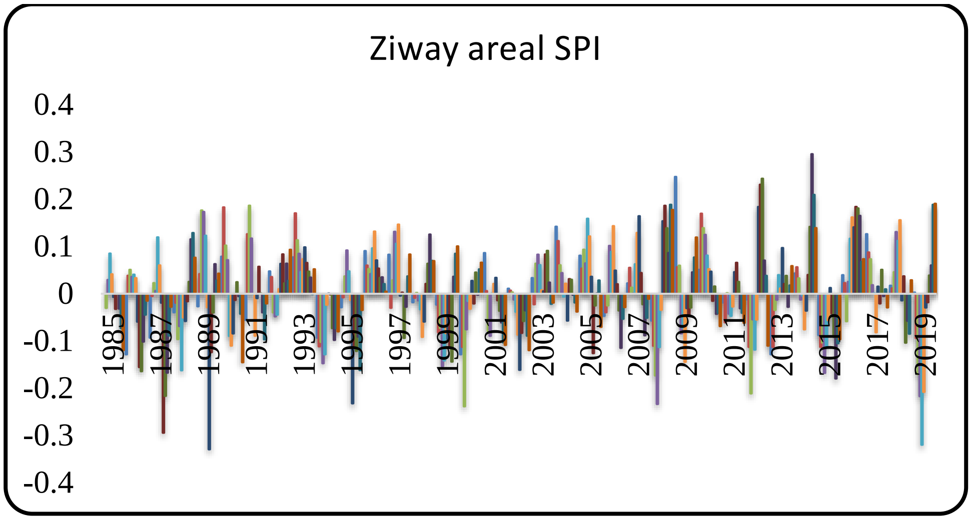

c)

Figure 4.9. Drought events identified using SPI for Ziway meteorological station with (a) 3-month time scale, (b) monthly time scale and (c) areal SPI

4.1.1. Characterizing SPI in terms of drought duration, severity and intensity

In this study, drought characteristics (duration, severity, and intensity) were analyzed using standardized precipitation index (SPI). The SPI series were computed for 9 meteorological stations in Central Rift Valley of Ethiopia from January 1985 to December 2019 at 3-month time scale to study the characteristics of drought. (Table 4.1) shows drought events occurred at different time scale during the study period.

The value of SPI-3 showed that 48 to 83, drought events occurred during 1985-2019, and most of the droughts recorded in Arsi Negele station followed by Ziway, Tora, Kulmsa, Assela, Degaga, Koshe, Bulbula and Langano. Results of SPI-3, calculation, obtained maximum duration of each station, these values were presented under section 4.1 above for each meteorological station, Feb-Dec/2015, Jan-Dec/2015 and Jan-Dec/2017 or very short until short duration for Arsi Negele station, Sep-Dec/1991, Apr-Sep/1999 and May-Dec/2012 for Assela station, Mar-Dec/2015, Mar-Dec/2015 and Jan-Dec/2016 for Bulbula station, Jan-Dec/2017, Jan-Dec/2018 and Jan-Dec/2018 for Dagaga station, Feb-Jul/2008, Jul-Dec/2017 and Jan-Aug/2003 for Koshe station, Jan-May/2008, Jan-Jun/2008 and Mar-Sep/2004 for Kulmsa station, Jun-Oct/1991, Jul-Dec/1991 and Jun-Dec/2017 for Langano station, Feb- Dec/2015, Mar-Dec/2015 and Feb-Dec/2015 for Tora station, at selected time series respectively.

Table 4.1. The numbers of drought events for meteorological station

Station	SPI3	Monthly SPI
Arsi negele	86	87
Bulbula	47	52
Koshe	54	55
Langano	46	42
Tora	65	60
Ziway	59	71
Assela	68	58
Degaga	65	62
Kulmsa	63	63
TOTAL	**564**	**550**

Table 4.2. Drought properties based on the SPI3(category for SPI according to (Table Table 2.1)

Station	Number of drought events			Max. intensity	Year of max. intensity
	moderate	severe	extreme		
Arsi negele	50	27	9	-3.01	2015(Oct.)
Bulbula	31	9	7	-3.42	2015(Apr.)
Koshe	31	12	11	-3.7	2019(Jul.)
Langano	34	8	4	-3.43	1991(Jun.)
Tora	43	12	10	-2.5	2000(Mar.)
Ziway	34	15	10	-3.8	1989(Jul.)
Assela	43	17	8	-3.32	2002(Jul.)
Degaga	29	17	19	-3.33	2018(Sep.)
Kulmsa	30	24	9	-3.3	2000(Mar.)
Total	**325**	**141**	**87**		

Table 4.3. Summary of SPI with longest duration and severity for each station

Station Name	Time scale	Year	Duration in (months)	Severity
Arsi negele	SPI3	2015	11	-22.70
	SPI1	2015	9	-20.70
Bulbula	SPI3	2015	10	-15.90
	SPI1	2013	11	-19.50
Koshe	SPI3	2008	6	-14.40
	SPI1	2001	6	-8.3
Langano	SPI3	1991	5	-10.46
	SPI1	2017	5	-6.75
Tora	SPI3	2015	11	-20.78
	SPI1	2015	7	-11.3
Ziway	SPI3	2015	4	-5.22
	SPI1	1991	8	-10.8
Assela	SPI3	1991	4	-9.28
	SPI1	2011	5	-6.2
Degaga	SPI3	2017	12	-27.80
	SPI1	2015	9	-16.6
Kulmsa	SPI3	2008	5	-10.41
	SPI1	2000	7	-11.56

The year 2015 had the worst droughts over Southern, central and western part of Central Rift Valley of Ethiopia. Similarly, (Ethiopian Panel on Climate Change, 20150) support our findings by mentioning that drought in 2015 and 2011 is one of the most severe droughts in the Horn of Africa. The result showed that among the extreme droughts that happened at Southern, central and western part of study area, in 1989 was the most severe drought with peak negative SPI-3 value −3.8 in Ziway station; followed by extreme drought which occurred in Koshe with SPI-3 value -3.7.

Table 4.4. Non-drought year and a drought year according to SPI3 values to each meteorological station

	Good year/non drought year/						Drought year					
Name	Sep	Oct	Nov	Dec	Jan	Feb	Sep	Oct	Nov	Dec	Jan	Feb
Arsi Negelle	2.2	2.1	1.8	0.5	2.1	0.8	-2.8	-3.0	-2.5	-1.6	-0.5	-1.0
Year	2004						2015					
Bulbula	2.7	1.8	1.5	0.6	0.5	3.2	-1.2	-1.4	-1.0	-2.2	-0.7	-0.9
Year	2012						2015					
Koshe	0.0	0.0	1.8	1.9	1.4	0.7	-1.5	-1.6	-2.1	-0.2	-0.2	-0.6
Year	2016						2019					
Langano	1.9	1.1	0.6	0.1	0.8	2.7	-2.2	-1.7	-0.8	0.0	-0.8	-0.4
Year	2010						1991					
Tora	1.6	2.4	1.3	1.2	0.5	1.4	-2.3	-2.7	-2.7	-1.5	-0.3	-1.0
Year	1993						2015					
Ziway	1.9	1.7	0.7	0.8	0.4	0.2	-1.0	-2.1	-1.1	-1.0	-1	-1.2
Year	2016						2015					
Assela	0.6	0.8	0.5	0.6	0.1	0.5	-1.7	-2.9	-3.3	-1.3	-1.0	-0.3
Year	2001						1991					
Degaga	1.0	2.1	1.7	0.8	0.2	1.3	-2.4	-2.1	-2.5	-2.6	-2.0	-1.4
Year	1988						2017					
Kulumsa	1.1	0.2	0.1	0.4	0.6	1.8	-1.7	-0.9	0.0	-0.1	-1.7	-1.6
Year	1990						2015					

SPI3 values for drought years and non-drought years have been presented in (Table 4.4) to show the pattern of SPI during these years. Results showed that 2015, 2019, 1991 and 2017 during September – February was drought year, whereas 2004, 2012, 2016, 2010, 2001, 1988 and 1990 was wet year.

It can be seen that during the drought years of 2015, the SPI3 values for Arsi Negele station in September, October and November, for Bulbula station in December, for Tora station, in September, October and December and for Ziway station, in October shows the condition of extremely drought as well as for Kulmsa stations severely dry condition observed in September, January and February. In 1991 at Langano station in September month and at Assela stations in October and November months the SPI3 value shows the condition of extremely dry, in Nov/2019 for Koshe station and in 2017 for Degaga station except in February extremely dry condition observed. SPI3 value for drought year in 2015 at Arsi Negele and Tora station during September-November and at Bulbula station in December month was found to be below (-2) which is considered to be a situation of extreme drought according to McKee (1993) drought classification. Also, SPI3 value obtained in the same year, as presented in (Table 4.4 which was found to be (-1.5 to -1.99) at Arsi Negele, Tora, Ziway and Kulmsa meteorological stations this indicated that were a severely dry year. Whereas SPI3 value which was found to be (-1 to -1.49) in February at Arsi Negele, during September – November at Bulbula, in February at Tora and during September-February at Ziway meteorological stations, which is considered to be a situation of moderately dry. As result shows that SPI3 value for drought year in 1991 at Langano meteorological station in September month and at Assela meteorological station during October- November months, in 2019 at koshe station at November month, in 2017 at Degaga station during September-January months was found to be below negative two (-2) which is considered to be a situation of extreme drought. SPI3 value for drought year obtained in the same meteorological stations found to be (-1 to -1.49) and (-1.5 to -1.99) identified as a situation of moderately dry and severe dry years respectively.

And also results can be showed that during the non-drought years there was positive values of SPI3, in 2016 at Koshe and Ziway, in 2001 at Assela, in 2010 at Langano, in 2004 at Arsi Negele, in 1988 at Degaga station, in 2012 at Bulbula station and in 1990 at Kulumsa stations as presented in (**Table 4.4**). This indicates that there had been high rainfall in these areas during September-January. During the non-drought years of 2004 at Arsi Negele in September, October and January, in 2012 at Bulbula in September and February, in 2010 at Langano in February, in 1993 at Tora in October and in 1988 at Degaga meteorological stations SPI3 value was greater than positive two which states that these years were extremely wet years. SPI3 value obtained in the same year, which was found to be (1.5 to 1.99) at Arsi Negele, Bulbula, Koshe, Langano, Tora, Ziway and kulmsa meteorological stations, this considered to be a situation of very wet years. The results of SPI3 for Assela rainfall stations in Central Rift Valley indicates that in 2001 dropped as low as 0.99 or found to be (-0.99 to 0.99) this considered to be a situation of near normal condition year.

Since SPI can be calculated at different time scales, it often serves as indicator of different drought types. 3-month SPI of September-February was used in the present work to quantify severity of drought for selected drought and wet years. In Fig. 4.11, ARC-GIS used in order to interpolate SPI3 value to determine the spatial pattern of meteorological drought (Monthly variation of Standard precipitation index (SPI3)) for the months of September, October, November, December, January and February. The interpolation of SPI3 was done by Inverse distance weighted (IDW) of spatial analyst tool. Sep (+ve) was interpolation of SPI3 done by using inverse distance weighted at all wet years of September months for all meteorological station. But Sep (-ve) was interpolation of SPI3 at all drought years of September months for all meteorological station. According to the result of Sep (+ve), Arsi Negele (1) in 2004 and Bulbula (2) in 2012 shows that extremely wet condition. Also, in the same month at Langano (4), Tora (5) and Ziway (6) in 2010, 1993 and 2016 respectively there was very wet (green color) condition is observed. The cream/shade of yellow/ color on the map represents the moderately wet condition for Kulmsa and Degaga meteorological station in 1990 and 1988 respectively. Yellow color on map at koshe (3) and Assela (7) stations indicates that there was near normal conditions in these area in 2016 and 2001 respectively. In otherwise, in Sep (-ve) or in drought years of September months Arsi Negele, Langano, Tora and Degaga meteorological stations showed the situation of extreme drought (red color) condition in 2015, 1991, 2015, 2017 respectively. The orange rust color on map represents that severely dry condition in drought years of September months for Assela and kulmsa meteorological station in 1991 and 2015 and all others indicated in fig. 4.11. In January and February major part of study shows moderately dry (Peach Melba – Orange) condition except in Dagaga ana kulmsa station which shows severely dry condition.

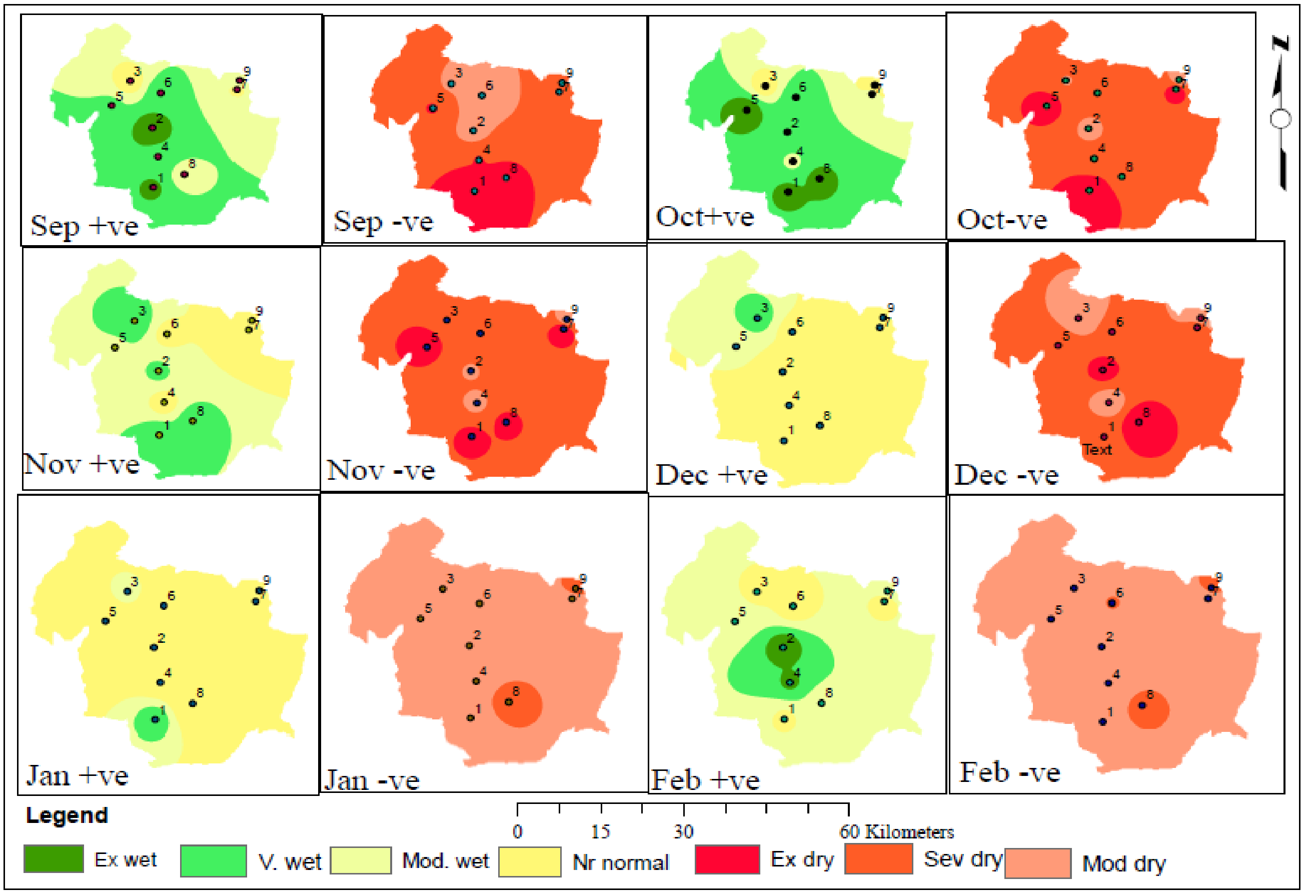

Note: -Nr normal = near normal, mod wet = moderately wet, v. wet = very wet, ex wet = extremely wet, sev dry = severely dry, Ex. dry = extremely dry and Mod. dry = moderately dry. 1=ArsiNegele,2=Bulbula,3=Koshe,4=Langano,5=Tora,6=Ziway,7=Assela,8=Dagaga and 9=Kulamsa (+ve) = non drought year, (-ve) = drought year.

Figure 4.11. Three month variation of Standard precipitation index (SPI3) values over selected drought and non-drought years from 1985-2019

4.2. Non-parametric Trend test for Historical Meteorological Drought

Based on the methodology explained under section (3.4-3.4.1) by following the MK test from the Z value and trend from Sen's Slope(β) estimation was computed based on monthly, seasonal, and annual rainfall data from 1985–2019 in the CRV, and the results are presented in the following tables. The sign of Z indicates the direction of the trend (Abdourahamane and Acar, 2018). The negative value of Z indicates a decreasing trend and vice versa. At the 5% significance level, the null hypothesis of no trend is rejected if the absolute value of Z is higher than 1.645. The significance of the change in monthly and annual stream flow was estimated using the MK test.

a) MK trend analysis result for Arsi Negele station

Table 4.5. Mann Kendall test output for monthly, seasonal and annual time series data for Arsi Negele station (from 1985-2019)

Variable	S-test	Z-test	Sen slope	VAR(S)	Remark
January	-106	-1.646	-0.019	4100	D.t@90%
February	-165	-2.54	-0.053	4164.33	D.t@95%
March	-138	-2.12	-0.049	4165.33	D.t@95%
April	-74	-1.13	-0.034	4165.33	n.t@95%
May	-96	-1.47	-0.019	4165.33	n.t@95%
Jun	-54	-0.82	-0.026	4165.33	n.t@95%
July	-136	-2.09	-0.042	4165.33	D.t@95%
August	50	-0.76	-0.029*	4165.33	I.t@95%
September	-135	-2.08	-0.042	4164.33	D.t@95%
October	-138	-2.12	-0.060	4165.33	D.t@95%
November	25	2.38	0.000*	3947.67	I.t @95%
December	-117	-1.93	0.000*	3600.33	D.t 90%
Belg(autumn)	-134	-2.06	-0.054	4165.33	D.t@95%
winter(bega)	-134	-2.06	-.061	4165.33	D.t@95%
summer(keremt)	-62	-0.95	-0.053	4165.33	n.t@95%
Annual	-66	-2.01	-0.040	4165.33	D.t@95%

Note: * mean not significant at 95% level; n.t mean no trend at 95%; D.t mean decreasing trend at 95%/90%., I.t mean increasing trend at 95%

The MK trend test on observed period monthly rainfall result reveals that no trend, insignificantly decreasing trend over certain meteorological station and increasing trend too. For Arsi Negele station during 1985-2019 in the MK test, positive Z-test value shows an increasing trend while a negative Z-test value showed a decreasing trend based on threshold Z value for 5% significance level. This value or $\mathbf{Z1{-}\alpha/2}$ value is 1.96 from the standard normal table or z table for 95% confidence level(Belay *et al.*, 2021). In other case hypotheses, Ho which says the nature of the monotonically increasing or decreasing trend is not significant (no trend) this happens when the absolute value of Z- test less than 5% significance level of threshold value. After analyzing the rainfall trend from 1985-2019, with the MK test and comparing with significant levels of 0.1% (0.001), 1% (0.01), 5% (0.05), and 10% (0.1), from (**Table 4.5**) results showed that there was negative, positive and no trend.

The MK trend test showed that there was a statically significant decreasing trend for the month of January, February, March, July, September and October at a 5% level of significance and there was no significant decreasing in rainfall trend that was observed at 90% confidence level or at 10% level of significance in December. Whereas no trend was observed in April, May, Jun and August, furthermore there was positive not significant trend observed at a 5% level of significance in November.

The monthly share of rainfall exhibited about 33.33% no trend, 50% negative trend, 8.33% not significant negative trend and 8.33% not significant positive trend in rainfall amounts. The results of trend analysis in monthly, seasonally, and annually rainfall found in this work are in agreement with the past research work in the some station found in the study area Eg. (Kassie *et al.*, 2014) they found that monthly, seasonally, and annually rainfall trend which are significantly decreasing, not significantly decreasing at a significant level alpha = 0.05 or at 95% confidence level. Generally strong decreasing trends in rainfall are apparent in the Arsi negele stations. Thus, the decreasing in rainfall particularly has significant impact on the initial growing stage of crop as well as the major cause meteorological drought. Observed trends in annual and seasonal rainfall were also presented in (**Table 4.5).** As shown in the Table during 1985-2019, trends in Belg(autumna) and winter(bega) rainfall were observed being negative for both seasons. As results shows that no trend was observed in summer

(keremt) season, whereas decreasing trend was observed annually. Seasonal trends are shown in Fig. 4.12 the seasonal rainfall variability for Belg, Kiremt, and Bega seasons were -1.3241mm/season, -1.8589mm/season and -0.8046mm/season respectively. Whereas the declining trend of Belg and bega season was statistically significant. The negative and positive values indicated decreasing and increasing pattern of rainfall distribution over the observed period respectively. As depicted in Fig. 4.12, Belg and bega rainfall showed a decreasing trend and significant. The Belg season rainfall is crucial for the farmers as the season determines the preparation and planting activities of the farmers in the study area. Annual trend shown in Figure 4.12(b) indicates rainfall variability for Arsi Negele station was -1.3392mm/year. As the result showed that the declining trend of annual rainfall was statistically significant.

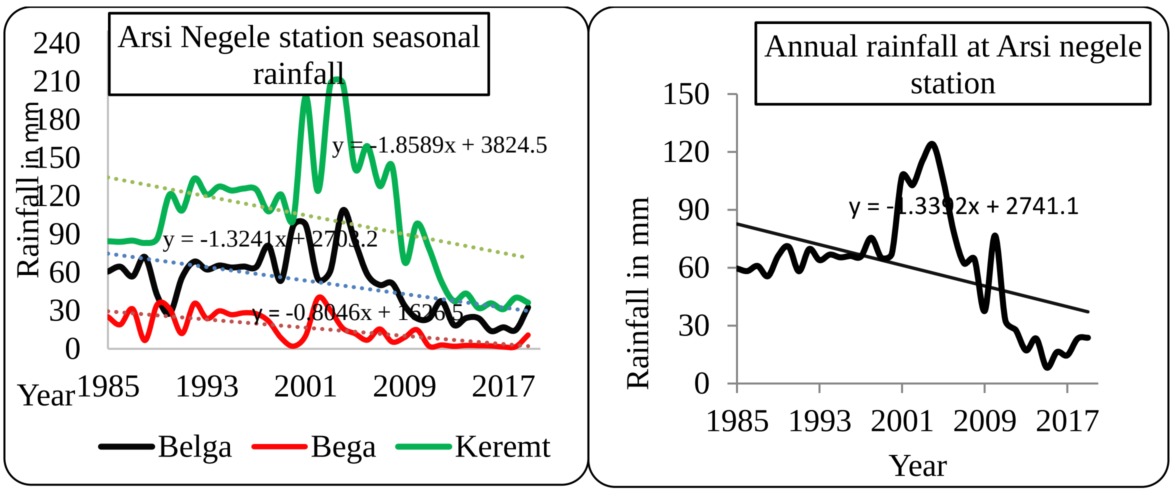

a). b).

Figure 4.12. Seasonal and Annual rainfall trends over the observed period for 1985–2019 Arsi Negele station.

b) Innovative trend analysis result for Arsi Negele station

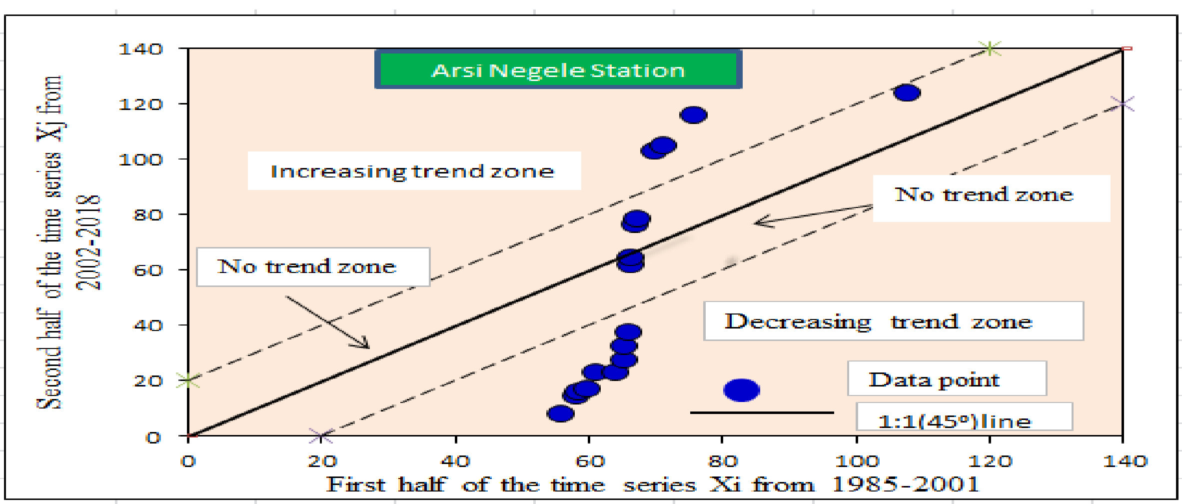

Figure 4.13. The innovative trend analysis (ITA) method shows increasing, decreasing and no trend zones

a) MK trend analysis result for Assela station

Table 4.6. Mann Kendall test output for monthly, seasonal and annual time series data for Assela station (from 1985-2019)

Variable	S-test	Z-test	Sen slope	VAR(S)	Remark
January	39	0.59	0.000*	4161.67	n.t@95%
February	-103	-1.51	-0.026*	4545.67	n.t@95%
March	-37	-0.53	-0.010*	4548.33	n.t@95%
April	-99	-1.45	-0.029*	4550.33	n.t@95%
May	86	1.26	0.026*	4549.33	n.t@95%
Jun	-58	-0.85	-0.013*	4549.33	n.t@95%
July	-56	-0.82	-0.013*	4549.33	n.t@95%
August	89	1.30	0.021*	4548.33	n.t@95%
September	52	0.76	0.014*	4549.33	n.t@95%
October	-11	-0.15	-0.005*	4548.33	n.t@95%
November	30	0.43	0.001*	4522.00	n.t@95%
December	-47	-0.69	-0.005*	4458.33	n.t@95%
Belg(autumn)	3	0.03	0.001*	4550.33	n.t@95%
winter(bega)	-58	-0.85	-0.012*	4549.33	n.t@95%
summer(keremt)	-43	-0.62	-0.017*	4550.33	n.t@95%
Annual	5	0.06	0.003*	4550.33	n.t@95%

The Sen's slope and Mann Kendall trend test were individually applied at Assela station. The tests were applied at each month and seasonal rainfall for the period 1985 to 2019 at 95% confidence levels. Observed trends in monthly and seasonal rainfall were presented in (Table 4.6). The MK trend test showed that there was a statically not significant trend observed for all months at a 95% level of confidence. As result shown during 1985-2019, in Belg(autumna), summer(keremt) and winter(bega) no trend were observed for all seasons. Seasonal trends were shown in Fig. 4.14 the seasonal rainfall variability for Belg, Kiremt, and Bega seasons were -0.05mm/season ,0.0358mm/season and –0.2793mm/season respectively. Generally, the

MK test result showed that there is no significant trend was observed in Assela station. Whereas the declining trend of Bega season was statistically not significant.

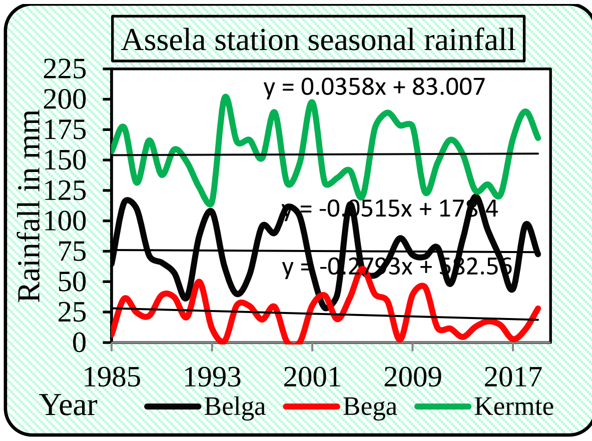

a).

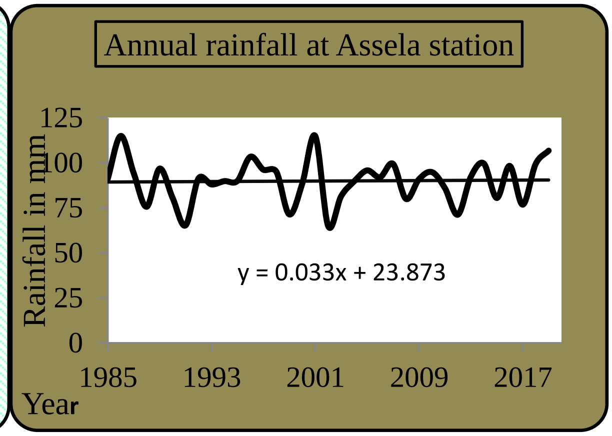

b).

Figure 4.14. Seasonal and Annual rainfall trends over the observed period for 1985–2019 Assela station.

The annual rainfall variability for Assela station was -0.033mm/year. As the result showed that there was no significant trend observed annually at Assela station (Table 4.6).

b) Innovative trend analysis result for Assela station

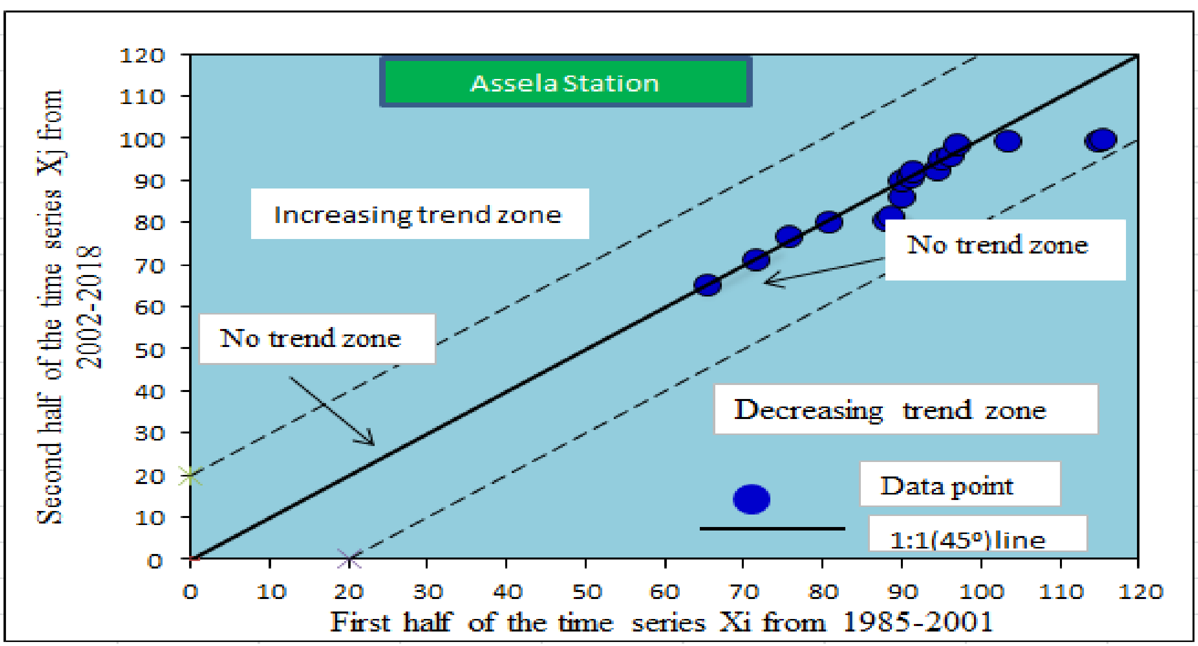

Figure. 4.15. The innovative trend analysis (ITA) method shows no trend zones for Assela station.

a) MK trend analysis result for Bulbula station

Table 4.7. Mann Kendall test output for monthly, seasonal and annual time series data for Bulbula station (from 1985-2019)

Variable	S-test	Z-test	Sen slope	VAR(S)	Remark
January	-71	-1.09	0.000	4121.00	n.t@95%
February	-92	-1.36	-0.011*	4484.00	n.t@95%
March	-78	-1.14	-.018	4528.00	n.t@95%
April	-144	-2.12	-0.036	4549.33	D.t@95%
May	-36	-0.52	-0.010*	4547.33	n.t@95%
Jun	-43	-0.62	-0.012*	4548.33	n.t@95%
July	-131	-1.93	-0.034	4548.33	D.t@90%
August	-141	-2.08	-0.033	4548.33	D.t@95%
September	10	0.13	0.004*	4549.33	n.t@95%
October	-58	-0.88	-0.017	4165.33	n.t@95%
November	109	1.66	0.004*	4213.00	I.t@90%
December	5	0.06	0.000*	3852.33	n.t@95%
Belg(autumn)	44	0.64	0.015*	4549.33	n.t@95%
winter(bega)	-83	-1.22	-0.017*	4546.33	n.t@95%
summer(keremt)	-168	-2.48	-0.037	4549.33	D.t@95%
Annual	-198	-2.92	-0.045	4549.33	D.t@95%

The MK trend test showed that there was a statically significant decreasing trend for the month of April, July and August at a 5% level of significance and also not significant positive trend at 10% of level of significance in November. Whereas no trend was observed in January, February, March May, Jun, September, October and December (Table 4.7). The monthly share of rainfall exhibited about 66.67% no trend, 25% negative trend, and 8.33% not significant positive in rainfall amounts. During 1985-2019, in Belg(autumna) and winter(bega) no trend were observed. But the result showed that there was negative trend in summer (keremt) season.

Seasonal trends were shown in Fig. 4.16 the seasonal rainfall variability for Belg, Kiremt, and Beg a seasons was 0.0972mm/season, -1.1715mm/season and -0.2823mm/season respectively. The positive trends of belga seasons were statistically not significant based on the result of Z and sen slope value.

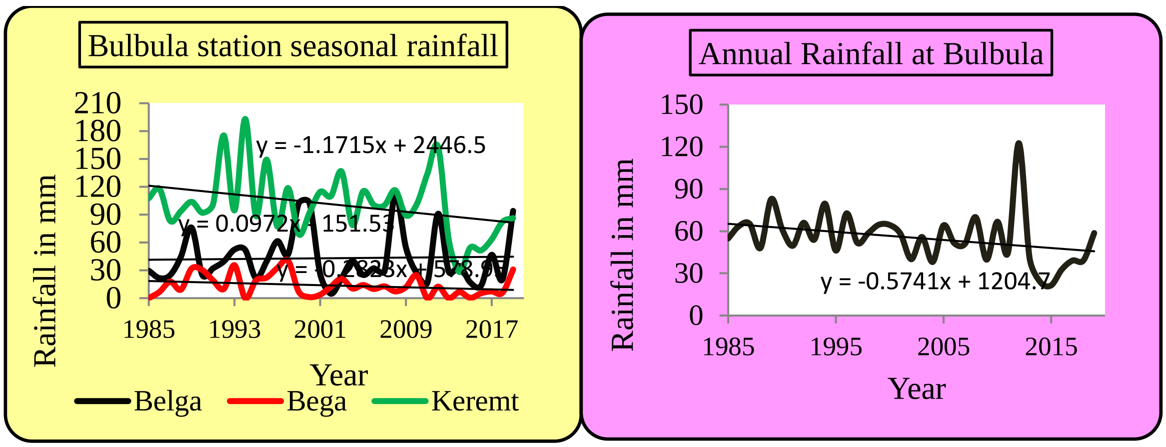

Figure 4.16. Seasonal and annual trend of Bulbula rainfall between 1985–2019

b) Innovative trend analysis result for Bulbula station

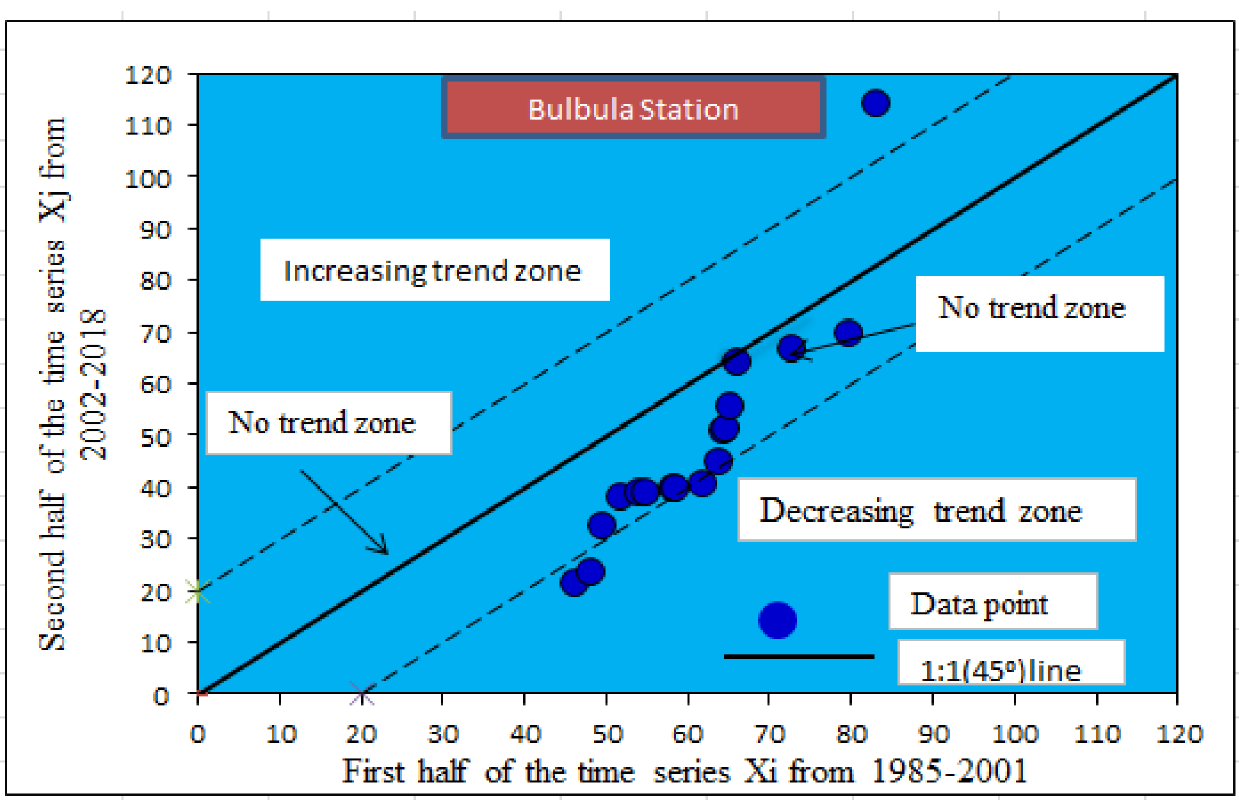

Figure 4.17. The innovative trend analysis (ITA) method for Bulbula station

a) MK trend analysis result for Degaga station

Table 4.8. Mann Kendall test output for monthly, seasonal and annual time series data for Degaga station (from 1985-2019)

Variable	S-test	Z-test	Sen slope	VAR(S)	Remark
January	-73	-1.07	-0.019*	4529.67	n.t@95%
February	-118	-1.81	-0.061	4165.33	D.t@90%
March	-133	-1.96	-0.036	4548.33	D.t@90%
April	-194	-2.86	-0.047	4549.33	D.t@95%
May	98	1.50	0.061	4165.33	n.t@95%
Jun	-44	-.64	-0.013	4544.67	n.t@95%
July	2	0.01	0.001*	4549.33	n.t@95%
August	-125	-1.84	-.029*	4548.33	D.t@90%
September	-112	-1.65	-0.032*	4547.33	D.t@90%
October	-48	-0.70	-0.011*	4547.33	n.t@95%
November	88	1.29	0.024*	4532.67	n.t@95%
December	-130	-1.94	-0.015*	4425.33	D.t@90%
Belg(autumn)	-48	-0.70	-0.011*	4549.33	n.t@95%
winter(bega)	-117	-1.72	-0.033*	4548.33	D.t@90%
summer(keremt)	-189	-2.79	-0.044*	4545.67	D.t@95%
Annual	-117	-1.72	-0.031*	4545.67	D.t@90%

The MK trend test showed that there was a statically significant decreasing trend for the month of February, March and April at a 10% level of significance and 5% level of significance as well as there was not significant decreasing in rainfall trend that was observed at 90% confidence level or at 10% level of significance in August, September and December. Whereas no trend was observed in January, May, Jun, July, October and November (Table 4.8). The monthly share of rainfall exhibited about 50% no trend, 25% negative trend, 25% not significant negative trend in rainfall amounts. As result shown during 1985-2019, in Belg(autumna) no trend were observed. But the result showed that, negative trend in summer (keremt), winter(bega) season and annual time series at 90% confidence level. Seasonal trends were shown in Fig. 4.18 the seasonal rainfall variability for Belg, Kiremt, and Bega seasons was -0.4525mm/season, -0.9665mm/season and –0.8737mm/season respectively. The negative trends of belga seasons were statistically not significant based on the result of Z and sen slope value.

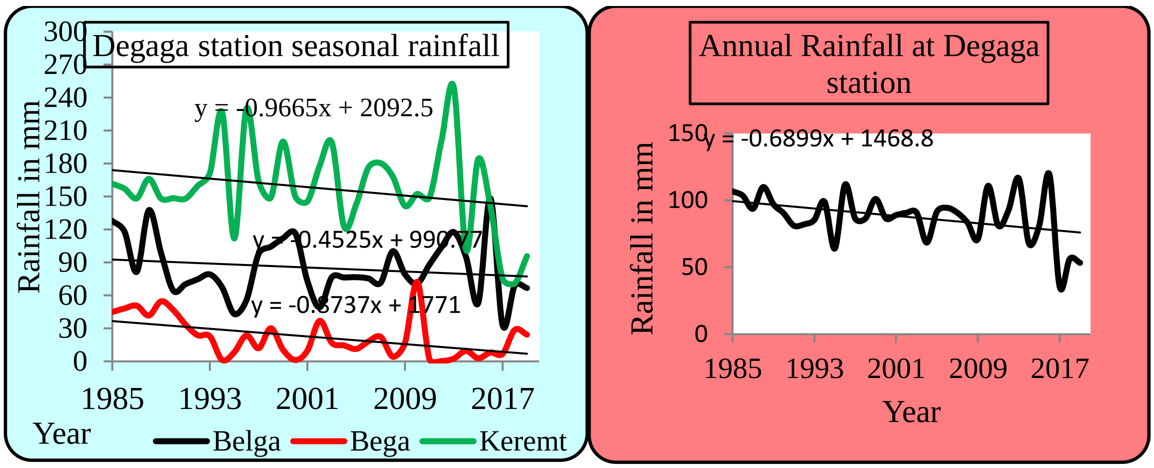

Figure 4.18. Seasonal and annual trend of Degaga rainfall between 1985–2019

b) Innovative trend analysis result for Degaga station

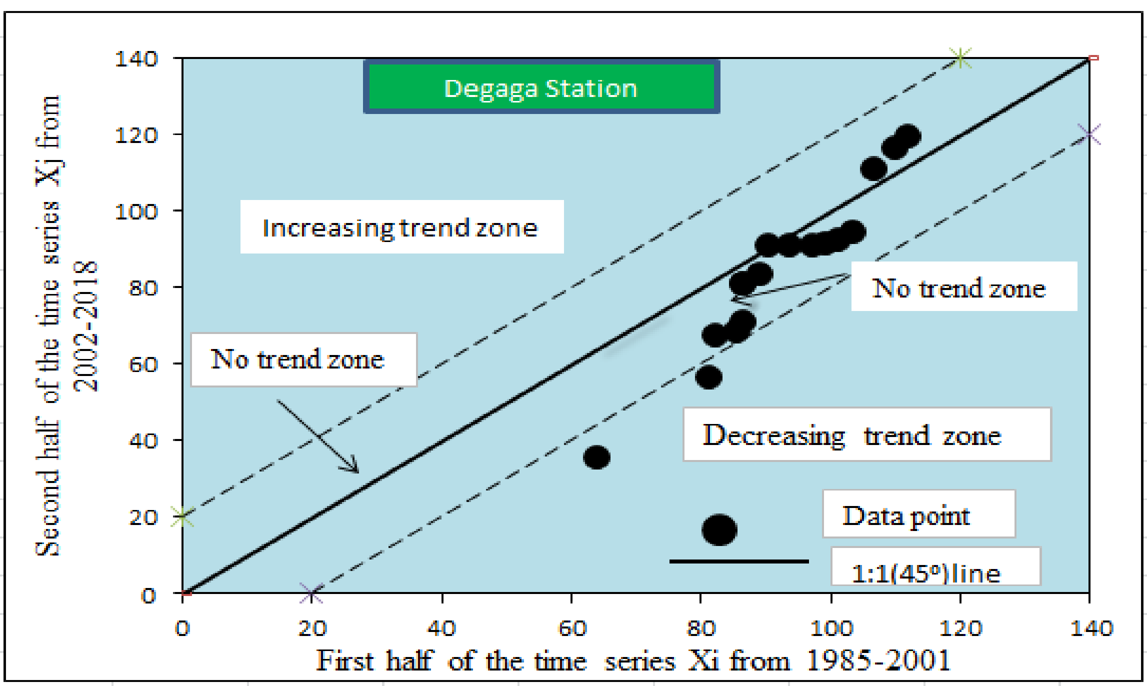

Figure 4.19. The innovative trend analysis (ITA) method for Degaga station

a) MK trend analysis result for Koshe station

Table 4.9. Mann Kendall test output for monthly, seasonal and annual time series data for Koshe station (from 1985-2019)

Variable	S-test	Z-test	Sen slope	VAR(S)	Remark
January	115	1.74	0.011*	4281.67	I.t@90%
February	-182	-2.70	-0.033	4484.00	D.t@95%
March	-22	-0.31	-0.009*	4549.33	n.t@95%
April	-76	-1.11	-0.019*	4547.33	n.t@95%
May	-3	-0.03	-0.001*	4548.33	n.t@95%
Jun	-60	-0.87	-0.018*	4549.33	n.t@95%
July	43	0.62	0.006*	4550.33	n.t@95%
August	-183	-2.70	-0.043	4550.33	D.t@95%
September	-75	-1.10	-0.017*	4548.33	n.t@95%
October	91	1.34	0.024*	4531.67	n.t@95%
November	142	2.46	0.000*	3292.67	I.t@95%
December	82	1.30	0.000*	3853.33	n.t@95%
Belg(autumn)	92	1.35	0 .021*	4547.33	n.t@95%
winter(bega)	-15	-0.21	-0.004*	4548.33	n.t@95%
summer(keremt)	-156	-2.01	-0.049	4548.33	D.t@95%
Annual	-119	-1.75	-0.036	4548.33	D.t@90%

The MK trend test showed that there was a statically significant decreasing trend for the month of February and August 5% level of significance as well as there was not significant decreasing in rainfall trend that was observed at 90% confidence level or at 10% level of significance in January. Also, there was positive trend at 5% level of significance in November, whereas no trend was observed in March, April, May, Jun, July, September October and December (Table 4.9). The monthly share of rainfall exhibited about 66.67% no trend, 16.66% negative trend, 8.33% not significant negative trend and 8.33% positive trend in rainfall amounts. As result shown during 1985-2019, in Belg(autumna) and winter(bega) no trend was observed at 95% confidence level. And also, there were negative trend observed in summer (keremt) season and annual time series at 95% and 90% confidence level respectively. Seasonal trends were shown in Fig. 4.20 the seasonal rainfall variability for Belg, Keremt, and Bega seasons was 0.2537mm/season, -1.7121mm/season and –0.4595mm/season respectively. The negative trends of keremt seasons were statistically significant based on the result of Z and sen slope value in (Table 4.9). But negative trend in bega and positive trend in belga is not statistically significant.

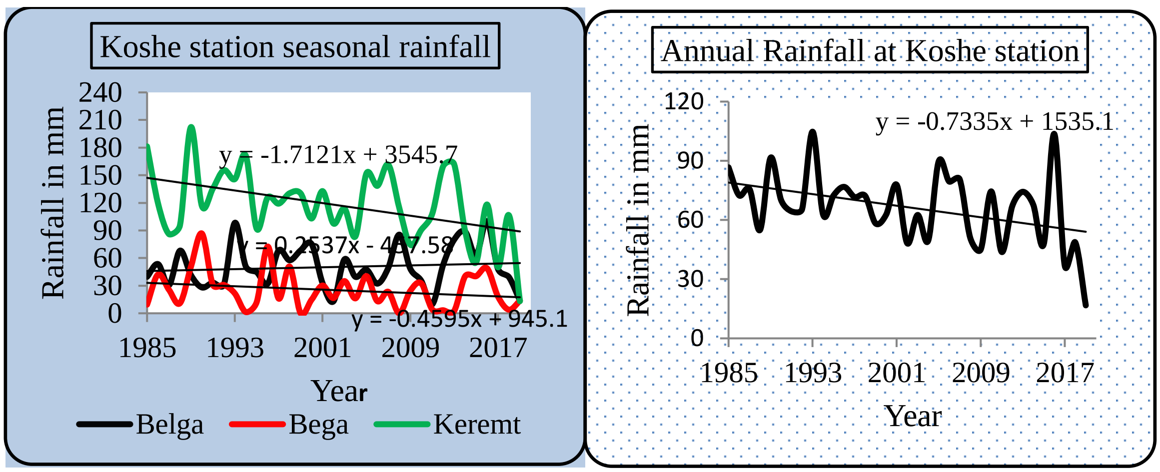

Figure 4.20. Seasonal and annual trend of Koshe rainfall between 1985–2019.

b) Innovative trend analysis result for Koshe station

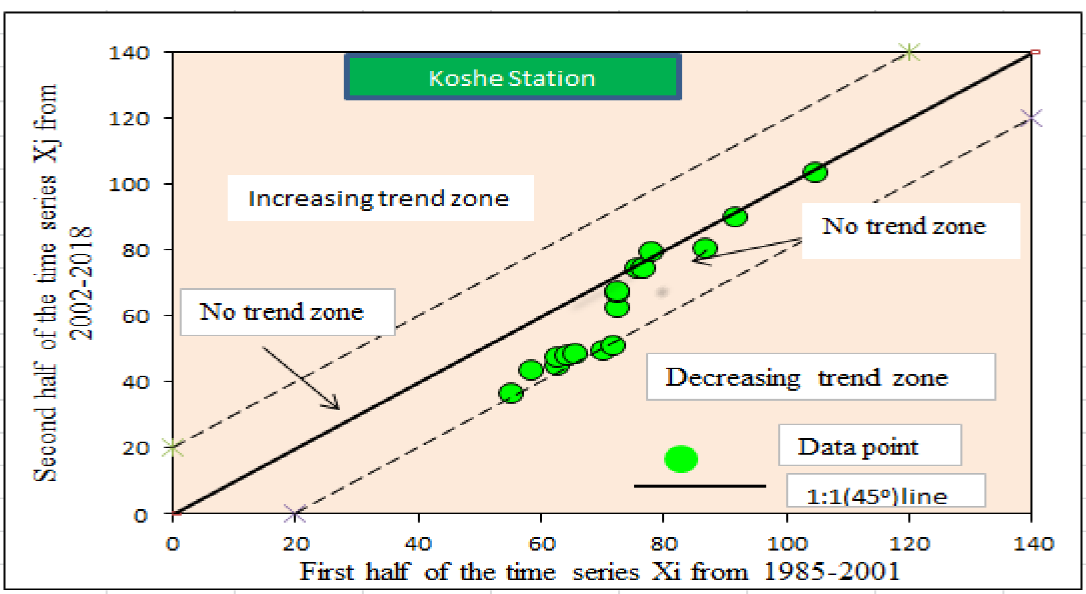

Figure 4.21. The innovative trend analysis (ITA) method for Koshe station.

a) MK trend analysis result for Kulmsa station

Table 4.10.Mann Kendall test output for monthly, seasonal and annual time series data for Kulmsa station (from 1985-2019)

Variable	S-test	Z-test	Sen slope	VAR(S)	Remark
January	-6	-0.07	0.000*	4504.00	n.t@95%
February	-143	-2.11	-0.038	4545.67	D.t@95%
March	-19	-0.27	-0.005*	4546.33	n.t@95%
April	-98	-1.44	-0.027*	4549.33	n.t@95%
May	157	2.31	0.000*	4548.33	I.t@95%
Jun	-4	-0.04	-0.003*	4549.33	n.t@95%
July	44	0.64	0.008*	4547.33	n.t@95%
August	-70	-1.02	-0.024	4549.33	n.t@95%
September	66	0.96	0.015*	4547.33	n.t@95%
October	-9	-0.12	-0.004*	4548.33	n.t@95%
November	48	0.70	0.003*	4482.00	n.t@95%
December	-148	-2.23	-0.012*	4336.67	D.t@95%
Belg(autumn)	57	0.83	0.014*	4548.33	n.t@95%
winter(bega)	-36	-0.52	-0.017*	4549.33	n.t@95%
summer(keremt)	-23	-0.42	-0.016*	4165.33	n.t@95%
Annual	-34	-0.49	-0.011*	4549.33	n.t@95%

At Kulmsa station the MK trend test showed that there was a statically significant decreasing trend for the month of February at 5% level of significance as well as there was not significant decreasing trend that was observed at 95% confidence level or at 5% level of significance in December. Also, there was not significant positive trend at 5% level of significance in May, whereas no trend was observed in January, March, April, Jun, July, August September, October and November (Table 4.10). The monthly share of rainfall exhibited about 75% no trend, 8.33% negative trend, 8.33% not significant negative trend and 8.33% positive trend in rainfall amounts. Seasonal rainfall variability for Belg, Keremt, and Bega seasons was 0.1054mm/season, -0.1143mm/season -0.7081mm/season respectively. The negative trends of bega, keremt seasons and annual time series data were not statistically significant at 95% confidence level based on the result of Z and sen slope value.

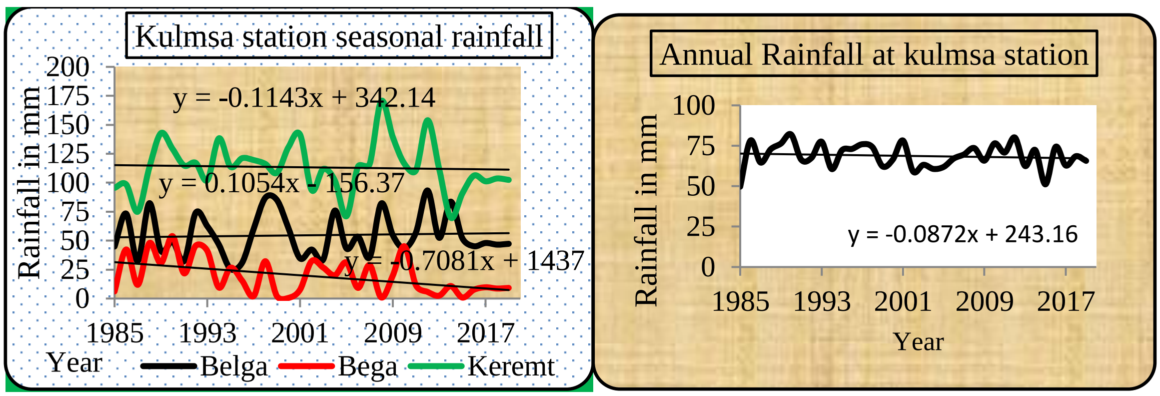

Figure 4.22. Seasonal and annual trend of Kulmsa rainfall between 1985–2019.

b) Innovative trend analysis result for Kulmsa station

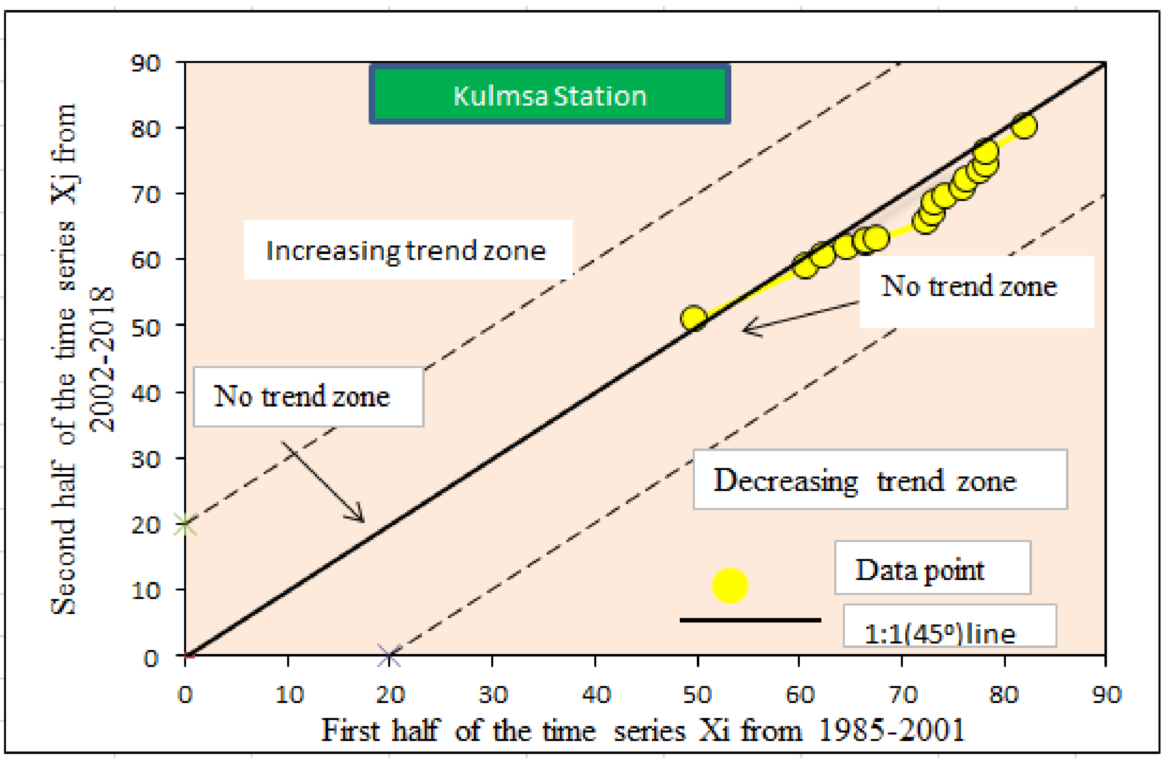

Figure.4.23. The innovative trend analysis (ITA) method for Kulmsa station.

a) MK trend analysis result for Langano station

Table 4.11. Mann Kendall test output for monthly, seasonal and annual time series data for Langano station (from 1985-2019)

Variable	S-test	Z-test	Sen slope	VAR(S)	Remark
January	-19	-0.29	0.000*	3850.33	n.t@95%
February	-35	-0.51	-0.002*	4483.00	n.t@95%
March	71	1.04	0.024*	4548.33	n.t@95%
April	-48	-0.70	-0.011*	4549.33	n.t@95%
May	104	1.60	0.040	4165.33	n.t@95%
Jun	42	0.61	0.011*	4547.33	n.t@95%
July	62	0.95	0.026	4165.33	n.t@95%
August	46	0.70	0.029	4165.33	n.t@95%
September	40	0.58	0.007*	4544.67	n.t@95%
October	-104	-1.61	-0.015	4100.00	n.t@95%
November	114	1.74	0.006*	4214.67	D.t@90%
December	35	0.58	0.000*	3453.67	n.t@95%
Belg(autumn)	-14	-0.20	0.003	4165.33	n.t@95%
winter(bega)	-10	-0.14	0.006	4165.33	n.t@95%
summer(keremt)	56	1.09	0.002*	4549.33	I.t@90%
Annual	26	0.39	0 .023	4165.33	n.t@95%

The MK trend test showed that there was a statically not significant decreasing trend for the month of November at 5% level of significance at Langano station. whereas no trend was observed in January, February, March, April, May, Jun, July, August, September, October and December (Table 4.11). The monthly share of rainfall exhibited about 91.67% no trend and 8.33% not significant negative trend in rainfall amounts during 1985-2019, in Belg(autumn), winter(bega) seasons and Annual time series data, no trend were observed at 95% confidence level. Summer(keremt) Season was showed not siginificant positive trend at 95% confidence level. Seasonal trends were shown in Fig. 4.24 the seasonal rainfall variability for Belg, Keremt, and Bega seasons was 0.1663mm/season,1.1442mm/season and -0.0399mm/season respectively.

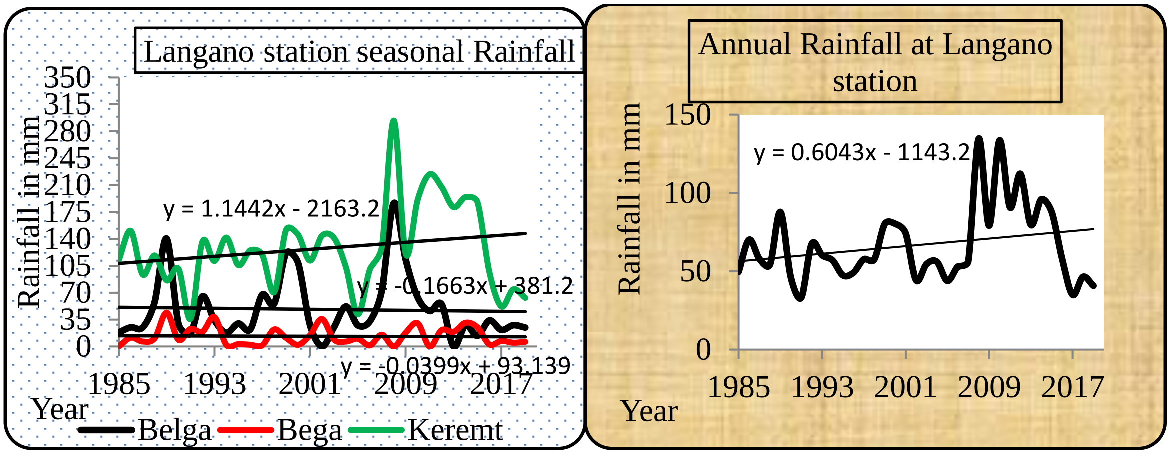

Figure 4.24. Seasonal and annual trend of Langano rainfall between 1985–2019.

b) Innovative trend analysis result for Langano station

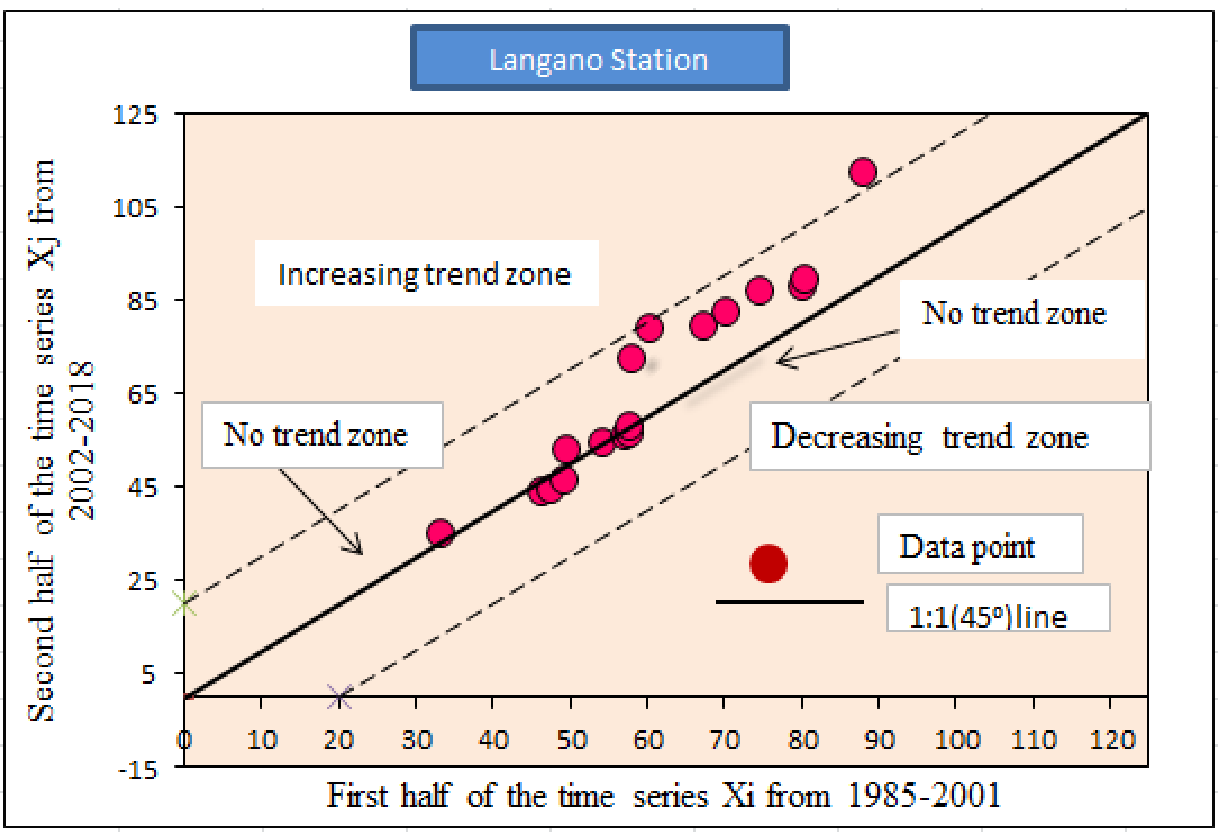

Figure 4.25. The innovative trend analysis (ITA) method for Langano station

a) MK trend analysis result for Tora station

Table 4.12. Mann Kendall test output for monthly, seasonal and annual time series data for Tora station (from 1985-2019)

Variable	S-test	Z-test	Sen slope	VAR(S)	Remark
January	30	0.44	0.000*	4385.33	n.t@95%
February	-104	-1.55	-0.017*	4425.33	n.t@95%
March	-90	-1.32	-0.021*	4549.33	n.t@95%
April	-164	-2.42	-0.044	4549.33	D.t@95%
May	-29	-0.42	-0.005*	4548.33	n.t@95%
Jun	-53	-0.77	-0.020*	4548.33	n.t@95%
July	-68	-0.99	-0.022*	4547.33	n.t@95%
August	-155	-2.28	-0.043	4550.33	D.t@95%
September	-160	-2.36	-0.043	4549.33	D.t@95%
October	-33	-0.48	-0.006*	4529.67	n.t@95%
November	15	0.24	0.000*	3291.67	n.t@95%
December	-14	-0.22	0.000*	3599.33	n.t@95%
Belg(autumn)	-116	-1.70	-0.027	4549.33	D.t@90%
winter(bega)	-121	-1.78	-0.029	4548.33	D.t@90%
summer(keremt)	-223	-3.29	-0.058	4548.33	D.t@99%
Annual	-144	-2.22	-0.058	4165.33	D.t@95%

The MK trend test showed that there was a statically significant decreasing trend for the month of April, August and September at a 5% level of significance. Whereas no trend was observed in January, February, March, May, Jun, July, October, November and December at 5% level of significance (Table 4.12). The monthly share of rainfall exhibited about 75% no trend and 25% negative trend in rainfall amounts. All seasons and annual time series data were indicated that statically significant decreasing trend were observed at 90%, 95% and 99% confidence level. Seasonal trends were shown in Fig.4.26 the seasonal rainfall variability for Belg, Keremt, and Bega seasons was -0.64mm/season, -1.1299mm/season and –0.528mm/year respectively.

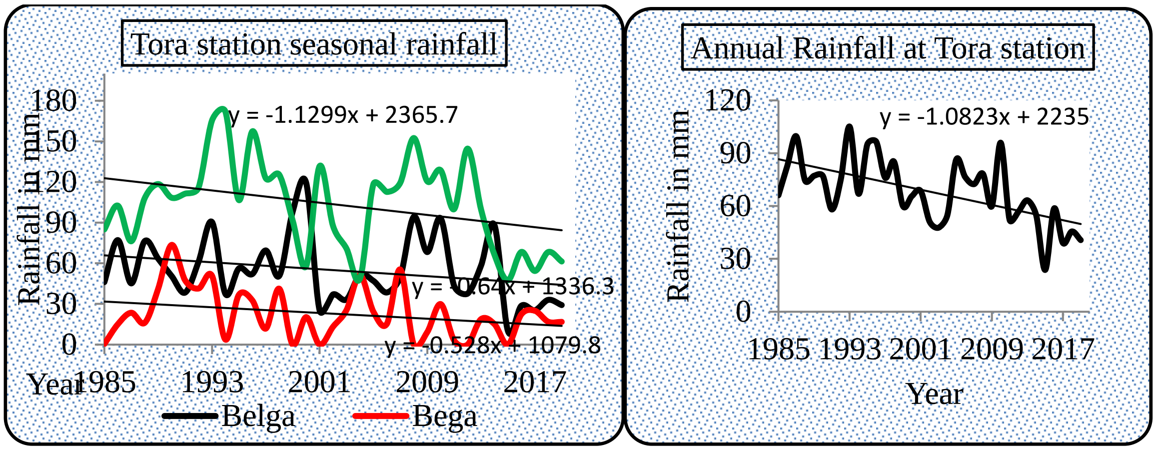

Figure 4.26. Seasonal and annual trend of Tora rainfall between 1985–2019

b) Innovative trend analysis result for Tora station

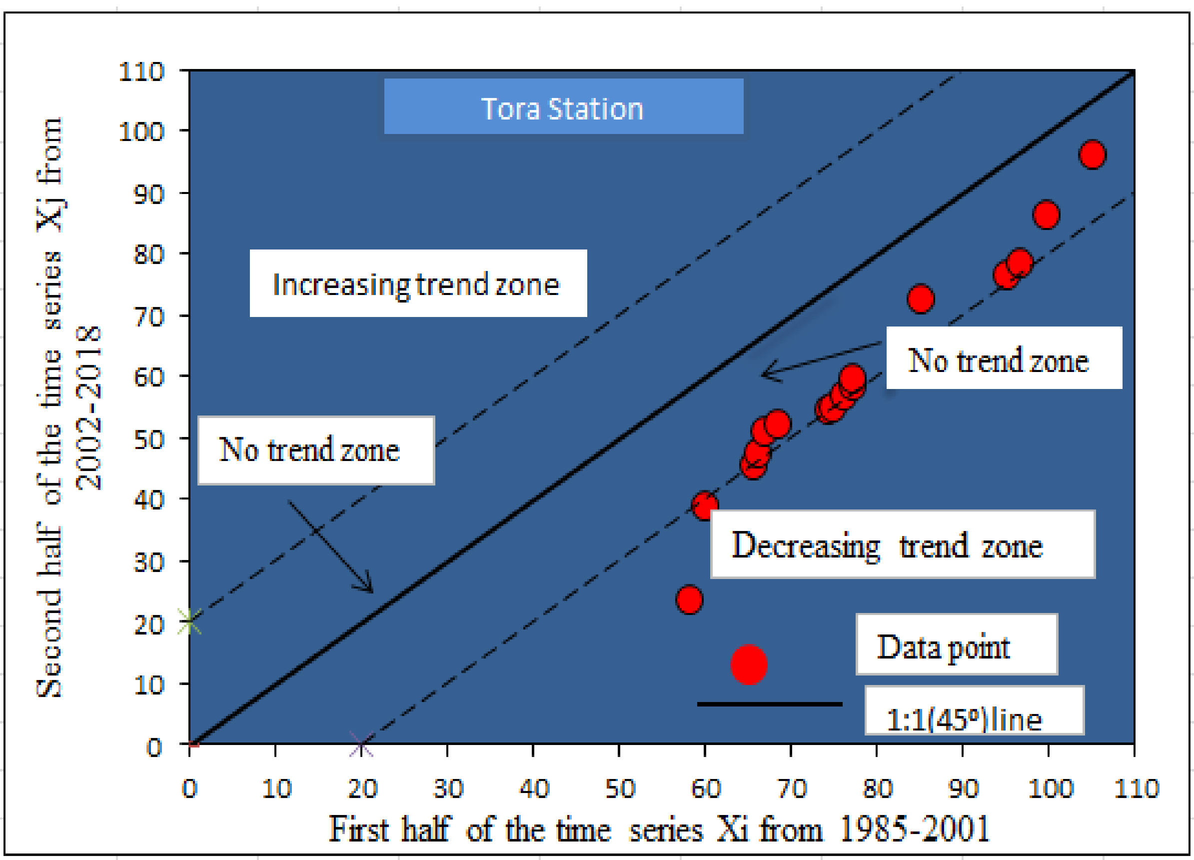

Figure 4.27. The innovative trend analysis (ITA) method for Tora station

a) MK trend analysis result for Ziway station

Table 4.13. Mann Kendall test output for monthly, seasonal and annual time series data for Ziway station (from 1985-2019)

Variable	S-test	Z-test	Sen slope	VAR(S)	Remark
January	55	0.83	0.000*	4281.67	n.t@95%
February	-81	-1.20	-0.010*	4424.33	n.t@95%
March	-16	-0.22	-0.001*	4547.33	n.t@95%
April	-25	-0.36	-0.007*	4550.33	D.t@95%
May	65	0.95	0.016*	4545.67	n.t@95%
Jun	83	1.22	0.025*	4550.33	n.t@95%
July	44	1.12	0.009	4549.33	I.t@95%
August	-44	-0.64	-0.009*	4549.33	n.t@95%
September	-2	-0.02	-0.005	4165.33	n.t@95%
October	-35	-0.51	-0.003*	4485.00	n.t@95%
November	145	2.32	0.000*	3852.33	I.t@95%
December	-59	-0.95	0.000*	3729.67	n.t@95%
Belg(autumn)	65	0.95	0.018*	4546.33	n.t@95%
winter(bega)	-18	-0.25	-0.003*	4549.33	n.t@95%
summer(keremt)	46	0.67	0.009*	4549.33	n.t@95%
Annual	115	1.69	0.003*	4548.33	I.t@90%

At Ziway station the MK trend test showed that there was not significant decreasing trend for the month of April at 5% level of significance. There was not significant positive trend at 5% level of significance in July, whereas no trend was observed in January, February, March, May, Jun, August, September, October, November and December (Table 4.13). The monthly share of rainfall exhibited about 83.34% no trend, not significant 8.33% negative and positive trend in rainfall amounts. As result shown in the above table during 1985-2019, in all seasons no trend was observed at 95% confidence level. But there was positive trend observed in annual time series data at 90% confidence level. Seasonal trends were shown in fig. 4.28 the seasonal rainfall variability for Belg, Keremt, and Bega seasons was 0.8397mm/season, 1.1853mm/season and 0.1434mm/season respectively.

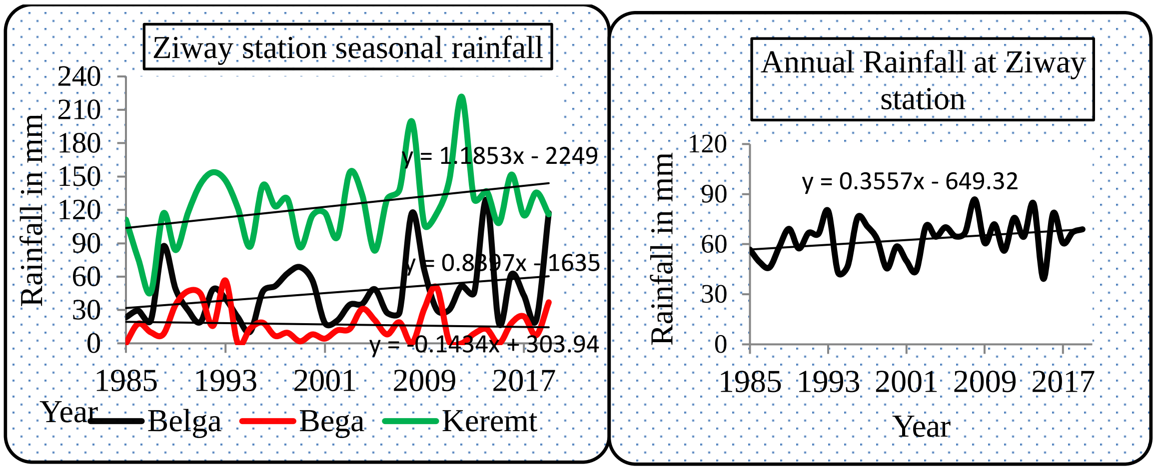

Figure 4.28. Seasonal and annual trend of Ziway rainfall between 1985–2019.

b) Innovative trend analysis result for Ziway station

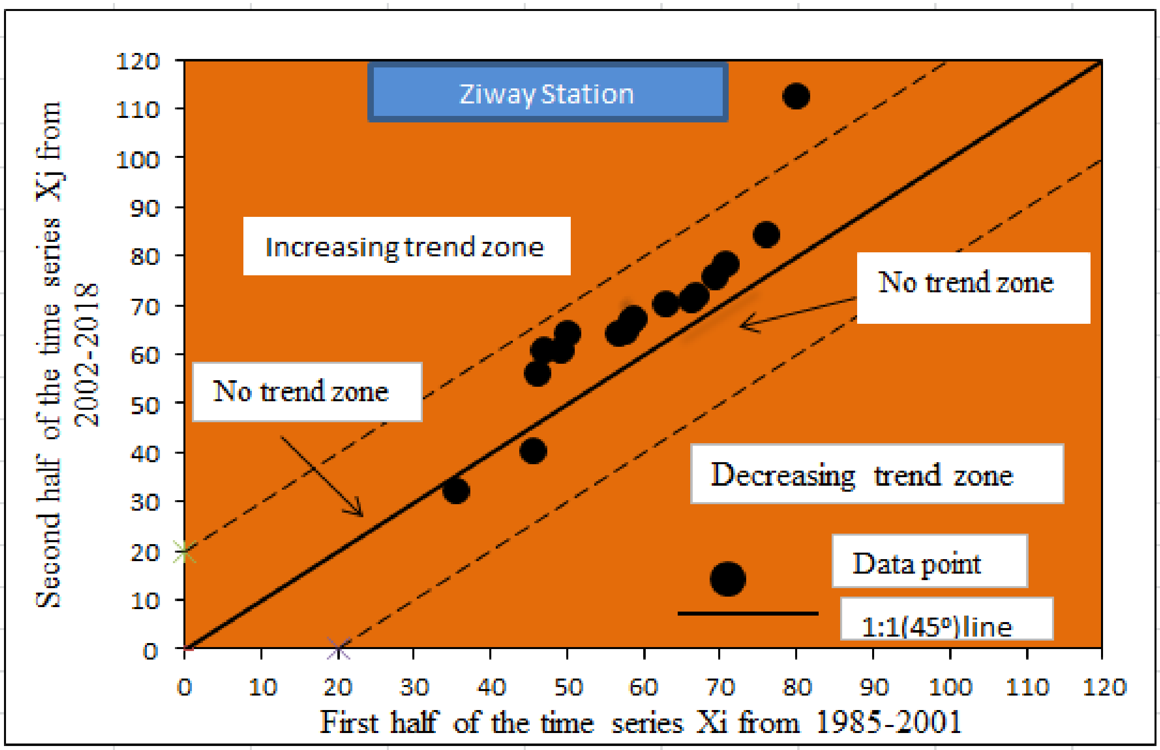

Figure 4.29. The innovative trend analysis (ITA) method for Ziway station

4.3.Projected Meteorological Drought by Using Standardized Precipitation Index (SPI) Under Representative Concentration Pathway (RCP4.5 and RCP8.5) Scenario

The coordinated regional climate downscaling experiment (CORDEX) series of daily precipitation projected data from 2020 to 2100, converted to monthly time series and have been used to compute selected drought indicators or the Standardized Precipitation Index (SPI). Monthly series of SPI3 and SPI1 have been computed for each meteorological station. Fig. 4.31-4.33 shows, examples of SPI3 series for projected precipitation data for each of the three analyzed periods that represent the recent past(historical), near future, future and far future for both RCP4.5 and RCP8.5 scenario.

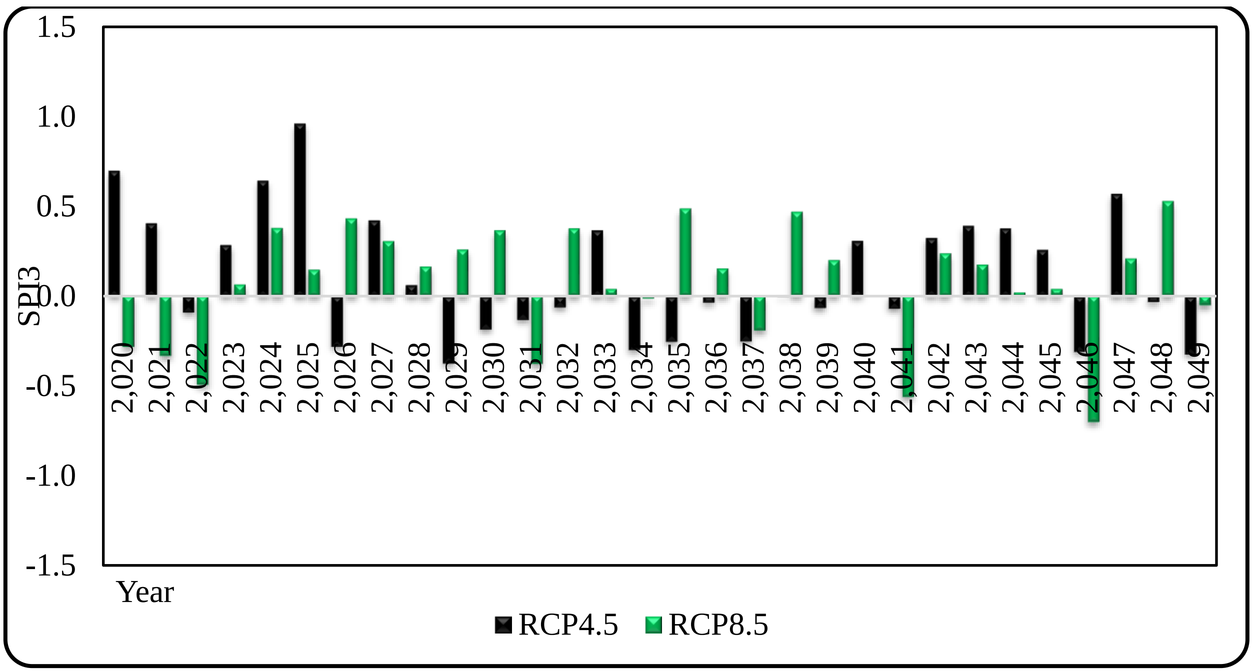

Figure 4.31. Average SPI-3 for all future meteorological station data for the near future (2020-2049).

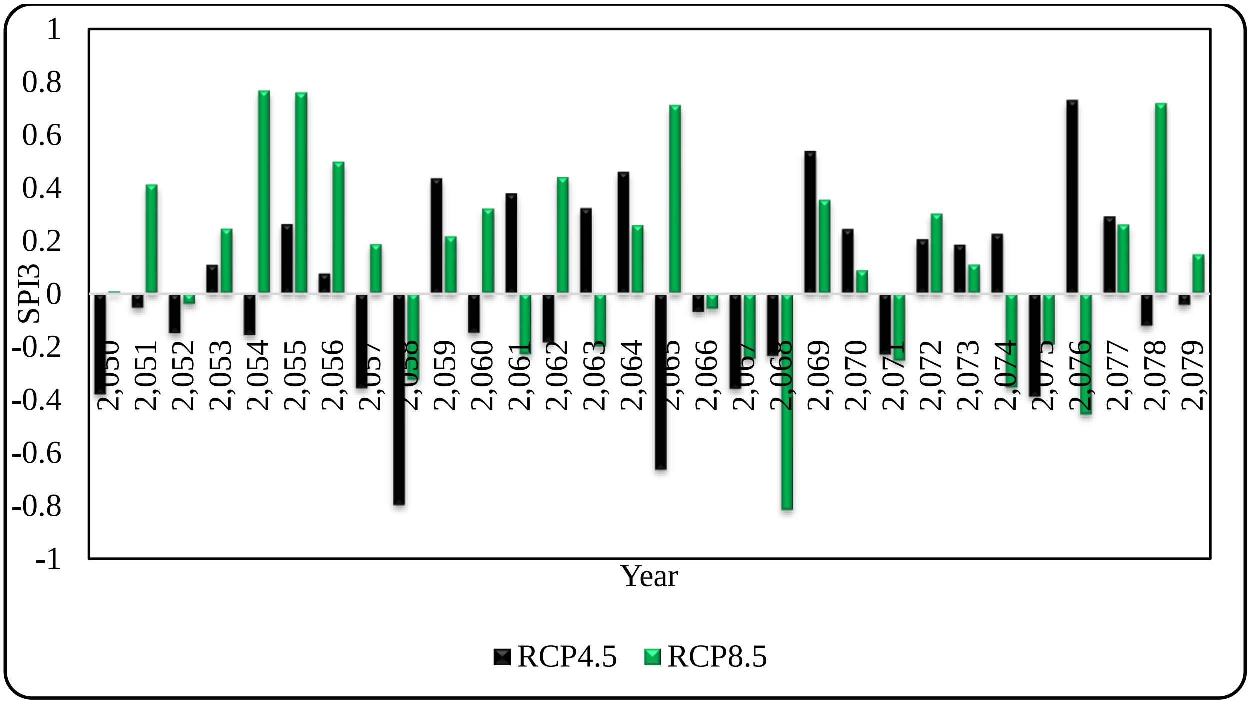

Figure 4.32. Average SPI-3 series for all future meteorological station data for the future (2050-2079)

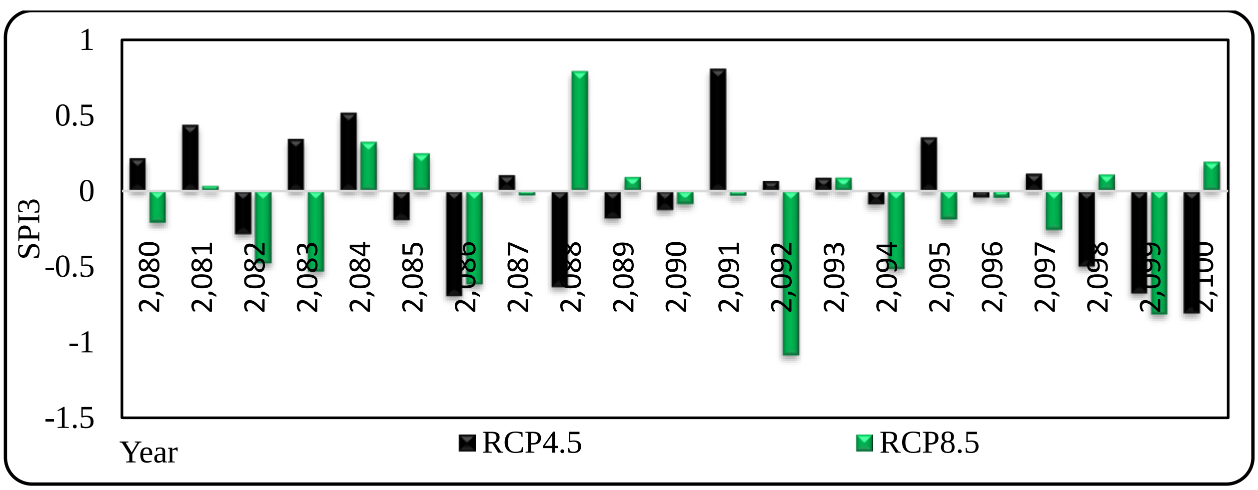

Figure 4.33. Average SPI-3 series for all future meteorological station data for the far future (2080-2100).

Here the change analysis is to refer a deviation of future climate condition from a historical (1985-2019) climate condition. Positive change indicates an increase from the historical period, whereas a negative change indicates a decrease from the historical period. The RCP 4.5 and RCP 8.5 drought projection noted a general negative increment pattern, except in the month of Dec/2084, Nov/2090, Jan/2070, Nov/2090 and Jul./2038, Oct./2038, Sep./2078, Oct./2035, Jul./2036 months which were observed extremely wet condition respectively according to the result of SPI3. As indicated in above fig.4.31- 4.33 of Feb/2076 (RCP4.5) and Aug/2078 (RCP8.5) under 2050-2079's, and Dec/2047(RCP4.5) and Jan/2048 (RCP8.5) under 2020-2049's shows positive increment in two RCPs, but Jul/2099(RCP8.5) and Jan/2100(RCP4.5) shows negative incremental of SPI3.

4.3.1. Characterizing SPI3 in terms of drought duration, severity and intensity for future data

Drought characteristics (duration, severity, and intensity) were analyzed using standardized precipitation index (SPI). The SPI series were computed in Central Rift Valley of Ethiopia from January 2020 to December 2100 at 3-, 6- and 12-month time scale to study the characteristics of drought.

Table 4.15. Summary of SPI with longest duration and severity for projected year at each station

Station Name (RCP4.5)	Time scale	Year	Duration in (months)	Severity
GP113212	SPI3	2059	9	-18.3
	SPI6	2069	11	-27.3
	SPI12	2070	12	-26.6
GP114211	SPI3	2076	8	-16.8
	SPI6	2076	10	-19.8
	SPI12	2025	12	-27.2
GP114212	SPI3	2083	6	-14.6
	SPI6	2076	5	-6.7
	SPI12	2083	8	-13.6
GP115212	SPI3	2090	7	-11.3
	SPI6	2070	8	-15.4

	SPI12	2090	8	-13.5
GP115212	SPI3	2070	10	-23.6
	SPI6	2090	8	-11.6
	SPI12	2091	7	-9.5

Table 4.16. Future drought properties based on the SPI3 (category for SPI according to (Table Table 2.1)

Station Name (RCP4.5)	Number of drought events				Max. Intensity	Year of Max. Intensity
	Near normal	Moderate	Severe	Extreme		
GP113212	605	95	41	21	-5.3	2038(Dec.)
GP114211	653	82	30	8	-4.6	2037(Dec.)
GP114212	662	72	26	15	-3.3	2038(Dec.)
GP115211	650	68	33	29	-3.43	2065(Apr.)
GP115212	662	75	41	22	-3.1	2037(Jul.)
Total	**3232**	**392**	**171**	**95**		
Station Name (RCP8.5)	Near normal	Moderate	Severe	Extreme	Max. Intensity	Year of Max.int.
GP113212	618	97	35	11	-3.4	2080(Dec.)
GP114211	661	79	24	11	3.7	2083(Oct.)
GP114212	655	95	16	4	-2.4	2083(Oct.)
GP115211	598	87	31	35	-4.7	2070(Apr.)
GP115212	610	98	36	19	-4.1	2094(Jun.)
Total	**3142**	**456**	**142**	**80**		

The drought and non-drought year was identified based on the value of SPI3. To show the spatial extent of droughts in the study area, SPI3 time series values of each meteorological station have been interpolated by Inverse Distance Weighted (IDW) method using the Spatial Analyst tool of ArcGIS.

Table 4.17. Non-drought and drought years according to SPI3 values near future (2020-2049)

RCP4.5	Good year/non drought year/						Drought year					
Station Name	Sep	Oct	Nov	Dec	Jan	Feb	Sep	Oct	Nov	Dec	Jan	Feb
GP113212	0.83	0.25	0.56	0.52	0.9	1.2	-2.3	-4.2	-3.4	-4.2	-1.3	-0.6
Year	2025						2022					
GP114211	0.98	1.59	1.64	1.59	0.83	0.07	-1.0	-1.6	-2.2	-3.6	-0.4	-0.4
Year	2025						2029					
GP114212	1.57	1.99	1.94	1.63	0.36	0.46	-0.8	-1.2	-2.4	-2.8	-0.8	-0.5
Year	2025						2029					
GP115211	0.87	2.69	1.7	1.54	0.56	0.16	-1.1	-0.5	-0.7	-0.2	-2.3	-1.3
Year	2020						2049					
GP115212	1.64	1.72	1.69	1.66	0.49	1.13	-0.9	-0.6	-0.2	-0.6	-0.9	-0.7
Year	2025						2026					
RCP8.5	Good year/non drought year/						Drought year					
GP113212	2.2	1.35	1.03	1.24	0.42	0.11	-2.1	-2.7	-2.4	-4	-3.2	-0.8
Year	2026						2046					
GP114211	2.08	3.35	1.09	0.52	0.02	0.54	-0.9	-2.6	-4	-1.7	-2.2	-0.4
Year	2035						2046					
GP114212	1.49	1.0	0.93	0.61	1.35	0.49	-0.1	-0.6	-3.7	-1.8	-0.8	0.10
Year	2038						2046					
GP115211	2.3	0.55	1.02	0.57	1.0	0.41	-2.4	-0.8	-0.9	-0.5	-1.0	-0.3
Year	2026						2046					
GP115212	0.25	0.76	1.00	1.12	1.59	0.72	-0.8	-0.9	-0.7	-0.9	-0.8	-0.6
Year	2048						2046					

From above (Table 4.17) results showed that 2022, 2029, 2049 and 2026 during September – February was drought years, whereas 2025 and 2020 was wet years for RCP4.5 and 2046 and 2026, 2035, 2038, 2026 was drought and wet years respectively for RCP8.5 scenario. From the fig. 4.35, it is evident that the extreme droughts observed at western part of study area according to the value of Standard precipitation index (SPI-3) over drought years for near future data in

September, October, November and December months for both RCP4.5 and RCP8.5 but for RCP8.5 data in November in addition to western part northern, southern and central part of study area shows extremely dry condition. Near normal drought were observed at eastern and central part of study area in these months. SPI3 values showed that severely dry conditions were observed in September and October at nearly western part, as well as in November and December at central part of study area for RCP4.5. But for RCP8.5 scenario severely dry conditions observed in December months at western and central part of study areas. Also, moderately dry condition analyzed in September, October, January and February months over drought years for RCP4.5 scenario which is not observed for RCP8.5. Whereas most of eastern and central part of study area for non-drought year indicate very wet and moderately wet (green, banana colors) in the study period from 2020 to 2049 for RCP4.5, as well as extremely wet condition observed at eastern part in October month. Also 100% and 60% of study area shows near normal drought for non-drought year in January and February months (fig. 4.35a). But extremely wet condition observed in September and October months for RCP8.5(fig.4.35b) and also there was very wet condition in September, October and January months at this scenario. 100% of results showed that moderately wet condition in November and near normal condition in February.

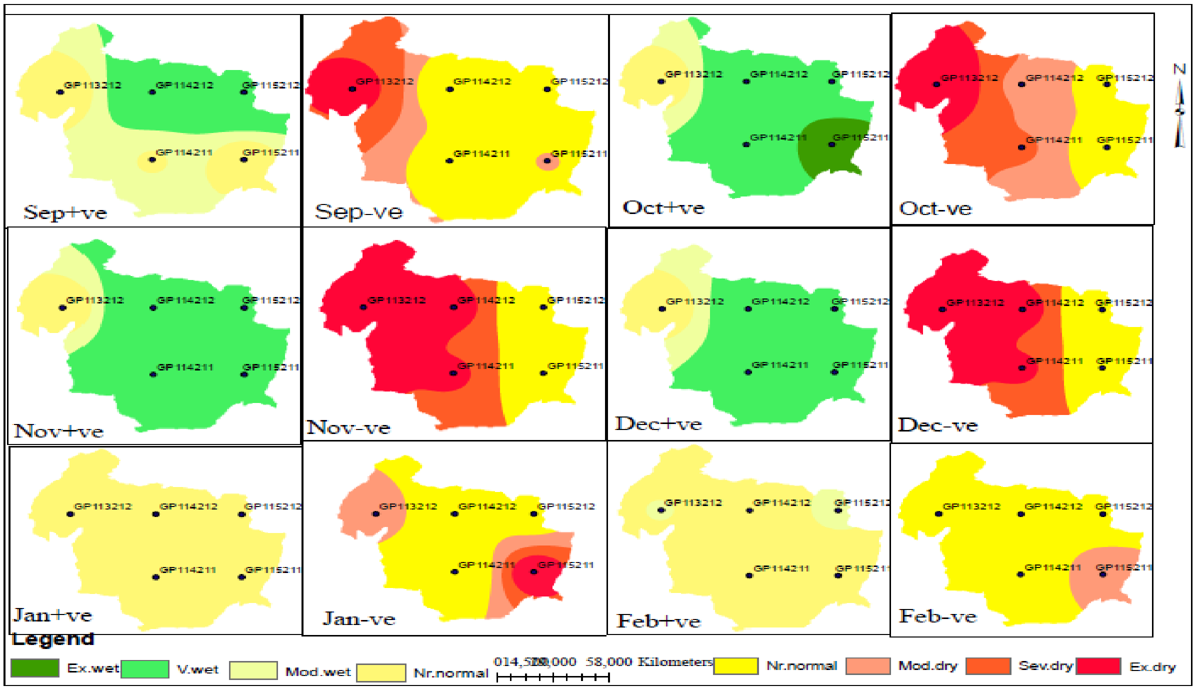

a.) RCP4.5

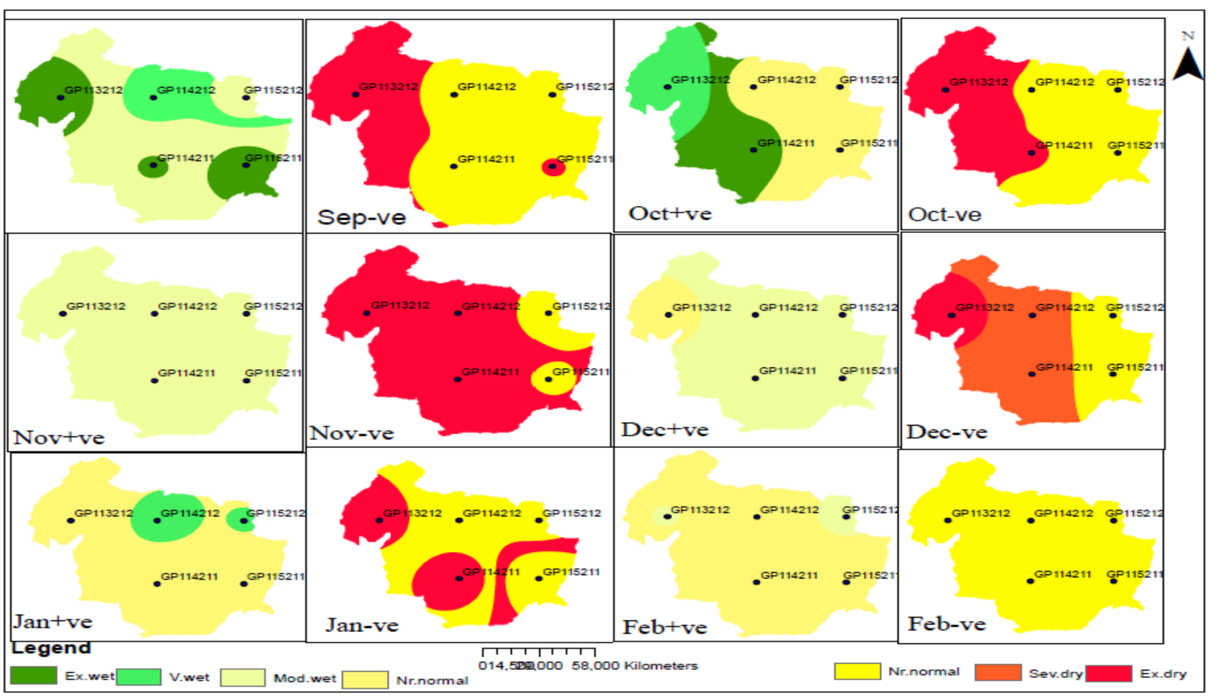

b.) RCP8.5

Figure 4.35. Projected change in drought according to three month variation of Standard precipitation index (SPI3) values over drought and non-drought years for 2020-2049 under emission scenario of both RCP 4.5 and RCP8.5

Table 4. 18. Non-drought and drought years according to SPI3 values mid future (2050-2079)

RCP4.5	Good year/non drought year/						Drought year					
Station Name	Sep	Oct	Nov	Dec	Jan	Feb	Sep	Oct	Nov	Dec	Jan	Feb
GP113212	1.06	1.38	1.27	1.52	0.9	0.9	-3.1	-0.6	-0.8	-0.8	-0.6	-0.3
Year	2076						2058					
GP114211	0.38	1.3	0.76	0.39	0.78	0.9	-2.5	-1.7	-0.5	-0.7	-0.8	0.30
Year	2076						2058					
GP114212	0.9	1.8	0.87	0.53	0.71	0.78	-1.3	-0.5	-0.5	-0.9	-0.5	-0.2
Year	2076						2065					
GP115211	3.41	2.82	2.70	2.67	0.9	0.63	-1.8	-0.7	-0.7	-0.1	-0.1	-0.4
Year	2069						2058					
GP115212	2.60	2.63	2.69	2.61	0.89	0.40	-0.6	-0.9	-0.7	-1.4	-0.1	-0.2
Year	2069						2065					
RCP8.5	Good year/non drought year/						Drought year					
GP113212	1.51	1.54	1.55	0.8	2.3	2.10	-1.1	-2.9	-1.3	-0.4	-2.6	-0.9
Year	2054						2061					
GP114211	0.04	0.61	1.5	0.71	1.91	2.85	-1.1	-1.8	-2.2	-0.9	-1.6	-1.1
Year	2054						2068					
GP114212	0.42	0.81	1.57	0.02	1.50	2.37	-1.5	-1.7	-0.7	-0.6	-2.5	-0.6
Year	2078						2068					
GP115211	0.3	0.51	0.89	0.87	2.46	2.6	-2.5	-2.3	-1.0	-0.4	-1.4	-1.0
Year	2054						2068					
GP115212	0.57	0.84	0.99	0.30	2.04	1.8	-3.5	-1.9	-2.7	-0.5	-2.1	-0.3
Year	2055						2068					

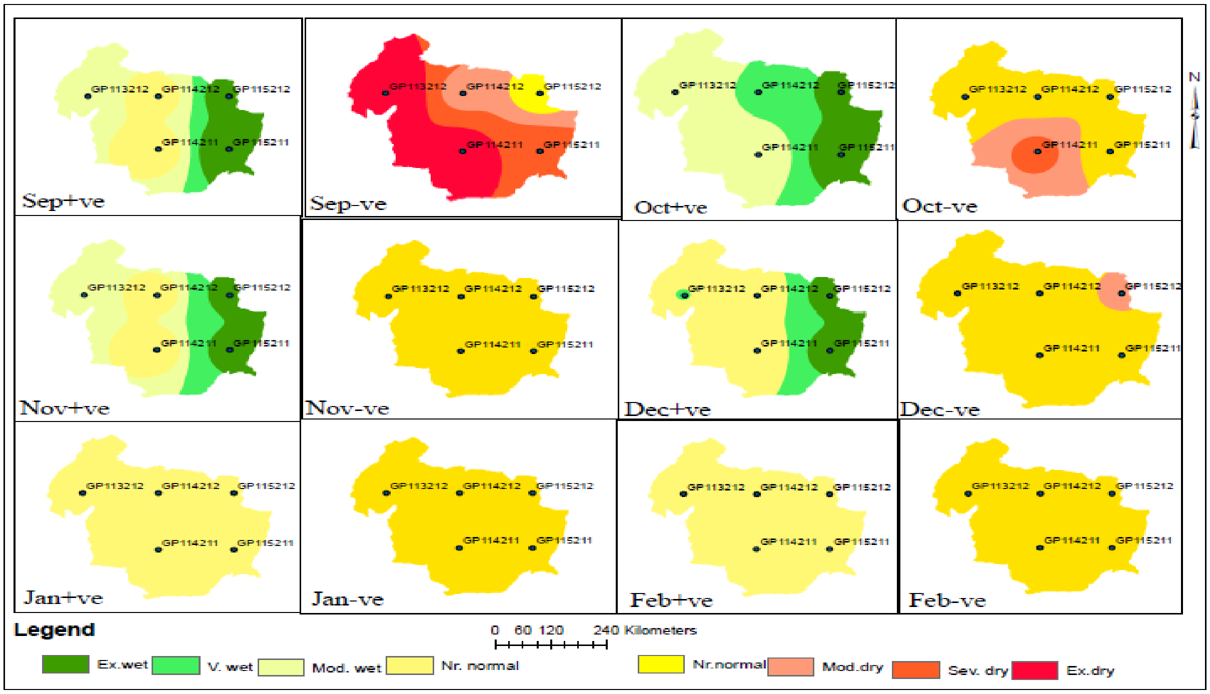

a.) RCP4.5

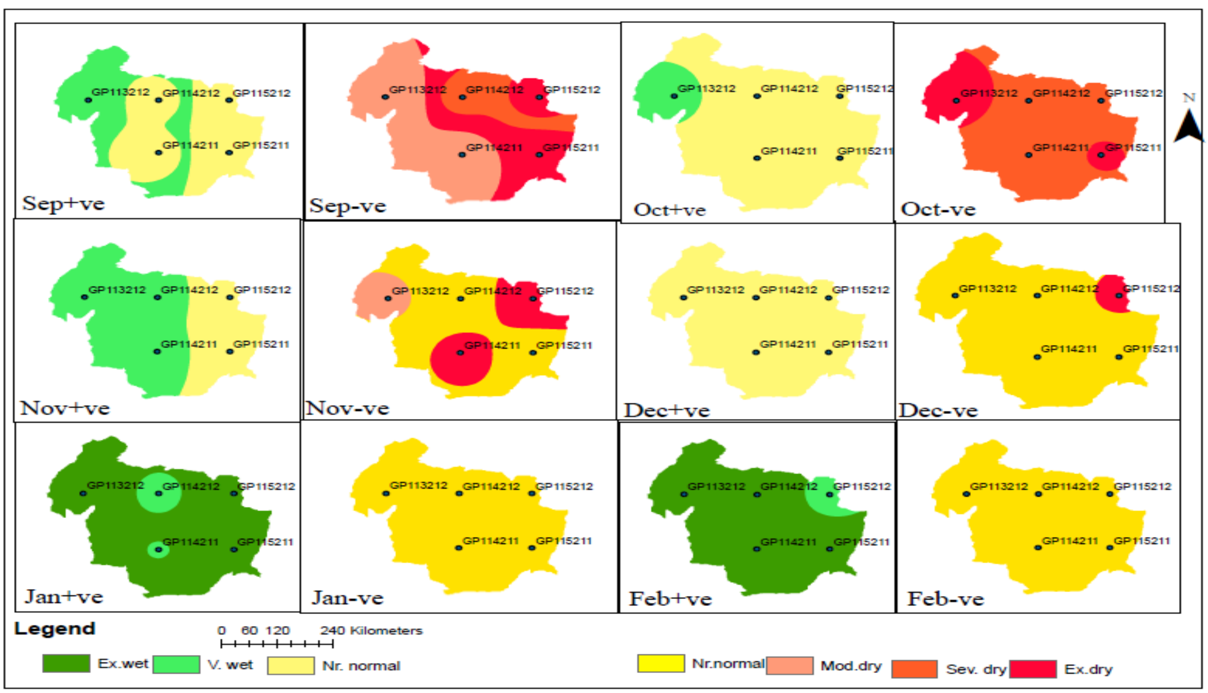

b.) RCP8.5

Figure 4.36. Projected change in drought according to three monthly variation of Standard precipitation index (SPI3) values over drought and non-drought years for 2050-2079 under m emission scenario of both RCP 4.5 and RCP8.5

Results shown in (**Table 4. 18),** in 2058 and 2065 during September – February was drought years, whereas 2076 and 2069 was wet years for RCP4.5 and 2061,2068 and 2054, 2078, 2055 was drought and wet years respectively for RCP8.5 scenario. In fig. 4.36, results showed that the extreme droughts were observed in western and south west part of CRV at drought years in September months as well as in October and December months there were moderate and severe drought situation observed for RCP4.5 scenario. Also 80% of December month and 100% of the November, January and February months shows near normal drought according to the value of Standard precipitation index (SPI-3) over drought years. For RCP8.5 scenario extremely dry condtion observed in september, october, november and december months as well as severely dry conditions observed in september and October months at northern and southern, eastern and central part of study areas. Also, moderately dry condition analyzed in September and november months over drought years for RCP8.5 scenario which is observed in september, october and december for RCP4.5. Whereas eastern part of study area for non-drought year indicates extremely wet and very wet in September, October, November and December months at RCP4.5 scenario which was observed for RCP8.5 in january, feburary, september, october and december months. Moderately wet droughts for non-drought year were observed in western and central part of study area in September, October and November months which is not observed in RCP8.5. 100% of study area shows near normal drought for non-drought year in January and February months for all station in RCP4.5, but as we observe from above fig.4.36 for RCP8.5 scenario extrmely wet and very wet condtion was observed in these months.

Note:- In fig.4.35, 4.36 Nr normal meaning near normal, mod wet meaning moderately wet, v. wet meaning very wet, ex wet meaning extremely wet, sev dry meaning severely dry, Ex. dry meaning extremely dry and Mod. dry meaning moderately dry, (+ve) meaning non drought year, (-ve) meaning drought year.

4.4.Non-parametric Trend test for Projected Meteorological Drought

According to the Z-values the trend test statistics taken on annual mean rainfall of RCP4.5 comparatively shows insignificantly increasing trend but RCP 8.5 shows significantly decreasing trend with the S-test value of -158 and with the Z-value is |Z|> 1.96 for 95% confidence level for near future projected climatic data. The tabular representation of the future two RCPs trends of long year means annual RF were shown below for near future (2020-2049), mid future (2050-2079) and far future (2080-2100) period of year.

Table 4.20. MK trend test results of rainfall under two RCPs (2020-2049) near future

Statistics	RCPs from (2020-2049)	
	RCP4.5	RCP8.5
Z-test	+0.72	-1.98
Significancy	Not significant	significant
S-test	56	-158

(–), (*) and (+) indicates decreasing, not significant and increasing trend

Table 4. 21. MK trend test results of rainfall under two RCPs (2050-2079) mid future

Statistics	RCPs from (2050-2079)	
	RCP4.5	RCP8.5
Z-test	-1.67	+0.66
Significancy	significant	Not significant
S-test	-102	+88

5. SUMMARY AND CONCLUSION

5.1. Summary

Drought is a natural and recurrent feature of climate, which characterized by its severity, duration and intensity. It is a deficiency in precipitation over an extended period, usually a season or more, resulting in a water shortage causing adverse impacts on vegetation, animals, and/or people. It can be categorized into four major categories related to precipitation (meteorological), soil moisture (agricultural), stream flow (hydrological) and socioeconomic droughts.

Meteorological droughts are quite common, and they are primarily classified by the extent of dryness in a given location and the length of the dry period. Although agricultural drought is linked to a lack of water needed to support crops, the drought does not always coincide with meteorological drought.

This thesis presents a study to identify past and projected meteorological drought using the standardized precipitation index (SPI) and Man-Kendall program to test drought trend as well as to show the spatial extent of droughts in the study area, SPI3 time series values of each meteorological station have been interpolated by inverse distance weighted (IDW) method using the spatial analyst tool of Arc GIS in the Central Rift Valley of Ethiopia.

The overall study was conducted in the four steps. First, a brief description of the study area showing the general characteristics of topographic, physiographic characteristics and the climate. Second, the data needed for the study were identified and collected from the available sources which is followed by proper data quality controls. Third, the overall characteristics of the collected meteorological data were evaluated on monthly, seasonal and annual time steps as needed. Finally, the fourth step is to conduct SPI determination, trend analysis using appropriate methodologies. To do that, we decided to firstly project the meteorological variables (precipitation,) which needed to determine SPI from the 1985s to 2019 and 2020-2100, thereafter compute the selected indicators (the SPI) on a monthly basis for these periods by using Rstudio software. By using historical precipitation data (monthly) from Ethiopian National Meteorological Agency during 1985-2019 and projected climatic data from coordinated regional climate downscaling experiment (CORDEX) series of daily precipitation from 2020 to 2100, which converted to monthly time series and have been used to compute selected drought indicators, afterward the historical drought and future drought identified according to Tom McKee drought classification for the Arsi Negele, Bulbula, Koshe, Langano, Tora, Ziway, Assela, Degaga and Kulamsa meteorological station as well as for projected climate data.

Drought events classified in seven magnitude classes, i.e., if SPI ranges between 1.5 and 1.99, it is very wet; 1.00 and 1.49, it is moderate wet; -0.99 and 0.99, it is near normal; -1.00 and -1.49, it is moderately dry; -1.5 and -1.99 severely dry and extreme drought if SPI is -2.00 or less as well as extremely wet if SPI value greater than two.

Based on SPI value calculated for 9 meteorological stations in Central Rift Valley of Ethiopia from January 1985 to December 2019 and January 2020 to December 2100 at 3- month time scale to study the characteristics of drought, results showed that (1991-1992), (2015-2016), (2017-2018) and 2019 were drought year for historical data and for projected climatic data in near future (2022, 2029 and 2046) in future (2058, 2065 and 2061,2068) and in far future (2099, 2085 and 2099,2083) which were among the drought years for both RCP4.5 and RCP8.5 respectively. Most of the drought years were associated for each station; even if for some station the occurrence of drought year varies by one year or more.

Almost all station indicts there was drought index in the study area even though the drought severity degree was different. The SPI value obtained in Arsi Negele station showed an extreme drought during 2015, 2016 and 2017 in October, December, march and Jun months for SPI3, SPI6, SPI12 and SPI1 value respectively which where, -3.01, -3.13, -3.03 and -2.81. Also, there were notable, SPI value was obtained in 2013, 2014, and 1991, which were -1.79, -1.62, -1.8 and -1.73 considered to be severely dry condition. For Assela station maximum drought obtained during 1991, 2008 and 2003 in November, April and February months for SPI3, SPI6 and SPI12 value respectively were -3.32, -2.71, -2.6 and -3.13 which were considered to be a situation of extreme drought. For Bulbula station standardized precipitation index values during 2014,2015 and 2016 at July, August, April and August months for SPI3, SPI6 and SPI12 value respectively were -3.42, -2.85 and -2.74 which were considered to be a situation of extreme drought. At Dagaga station in 2018, 2017, 2018 and 2019 at September, December and march SPI3, SPI6, SPI12 values were -3.33, -3.3 and -4.42 which identified as extreme drought condition. Also, severely dry condition observed in 2009, 1991 and 1985 respectively at (April, August and May).

The value of SPI-3 showed that 48 to 83, drought events occurred during 1985-2019, and most of the droughts recorded in Arsi Negele station followed by Ziway, Tora, Kulmsa, Assela, Degaga, Koshe, Bulbula and Langano. In addition, during this year, 48 to 93 and 42 to 93 drought events were recorded in six months and twelve months' time scale respectively. SPI-3, SPI-6 and SPI-12 value indicated that most of the drought events occurred in Arsi Negele meteorology station.

The highest severity recorded at the Dagaga meteorological station in 2018 at SPI12 which was -32.30. SPI12 showed maximum drought duration at Arsi Negele in 2015 and 2017 which is 12 months with severity of -25.7 as well as at Bulbula in 2016 with severity -18.3.

The MK trend test on observed period monthly rainfall result reveals that no trend, insignificantly decreasing trend over certain meteorological station and increasing trend too. In Arsi Negele station monthly share of rainfall exhibited about 33.33% no trend, 50% negative trend, 8.33% not significant negative trend and 8.33% not significant positive trend in rainfall amounts and seasonal rainfall variability for Belg, Kiremt, and Bega seasons was -1.3241mm/season, -1.8589mm/season and -0.8046mm/season respectively. The MK trend test showed that at Assela station there was a statically not significant trend observed for all months at a 95% level of confidence and seasonal rainfall variability for Belg, Kiremt, and Bega seasons were -0.05mm/season ,0.0358mm/season and –0.2793mm/season respectively. At Bulbula station the monthly share of rainfall exhibited about 66.67% no trend, 25% negative trend, 8.33% in rainfall amounts and seasonal rainfall variability for Belg, Kiremt, and Bega seasons was 0.0972mm/season, -1.1715mm/season and -0.2823mm/season respectively. The monthly share of rainfall at Dagaga station exhibited about 50% no trend, 25% negative trend, 25% not significant negative trend in rainfall amounts.

The RCP 4.5 and RCP 8.5 drought projection noted a general negative increment pattern, except in the month of Dec/2084, Nov/2090, Jan/2070, Nov/2090 and Jul./2038, Oct./2038, Sep./2078, Oct./2035, Jul./2036 months which were observed extremely wet condition respectively according to the result of SPI3.

The highest severity recorded at the GP113212 meteorological station in 2069 at SPI6 which was -27.3. SPI12 showed maximum drought duration at GP113212 in 2070 which is 12 months with severity of -26.6 as well as at GP114211 in 2025 with severity -27.2. SPI3 values of drought years showed that severely dry conditions in September and October at nearly western part, as well as in November and December at central part of study area for RCP4.5. But for RCP8.5 scenario severely dry conditions observed in December months at western and central part of study areas. Results showed that the western part of Central Rift Valley is projected to be drier in the near future than in the recent past, also, the SPI value indicated that, the central and eastern part of the study area were projected to be wetter, in particular around Kulmsa, Ziway, Dagaga and Assela.

According to the Z-values the trend test statistics taken on annual mean rainfall of RCP 8.5 shows significantly decreasing trend with the S-test of -158, Z-test of -1.98 and with the Z-value |Z|> 1.96 at near future, (S-test= -122, Z=-2.3) at far future for 95% confidence level. But RCP4.5 shows decreasing trend at mid future (S-test=-106, Z= -1.67) for |Z|> 1.64 at 90% confidence level.

5.2. **Conclusion**

Based on standardized precipitation index value calculated for 9 meteorological stations results showed that (1991-1992), (2015-2016) and (2017-2018) were drought year and extremely, severely, moderately and near normal drought condition were observed in these year for historical rainfall data.

The average monthly share of rainfall in CRV showed about, 71.3% no trend, 16.67% decreasing trend, 7.4% not significant decreasing trend 1.85% increasing trend and 2.8% not significant increasing trend in historical period.

For projected climatic data in near future (2022, 2029 and 2046) in future (2058, 2065 and 2061,2068) and in far future (2099, 2085 and 2099,2083) which were among the drought years for both RCP4.5 and RCP8.5 respectively.

The trend test statistics taken on annual mean rainfall of RCP 8.5 shows significantly decreasing trend with the S-test of -158, Z-test of -1.98 and with the Z-value |Z|> 1.96 (95% confidence level) at near future, (S-test= -122, Z=-2.3) at far future. But RCP4.5 shows decreasing trend at mid future (S-test=-106, Z= -1.67) for |Z|> 1.64 (at 90%) .

5.3. Recommendations

Based on the findings of this thesis, the trends of meteorological drought increase from year to year in most of studded area station, so that it is importance to recommended the following: -

- Governmental and non-governmental sectors which are working with these issues evaluate the risk of drought and revise drought preparedness and response plan every year.
- For rural farmers who have been vulnerable to drought, water stress and erratic nature of rainfall, appropriate adaptation strategies should have to be designed and implemented.

Generally, this research was conducted for identification of meteorological drought by using standardized precipitation index (SPI) which is only require precipitation data as an input rather than considering temperature, water-balance component (ET/PET). Because of this limitation, directions for future research to improve our understanding of droughts and their impacts in different economic sectors should include efforts to improve and extend the database of past drought events and their impacts.

REFERENCES

Abdourahamane, Z. S. and Acar, R. (2018). Analysis of meteorological drought variability in Niger and its connection with climate indices, Hydrological Sciences Journal, 63(8), pp. 1203–1218. doi: 10.1080/02626667.2018.1489542.

Adisa, O. M., Botai, J. O., Adeola, A. M., Botai, C. M., Hassen, A., Darkey, D., Tasfamariam, A. T., Adisa, A. T., & Adisa, A. F. (2019). Analysis of drought conditions over major maize pro-ducing provinces of South Africa.Journal of Agriculture Meteorology, 75, 173–182. https://doi.org/10.2480/agromet.D-18-00049

Amsalu, S. (2019). Review on the Cause and Effects of Recurrent Drought on Ethiopian.

Araya, A., Stroosnijder, L., Girmay, G., Keesstra, S.D. (2011). Crop coefficient, yield response to water stress and water productivity of teff (Eragrostis tef (Zucc.)). Agric Water Manag 98,775–783.

Araya, A., Stroosnijder, L., Habtu, S., Keesstra, S.D., Berhe, M., Hadgu, K.M. (2012). Risk assessment by sowing date for barley (Hordeum vulgare) in northern Ethiopia. Agric For Meteorol 154, 30–37.

Araya, A., and Stroosnijder, L. (2011). Assessing drought risk and irrigation need in northern Ethiopia. Agric. For. Meteorol. 151, pp.425 – 436.

Arnell, N.W. & Reynard, N.S. (2016). The Effects of Climate Change Due to Global Warming on River Flows in Great Britain. Journal of Hydrology. pp 397-424.

Ayenew, T., & GebreEgziabher, M. (2015). Morphometric Characteristics and Hydrology of Selected Ethiopian Rift Lakes (pp. 275-287).

Ayenew, T. (2002). Recent changes in the level of Lake Abiyata, central main Ethiopian Rift.Hydrological Sciences-Journal'des Sciences Hydrologiques, 47(3) 493-503. journal of hydrology pp. 418–429.doi: 10.1016/j.jhydrol.2013.10.052.

Baloutsos, G., Gountoufas, E., and Kaimaki, S. (1993). Characteristics of Meteorological Droughts of the Last 132 Years in the Plain of Attika, Greece, Geotechnical Scientific Topics, 4(2), Geotechnical Chambre of Greece.

Batisani, N. and Yarnal, B. (2010). Rainfall variability and trends in semi-arid Botswana: implications for climate change adaptation policy. Applied Geography, 30(4), pp.483-489.

Belay, A. et al. (2021). Analysis of Climate Variability and Trends in Southern Ethiopia, Climate, 9(6), p. 96. doi: 10.3390/cli9060096.

Belayneh, A. et al. (2014). Long-term SPI drought forecasting in the Awash River Basin in Ethiopia using wavelet neural network and wavelet support vector regression models.

Benson C, Clay EJ. (1998). The impact of drought on sub-Saharan African economies: a preliminary examination. World Bank Technical Paper 401, Library of Congress Cataloging, Washington D.C., ISBN 0-8213-4180-4, ISSN 0253-7494.

Birsan, M.-V., Molnar, P., Burlando. (2017). Streamflow trends in Switzerland. J. Hydrol. 2005, 314, pp.312–329.

Blackmore, D. and Sadoff, C. (2013). Implications of climate change for water resources development in the Ganges basin, 15, pp. 26–50. doi: 10.2166/wp.2013.107.

Blumenstock, G. (1942). Drought in the United States analyzed by means of the theory of probability, Technical Bulletin No. 819, U.S. Department of Agriculture. Campbell, D., 1968, Droughts, Causes, Effects, Solutions. F. W. Cheshire,Melbourne, Australia.

Bobadoye, A.et al. (2019). Assessment of Meteorological drought using Standardized Precipitation Index (SPI) in Kajiado County, Keny, Journal of Forestry Research and Management, 16(1), pp. 154–163.

Boko M et al., (2007). Africa in Parry M L et al. Climate Change 2007: Impacts, Adaptation and Vulnerability. Contribution of Working Group II to the Fourth Assessment Report of the Intergovernmental Panel on Climate Change, Cambridge, Cambridge University Press. Pp.433-467.

Bordi, I., K., Fraedrich, and A. Sutera. (2009). Observed drought and wetness trends in Europe: an update, Hydrology and Earth System Sciences, 13, pp.1519–1530.

Bordi, I., S. Frigio, P. Parenti, A. Speranza, and A. Sutera. (2001). The analysis of the Standardized Precipitation Index in the Mediterranean area: large-scale patterns, Annalidi Geofisica, 44(5-6), 979–993.

Brunetti M., Caloiero, T., Coscarelli, R., Gullà, G., Nanni, T. and Simolo, C. (2016). Precipitation variability and change in the Calabria region (Italy) from a high-resolution daily dataset. Int. J. Climatol. 2012, 32, 57–73. [CrossRef].

Burke, E. (2011). Understanding the sensitivity of different drought metrics to the drivers of drought under increased atmospheric CO2, Journal of Hydrometeorology, 12(6), pp.1378–1394.

Burke EJ, Brown SJ. (2008). Evaluating uncertainties in the projection of future drought. Journal of Hydrometeorology 9(2): pp.292-299.

Cacciamani C, Morgillo A, Marchesi S. Pavan V. (2007). Monitoring and forecasting drought on a regional scale: Emilia-Romagna region. Methods and tools for drought analysis and management. Springer.

Campbell, D. (1968). Droughts, Causes, Effects, Solutions. F. W. Cheshire, Melbourne, Australia

Chimdesa, G. (2016). Climate Change Impacts and Adaptation Actions in Central Rift Valley of Ethiopia, 6(3), pp. 84–93.

Chopra, P. (2006). Drought Risk Assessment Using Remote Sensing and GIS: Available at: http://www.itc.nl/library/papers_2006/msc/iirs/chopra.pdf.

Chu, J., Xia, J., Xu, C.-Y., and Singh, V. (2010). Statistical downscaling of daily mean temperature, pan evaporation and precipitation for climate change scenarios in Haihe River, China. Theoretical and Applied Climatology, 99(1-2), 149-161.

Collins, W., et al. (2011). Development and evaluation of an Earth-system model–HadGEM2, Geosci. Model Dev, pp.1051–1075.

Conway, D., Mould, C., Bewket,W. .(2004). Over one century of rainfall and temperature observations in Addis Ababa, Ethiopia. Int. J. Climatol. 24: 77-91.

Conway, D. (2000). The climate and hydrology of the Upper Blue Nile, Ethiopia. Geog. J. 166, pp. 49-62.

Conway, D., Schipper, E.L.F. (2011). Adaptation to climate change in Africa: Challenges and opportunities identified from Ethiopia. Global Environmental Change 21, pp. 227-237.

Dai, A. (2011). Drought under global warming: a review, Wiley Interdisciplinary Reviews: Climate Change, 2(1), pp.45–65.

Demenocal, P. B. (2001). Cultural responses to climate change during the late Holocene. Science, 292(5517), pp. 667-673.

Feye Lema. (2021). Trend Analysis of Hydro-Meteorological Data p.36. (URl http://etd.aau.edu.et/handle/123456789/26724).

Fitsum. (2020). Wetland Management in the Central Rift Valley of Ethiopia.

Fleig, A. L. Tallaksen, H. Hisdal, and S. Demuth. (2006). A global evaluation of stream-flow drought characteristics, Hydrology and Earth System Sciences.

Frederick, K., and D. Major. (1997). Climate Change and Water Resources, Climatic Change.

Frieler, K., M. Meinshausen, T. Schneider von Deimling, T. Andrews, and P. Forster. (2011). Changes in global-mean precipitation in response to warming, greenhouse gas forcing and black carbon, Geophysical Research Letters.

Gebre SL, Getahun YS. (2016). Analysis of Climate Variability and Drought Frequency Events on Limpopo River Basin, South Africa.

Gebrehiwot, T., Veen, A. Van Der, & Maathuis, B. (2011). International Journal of Applied Earth Observation and Geoinformation Spatial and temporal assessment of drought in the Northern highlands of Ethiopia pp.309–321.

Gemechu, T. et al. (2015). The Current and Future Trend of Rainfall and Its Variability in Adami-Tulu Jido-Kombolcha Woreda.

Giannini, A., Biasutti, M., and Verstraete, M. M. (2008) A climate model-based review of drought in the Sahel: desertification, the re-greening and climate change, Global Planet. Change, 64,5 p119–128.

Gidey, E., Dikinya, O., Sebego, R., Segosebe, E., & Zenebe, A. (2018). Predictions of future meteorological drought hazard (*2070) under the representative concentration path (RCP) 4.5climate change scenarios in Raya, Northern Ethiopia.ModelEarth System and Environment, 4, 475–488. https://doi.org/10.1007/s40808-018-0453-x.

Giorgi et al., F. Giorgi, C. Jones, G.R. Asrar, (2009). Addressing climate information needs at the regional level: the CORDEX framework World Meteorological Organization (WMO) Bulletin, 58 (2009), p. 175.

Glantz, M. H. (1966). The Policy of National Disaster: The Case of the Sahel Drought, Praeger, New York.

Greene M. (1974). Impact of the Sahelian drought in Mauritania West Africa.

Guhathakurta, P., Pai, D. S. and Rajeevan, M. N. (2017). Variability and Trends of Extreme Rainfall and Rainstorms, Springer Geology. doi: 10.1007/978-981-10-2531-0_3.

Guteirrez, Anna P.A., Engle, Nathan L., Erwin De Nys, Molejon, Carmen, Martins,Edwardo Savio, .2014. Drought Preparedness in Brazil. Published in Weather and Climate Extremes. Elsevier 2014.

Guttman, N.B. (1999). Accepting the standardized precipitation index: a calculation algorithm, JawraJournal of the American Water Resources Association, Vol. 35 No. 2, pp. 311-322.Meteorological drought assessment.

Haied, N. et al. (2017). Drought assessment and monitoring using meteorological indices in a semi-arid region', Energy Procedia, 119, pp. 518–529. doi: 10.1016/j.egypro.2017.07.

Haile, G. G., Tang, Q., Hosseini-Moghari, S. M., Liu, X., Gebremicael, T. G., Leng, G., Kebede, A., Xu, X., & Yun, X.(2020b). Projected impacts of climate change on drought patternsover East Africa.Earth's Future, 8(7), e2020EF001502.

Halim, N.S. (2010). AgricultureMeetingtheWaterChallenge.http://water.jhu.edu/magazine/agriculturemeeting-the-water.

Hamed, K. H. and Rao, A. R. (1997). A modified Mann-Kendall trend test for autocorrelated data', Journal of Clinical Oncology, 36(15_suppl), pp. 522–522. doi: 10.1200/jco.2018.36.15_suppl.522.

Harou J.J. Medellín Azuara J, Zhu T, Tanaka SK, Lund JR, Stine S, Olivares MA, Jenkins MW. (2010). Economic consequences of optimized water management for a prolonged, severe drought in California. Water Resources Research 46(5), May 2010.

Harrigan, S. et al. (2019). Using R in hydrology: a review of recent developments and future directions, Hydrology and Earth System Sciences, (February), pp. 1–33.

Hasegawa, A., Gusyev, M. and Iwami, Y. (2016). Meteorological drought and flood assessment using the comparative SPI approach in Asia under climate change, Journal of Disaster Research, 11(6), pp. 1082–1090. doi: 10.20965/jdr. 2016.p1082.

Hassanzadeh, H., Eslamian, S., Abedi-Koupaei, J., and Gheysari, M. 2011. (2011). Application of L-moment for evaluating drought indices of cumulative precipitation deficit (CPD) and maximum precipitation deficit (MPD) based on regional frequency analysis. International Journal of Hydrology Science and Technology, 1(1):88-104.

Hayes, M. J. and Svoboda, M. D., (1999). Monitoring the 1996 drought using the Standardized Precipitation Index. BAMS Vol. 80. pp. 429-438.

Haylock, D. Collins, B. Trewin, F. Rahimzadeh, A. Tagipour, K. Rupa Kumar, J.Revadekar, G. Griffiths, L. Vincent, D. Stephenson, J. Burn, E. Aguilar, M. Brunet, M. Taylor, M. New, P. Zhai, M. Rusticucci, and J. Vazquez-Aguirre (2006), Global observed changes in daily climate extremes of temperature and precipitation, Journal of Geophysical Research, 111, D05,109.

Heim, R. R. J. (2000). Drought Indices Assessment", Routledge. Vol.1, pp. 159-167.

Heim Jr. RR. (2002). A review of twentieth-century drought indices used in the United States. Bulletin of the American Meteorological Society p: 1149-1165.

Held, I., and B. Soden. (2006). Robust Responses of the Hydrological Cycle to Global Warming, Journal of Climate, 19(21), pp.5686–5699.

Hengsdijk, H., van Driel, J., Haile, A., Argaw, M., & Jansen, H. (2010). Competing claims for water resources in the Central Rift Valley of Ethiopia: Global drivers and local opportunities. Wageningen: Plant Research International.

Hengsdijk, H., Legesse, D. and Jansen, H. (2007). 'Ethiopian Central Rift Valley: Current status, developments and policy implications', Plant research International.

Hirabayashi, Y., S. Kanae, S. Emori, T. Oki, and M. Kimoto. (2008). Global projections of changing risks of floods and droughts in a changing climate, Hydrological Sciences Journal, 53(4), 754–772.

Hirsch, R. M. and Slack, J. R. (1984). A Nonparametric Trend Test for Seasonal Data With Serial Dependence', Water Resources Research, 20(6), pp. 727–732. doi: 10.1029/WR020i006p00727.

Hoerling, M., and A. Kumar. (2003). The perfect ocean for drought, Science, 299(5607), pp.691–694.

Hong, X. Guo, S. (2015). Spatial and temporal analysis of drought using entropy-based standardized precipitation index: A case study in Poyang Lake basin, China.

[https://www.r-project.org/foundation/Rfoundation-statutes.pdf (2021) 28 March, at 23:55 (UTC]

Ibrahim, A. M. (2001) Contract Research project on Application of Agro-ecological Zones Database in Drought Management and Water Availability Assessment, Bangladesh Agricultural Research Council (BARC) and Ministry of Water Resources, Government of Bangladesh, pp. 2-8.

IFPRI, (2012). Zambia: Private agricultural research and innovation. Country Note, June. Rome: Agricultural Science and Technology Indicators (ASTI). International Food Policy Research Institute (IFPRI). Impact Assessments Opportunities and Challenges. Climate and Development, 4(1), pp.26-39.

IPCC, (2007). The Physical Science basis and Contribution of Working Group I to the Fourth Assessment Report of the Intergovernmental Panel on Climate Change.

IPCC (2012). Managing the Risks of Extreme Events and Disasters to Advance Climate Change Adaptation, in: A Special Report of Working Groups I and II of the Intergovernmental Panel on Climate.

Isabella bordi, Sandro Frigio, Patrizia Parenti, Antonio Speranza and Alfonso Sutera, (2001). The analysis of the Standardized precipitation Index in the Mediterranean area: large-scale Patterns. Annali Di Geofisica, Vol.44, N.5/6.

James Verdin (2007). Drought Mapping, Assessment and Monitoring -2nd Asian Ministerial Conference on Disaster Risk Reduction, New Delhi

Jang Y.K. Kim, S.D. (2006). A Study of Drought Spatio-temporal Characteristics Using SPI-EOF Analysis. J. Korea Water Resour. Assoc. 2006, 39, pp.691–702.

Jansen, H., Hengsdijk, H., Legesse, D., Ayenew, T., Hellegers, P., & Spliethoff, P. (2007). Land and water resources assessment in the Ethiopian Central Rift Valley. Project: ecosystems for water, food and economic development in the Ethiopian Central Rift Valley. Wageningen, Alterra, Alterra-rapport 1587, ISSN 1566-7197.

Johannes GM, Mebratu K (2009) Local innovation in climate change adaptation by Ethiopian pastoralists. PROLINNOVA-report, Addis Ababa, Ethiopia.

Jones P.G., Thornton P.K. (2000). MarkSim: software to generate daily weather data for Latin America and Africa. Agron J 92: pp.445–453.

Jones P.G., Thornton, P.K. (2013). Generating downscaled weather data from a suite of climate models for agricultural modeling applications.

Jones, P.G., Thornton, P.K. (2003). The potential impacts of climate change in tropical agriculture: the case of maize in Africa and Latin America in 2055. Global Environ. Change 13, pp 51–59.

Jubb, I., Canadell, P. and Dix, M. (2013). Representative Concentration Pathways.Australian Government, Department of the Environment, pp. 1–19.

Kendall, S. B. (1975). Enhancement of Conditioned Reinforcement by Uncertainty 1, Journal of the Experimental Analysis of Behavior, 24(3), pp. 311–314. doi: 10.1901/jeab.1975.24 311.

Karamouz, M., Nazif S., Fallahi, M. (2010). Rainfall downscaling using statistical downscaling model and canonical correlation analysis: a case study. In: Palmer, R.N. (Ed.), Proceedings of the World environmental and water resources congress ASCE, Preston, pp.4579-4587.

Karlsen, S. R., Tolvanen, A., Kubin E., Poikolainen, J., Hogda, K. A., Johansen, B., Danks, F. S., Aspholm, P., Wielgolaski, F. E. and Makarova, O. (2008). "MODIS-NDVI-based mapping of the length of the growing season in northern Fennoscandia", International Journal of Applied Earth Observation and Geo-information Vol. 10, pp. 253–266.

Kassie, B.T., Van Ittersum, M.K., Hengsdijk H., Asseng, Wolf, S., Rötter, R.P. (2014). Climate-induced yield variability and yield gaps of maize (Zea mays L.) in the Central Rift Valley of Ethiopia. Field Crops Res.160: pp.41–53.

Kassie, B.T., Rötter, R.P., Hengsdijk, H., Asseng, S., Van Ittersum, M.K., Kahiluto, H.,Van Keulen, H., 2013. Climate variability and change in the Central Rift Valley of Ethiopia: challenges for rainfed crop production. J. Agric. Sci. 152, 58–74.

Kassie, B. T. et al. (2014). Climate variability and change in the Central Rift Valley of Ethiopia: Journal of Agricultural Science, 152(1), pp. 58–74. doi: 10.1017/S0021859612000986.

Kassie, M., Zikhali, P., Manjur, K., Edwards, S. (2009). Adoption of sustainable agriculture practices: Evidence from a semiarid region of Ethiopia. Natural Resources Forum 33, pp.189–198.

Kim, B.S.; Sung, J.H.; Kang, H.S. Cho, C.H. (2016). Assessment of Drought Severity over South Korea using Standardized Precipitation Evapotranspiration Index.

Kim, B.S.; Sung, J.H.; Lee, B.H.; Kim, D.J. (2013). Evaluation on the Impact of Extreme Droughts in South Korea using the SPEI and RCP8.5.

Kim, Y., and Chung, E. S. (2012). Integrated assessment of climate change and urbanization impact on adaptation strategies: a case study in two small Korean watersheds. Climatic change, 115(3-4), 853-872.

Komala Dhanapal Sagadevan Eng, by B. and Tech, M. (2017). Meteorological Drought Projections for New Zealand using CMIP5 Data.

Kwak, J. et al. (2016). Assessment of Meteorological Drought in Korea under Climate Change Advances in Meteorology, 2016(Dm). doi: 10.1155/2016/1879024.

Lebel, T., Cappelaere, B., Galle, S., Hanan, N., Kergoat, L, Levis, S., Vieux, B., Descroix, L., Gosset, M., Mougin, E., Peugeot, C., and Seguis, L. (2009). AMMA-CATCH studies in the Sahelian region of West-Africa: an overview, J. Hydrol., 375, 3–13, doi: 10.1016/j.jhydrol.2009.03.020.

Lei Y, Duan A. (2011). Prolonged dry episodes and drought over China. International Journal of Climatology 31(12): 1831-1840.

Liverman DM. (1990). Drought impacts in Mexico: climate, agriculture, technology, and land tenure in Sonora and Puebla. Annals of the Association of American Geographers 80(1): pp.49-72.

Lloyd-Hughes B, Saunders MA. (2002). A drought climatology for Europe. Int J Climatol pp. pp.1571–1592.

Lobell, D. B., Burke, M. B., Tebaldi, C., Mastrandrea, M. D., Falcon, W. P., Naylor, R. L. (2008). Prioritizing climate change adaptation needs for food security.

Lobell, D.B., Burke, M.B. (2010). On the use of statistical models to predict crop yield responses to climate change. Agric. For. Meteorol. 150, pp.1443–1452.

Lynch, (2014). The Emergence of Numerical Weather Prediction, Cambridge University Press, Cambridge.

Mann, H. B. (1945). Non-Parametric Test Against Trend, Econometrica, 13(3), pp. PP.245–259.

Mark Svoboda; Michael Hayes; Deborah A. Wood (1987). Standardized Precipitation Index User Guide Journal of Applied Bacteriology, 63(3), pp. 197–200.

Masih, I. et al. (2014). The extreme droughts of 1972-1973', Hydrol. Earth Syst. Sci. Discuss, 11, pp. 2679–2718. doi: 10.5194/hessd-11-2679-2014.

Mathbout, S.; Lopez-Bustins, J.A.; Martin-Vide, J.; Bech, J.; Rodrigo, F.S. (2018). Spatial and temporal analysis of drought variability at several time scales in Syria during.

Mavromatis, T. (2007). Drought Index Evaluation for Assessing Future Wheat Production in Greece.

McDaniels TL, Axelrod LJ, Cavanagh NS, Slovic P. (1997). Perception of ecological risk to water environments.

Mckee, T.B.; Doesken, N.J.; Kleist, J. (1993). The Relationship of Drought Frequency and Duration to Time Scales, Preprints. pp. 179–184.

Meehl, C. Covey, T. Delworth et al., (2018) The WCRP CMIP3 multimodal dataset: a new era in climate change research, Bulletin of the American Meteorological Society, vol. 88, no. 9, pp. 1383–1394, 2007.

Meinshausen, S. J. Smith, K. Calvin et al., (2011). The RCP greenhouse gas concentrations and their extensions from 1765 to 2300, Climatic Change, vol. 109, no. 1-2, pp. 213–241, 2011.

Mengesha, G., Bekele, A., Fraser, G., & Mamo, Y. (2014). Land use, land cover and climate change impacts on the bird community in and around Lake Zeway, Ethiopia. International Journal of Biodiversity and Conservation 6(3):256-270.

Mengesha, G., Elphick, C. S., Field, C. R., Bekele A., & Mamo, Y. (2015). Abundance and temporal patterns in wetland birds in and around Lake Ziway, Ethiopia. Journal of Biodivers Manage Forestry, 4(1), 1-9, doi:10.4172/2327-4417.100013.

Mera, G. A. (2018). Drought and its impacts in Ethiopia, Weather and Climate Extremes, 22(September), pp. 24–35. doi: 10.1016/j.wace.2018.10.002.

Mesfin, D. (2018). Adaptive Capacity of Woodland Dependent Households to Climate Change in the Central Rift Valley of Ethiopia (Doctoral dissertation, Addis Ababa University.

Ministry of Environment and Forest (2015). Ethiopia's Second National Communication to the United Nations Framework Convention on Climate Change (UNFCCC). The Federal Democratic Republic of Ethiopia. URL: https://unfccc.int/resource/docs/natc/ethnc2.pdf.

Mishra, A. K. and Desai, V. R. (2006). Drought forecasting using feed-forward recursive neural network, Ecological Modelling, 198(1–2), pp. 127–138. doi: 10.1016/j.ecolmodel.2006.

Mohammed, Y. et al. (2018). Meteorological drought assessment in north east highlands of Ethiopia International Journal of Climate Change Strategies and Management, 10(1), pp. 142–160. doi: 10.1108/IJCCSM-12-2016-0179.

Montz BE, Tobin GA. (2011). Natural hazards: an evolving tradition in applied geography. Applied Geography 31(1): 1-4.

Morris J, Graves A, Daccache A, Hess T, Knox J. (2010). Towards a framework for the economic assessment of drought risk pp.139-148.

MoWR and NMSA. (2007). Climate Change National Adaptation Programme of Action (NAPA) of Ethiopia National Meteorological Agency, Addis Ababa.

MoWR and NMSA. (2001). Initial National Communication of Ethiopia to the United Nations Framework Convention on Climate Change (UNFCCC) Addis Ababa, Ethiopia.

Mpelasoka, F., K. Hennessy, R. Jones, and B. Bates. (2008). Comparison of suitable drought indices for climate change impacts assessment over Australia towards resource, International Journal of Climatology, 28(10), pp.1283–1292.

Muzein, B. S. (2006). Remote Sensing and GIS for Land Cover/Land Use Change Detection and Analysis in the Semi-Natural Ecosystems and Agriculture Landscapes of the Central Rift Valley. PhD Thesis. Institute of Photogrammetry and Remote sensing, Technology University of Dresden, Dresden.

M. Wambua, R. (2014). Drought Forecasting Using Indices and Artificial Neural Networks for Upper Tana River Basin, Kenya-A Review Concept', Journal of Civil & Environmental Engineering, 04(04). doi: 10.4172/2165-784x.1000152.

Nam, J.E.; Lee, Y.H.; Jung, K.Y. (2012). Analysis of Evapotranspiration Effect on Drought by Comparison of SPI and SPEI Drought Indices. In Proceedings of the Autumn Meeting of KMS, Daegu, Korea, 1–2 November 2012; pp. 390–391. (In Korean).

Nasir, J. et al. (2021). Meteorological Drought in Northwestern Escarpment of Ethiopian Rift Valley: detection seasonal and spatial trends, Environmental Systems Research, 10(1). doi: 10.1186/s40068-021-00219-3.

Naumann, G., Dutra, E., Barbosa, P., Pappenberger, F., Wetterhall,F., & Vogt, J. V. (2014). Comparison of drought indicatorsderived from multiple data sets over Africa.Hydrology EarthSystem Science, 18, 1625–1640. https://doi.org/10.5194/hess-18-1625-2014

Nel JL, Le Maitre DC, Nel DC, Reyers B, Archibald S, van Wilgen BW, Forsyth GG, Theron AK,O'Farrell PJ, Mwenge Kahinda J-M, et al.(2014). Natural hazards in a changing world. doi: 10.1371/journal.pone.0095942.

Nikulin et al., (2012), G. Nikulin, C. Jones, F. Giorgi, G. Asrar, M. Büchner, R. Cerezo-Mota, O.B. Christensen, M. Déqué, J. Fernandez, A. Hänsler. Precipitation climatology in an ensemble of CORDEX-Africa regional climate simulations

NMSA. (2001). Initial National Communication of Ethiopia to the United Nation Framework Convention on Climate Change (UNFCCC). National Meteorological Services Agency, Addis Ababa, Ethiopia.

OECD. (2012). Incorporating climate change impacts and adaptation in Environmental

Olesen JE, Bindi M. (2002). Consequences of climate change for European agricultural productivity, land use and policy. European journal of agronomy 16(4): 239-262.

Quiring, S. M. (2017). Monitoring drought: An evaluation of meteorological drought indices. Geography Compass, 3, pp.64-88.

Pahl-Wostl, C. (2007). Transitions towards adaptive management of water facing climate and global change. Water resources management, 21(1), pp.49-62.

Palmer, W.C. (1965), Meteorological Drought, Research Paper No. 45, U.S. Weather Bureau, Washington, D.C.

Panu, U. and T. Sharma. (2002). Challenges in drought research: some perspectives and future directions, Hydrological Sciences Journal, 47(1), pp.19–30.

Pascual Ferre, J., & Candela, L. (2015). Water Balance on the Central Rift Valley', in Case studies for developing globally responsible engineers, GDEE (eds.), Global Dimension in Engineering Education, Barcelona.

Patil, S. R. (2012). Analyses of Spatial Performance of Meteorological Drought Indices, p. 142.

Paulo, A. A., Rosa, R. D. and Pereira, L. S. (2012). Climate trends and behavior of drought indices based on precipitation and evapotranspiration in Portugal. Nat. pp.1481-1491.

Pohlert T (2020) Non-Parametric Trend Tests and Change-Point Detection.

https ://creat iveco mmons .org/licen ses/by-nd/4.0/

Rahmat, S. N., Jayasuriya, N. and Bhuiyan, M. (2015). Assessing droughts using meteorological drought indices in Victoria, Australia', Hydrology Research, 46(3), pp. 463–476. doi: 10.2166/nh.2014.105.

Ramanathan, V. and Y. Feng. (2009). Air pollution, greenhouse gases and climate change: Global and regional perspectives, Atmospheric Environment, 43(1), 37–50.

Richard, Y., Fauchereau, N., Poccard, I., Rouault, M., and Trzaska, S. (2011). 20th century droughts in southern Africa: spatial and temporal variability, teleconnections with oceanic and atmospheric conditions, Int. J. Climatol., 21, 873–885, doi:10.1002/joc.656, 2001. Roderick, M. L., Sun, F., Lim, W. H., & Farquhar, G. D.

Roe JH, Rees M, Georges A. (2011). Suburbs: dangers or drought refugia for freshwater turtle populations. The Journal of Wildlife Management 75(7): pp.1544-1552.

Rosenberg, N. J. (ed). (1980). Drought in the Great Plains, Research on Impact and Strategies, Water Resources Publications, Fort Collins, Colorado.

Russel, C. S. et al. (1970). Drought and Water Supply; Implications of the Massachusetts Experiences for Municipal Planning, Johns Hopkins Press, Baltimore, Maryland.

Salehnia, N. et al. (2017). Estimation of meteorological drought indices based on AgMERRA precipitation data and station-observed precipitation data', Journal of Arid Land, 9(6), pp. 797–809. doi: 10.1007/s40333-017-0070-y.

Segele, Z.T., Lamb, P.J. (2005). Characterization and variability of Kiremt rainy season over Ethiopia. Meteorol Atmos154 ,pp153–180.

Segal, M., Pan, Z., Turner, R.W. and Takle, E. S. (1998). On the potential impact of irrigated areas in North America summer rainfall caused by large-scale systems. J. Appl. Meteor., 37, pp.325–331.

Seleshi Y, Zanke U. (2004). Recent changes in RF and rainy days in Ethiopia. Inter. J. Climatol., 24: pp.973-983.

Samuelsson et al., (2011), P. Samuelsson, C.G. Jones, U. Will´ En, A. Ullerstig, S. Gollvik, U. Hansson, E. Jansson, M.C. Kjellstro¨, G. Nikulin, K. Wyser. The rossby centre regional climate model RCA3 description and performance, pp. 4-23

Sen, P.K. (2018). Estimates of the regression coefficient based on Kendall's tau.

Sen Z. (2012). Innovative trend analysis methodology. J Hydrol Eng 17(9):1042–1046

Sen Z. (2014). Trend identification simulation and application. J Hydrol Eng 19(3):635–642

Sen Z. (2017a). Hydrological trend analysis with innovative and over whitening procedures. Hydrol Sci J 62(2):294–305

Sen Z. (2017b). Innovative trend methodologies in science and engineering.

Sen Z. (2017c). Innovative trend significance test and applications. Theoret Appl Climatol 127(3): pp.939–947.

Sen Z, S¸ E, Dabanli I. (2019). Innovative Polygon Trend Analysis (IPTA) and applications. J Hydrol 575: pp.202–210.

Shahid, S., Wang, X.-J., Harun, S. B., Shamsudin, S. B., Ismail, T., and Minhans, A. (2016). Climate variability and changes in the major cities of Bangladesh: observations, possible impacts and adaptation. Regional Environmental Change, 16(2), pp.459-471.

Shanahan, T. M., Overpeck, J. T., Anchukaitis, K. J., Beck, J. W., Cole, J. E., Dettman, D. L., Peck, J. A., Scholz, C. A., and King, J. W. (2009) Atlantic forcing of persistent drought in West Africa, Science, 324, 377–380, doi:10.1126/science.1166352.

Sheffield, J., and E. Wood. (2008). Global Trends and Variability in Soil Moisture and Drought Characteristics, 1950-2000, from Observation-Driven Simulations of the Terrestrial Hydrologic Cycle, Journal of Climate, 21(3), 432–458.

Sheffield, J., and E. Wood. (2011). Projected changes in drought occurrence under future global warming from multi-model, multi-scenario, IPCC AR4 simulations, Climate Dynamics, 31(1), 79–105.

Shaowei, Z.; Hongchao, Z.; Pengcheng, R.; Guangjie, X.; Bangdong, L.; Wencheng, D.; Liying, W. (2013). Application of Standardized Precipitation Evapotranspiration Index in China.

Siccardi, F. and Bras, R. L. (eds). (1989). Natural Disasters in European Mediterranean Countries, NRC Group for Prevention from Hydrogeological Disasters, Genoa.

Sivakumar, M.V.K. .2014. Impact of Natural Disaster in Agriculture: An Overview. WMO. Geneva, Switzerland, 2014.

Smakhtin V U, Hughes D A. (2007). Automated estimation and analyses of meteorological drought characteristics from monthly rainfall data. Environmental Modelling & Software, 22(6): 880–890.

Society, T. E. et al. (2016). Water Tower of the Yellow River in a Changing Climate: Toward an integrated assessment, Water Resources Management, 13(3), pp. 245–259.

Spinoni, J.; Naumann, G.; Carrao, H.; Barbosa, P.; Vogt, J. (2018). World drought frequency and duration.

Tagel, G., Veen, A.V.D. and Maathuis, B. (2011). Spatial and temporal assessment of drought in the Northern highlands of Ethiopia International Journal of Applied Earth Observation and Geoinformation, Vol. 13, pp. 309-321.and severity for 1951–2010. Int. J. Clim. 2014, 34, 2792–2804.

Tallaksen LM, Van Lanen HAJ. (2014). Hydrological drought: processes and estimation methods for streamflow and groundwater. In: Developments in Water Science, vol.48. Amsterdam, the Netherlands: Elsevier Science B.V.;2004.

Tamoffo et al., (2019), A.T. Tamoffo, W. Moufouma-Okia, A. Dosio, R. James, W.M. Pokam, D.A. Vondou, T.C. Fotso-Nguemo, G.M. Guenang, P.H. Kamsu-Tamo, G. Nikulin Process-oriented assessment of RCA4 regional climate model projections over the Congo Basin under 1.5°{C} and 2°{C} global warming levels.

Tannehill, I. R. (1947). Drought: Its Causes and Effects, Princeton University Press, Princeton, New Jersey.

Tao, H.; Borth, H.; Fraedrich, K.; Su, B.; Zhu, X. (2014). Drought and wetness variability in the Tarim River Basin and connection to large-scale atmospheric circulation. Int. J. Clim. 2014, 34, 2678–2684.

Tardieu, H. and Plus, B. (1989). Apres la secheresse des annees 1984-87 dans le basin de la Garonne (France), La Houille Blanche No. 7-8.

Taylor, K. E., R. J. Stouffer, and G. A. Meehl. (2012). An overview of CMIP5 and the experiment design, Bulletin of the American Meteorological Society, 93, 485–498.

Teegavarapu, R. S. V. (2018) Methods for analysis of trends and changes in hydroclimatological time-series, Trends and Changes in Hydroclimatic Variables: Links to Climate Variability and Change. Boca Raton, United States: Elsevier Inc. doi: 10.1016/B978-0-12-810985-4.00001-3.

Temesgen, H., Nyssen, J., Zeneber, A., Haregeweyen, N., Kindu, M., Lemenih, M., & Haile M. (2013). Ecological succession and land use changes in a lake retreat area (Main Ethiopian Rift Valley). Journal of Arid Environments, 91: 53-60.

Teutschbein, C., Seibert, J. (2010). Regional climate models for hydrological impact studies at the watershed scale: A review of recent modeling strategies.

Teutschbein, C., Seibert, J. (2012). Bias correction of regional climate model simulations for hydrological climate-change impact studies: Review and evaluation of different methods. Journal of Hydrology, p 456- 457.

Thomas B. McKee, N. J. D. and J. K. (1993). Analysis of Standardized Precipitation Index (SPI) data for drought assessment, Water (Switzerland), 26(2), pp. 1–72. doi: 10.1088/1755-1315/5.

Thomson, A. M. et al. (2011). RCP4.5: A pathway for stabilization of radiative forcing by 2100, Climatic Change, 109(1), pp. 77–94. doi: 10.1007/s10584-011-0151-4.

Thornton, P, Jones, P, Owiyo, T, Kruska, R, Herrero, M, Kristjanson, P, Notenbaert, A, Bekele, N.& Omolo, A. (2006). Mapping climate vulnerability and poverty in Africa. Nairobi: International Livestock Research Institute.

Tirivarombo, S.; Osupile, D.; Eliasson, P. (2018). Drought monitoring and analysis: Standardised Precipitation Evapotranspiration Index (SPEI) and Standardised Precipitation Index (SPI).

Totaro, V., Gioia, A. and Iacobellis, V. (2020). Numerical investigation on the power of parametric and nonparametric tests for trend detection in annual maximum series, Hydrology and Earth System Sciences, 24(1), pp. 473–488. doi: 10.5194/hess-24-473 2020.

Touchan, R., Anchukaitis, K. J., Meko, D. M., Attalah, S., Baisan, C., and Aloui, A. (2011) Long term context for recent drought in northwestern Africa, Geophys. Res. Lett., 35, L13705, doi:10.1029/2008gl034264.

Tsakiris G, Vangelis H. (2005). Establishing a drought index incorporating evapotranspiration. European Water 9(10): pp.3-11.

Tsakiris G, Pangalou D, Vangelis H. (2007). Regional drought assessment based on the Reconnaissance Drought Index (RDI). Water Resources Management 21(5): 821-833.

Ukkola, A. M., De Kauwe, M. G., Roderick, M. L., Abramowitz,G., & Pitman, A. J. (2020). Robust future changes in meteoro-logical drought in CMIP6 projections despite uncertainty inprecipitation. GeophysicalResearchLetters,47(11),e2020GL087820

Urbistondo, R. and Bays, L. (eds). (1987). Drought and famine, Water Supply No, 5.

USDA, (1994). Major world crop areas and climatic profiles, World Agricultural Outlook Board, US department of Agriculture, Agricultural Handbook No. 664, pp. 157–170.

van Gelder, P. H. A. J. M. (1999). Statistical Methods for Risk-Based Design of Civil Structures. PhD Thesis, Delft University of Technology, The Netherlands.

Van Lanen, H., L. Tallaksen, and G. Rees. (2015). Droughts and climate change, in: Commission Staff Working Document Impact Assessment (SEC (2007) 993), Accompanying document to Communication Addressing the challenge of water scarcity and droughts in the European Union (COM (2007) 414), Commission of the European Communities, Brussels, Belgium.

Van Loon, A. F. (2015). Hydrological drought explained', WIREs Water, 2(4), pp. 359–392. doi: 10.1002/wat2.1085.

Verschuren, D.(2000). Decadal and century-scale climate variability in tropical Africa during the past 2000 years, in: Past Climate Variability Through Europe and Africa, edited by: Battarbee, R. W., Gasse, F., and Stickley, E., Springer, Dordrecht, 139–158.

Vincente, S.M. Begueria, S. Lopez-Moreno, J.I. (2010). A Multiscalar Drought Index Sensitive to Global Warming:The Standardized Precipitation Evapotranspiration Index. J. Clim. 2010, 23, 1696–1718.

Vicente-Serrano SM, Beguería S, López-Moreno JI, Angulo M, El Kenawy A. (2010b). A new global 0.5 gridded dataset (1901-2006) of a multiscalar drought index: comparison with current drought index datasets based on the Palmer Drought Severity Index.

Von Storch, H., Langenberg,H., Feser,F. (2000). A Spectral Nudging Technique for Dynamical Downscaling Purposes.

Von Braun, J. (1991). A policy agenda for famine prevention in Africa.

Vidal, J.-P., and S. Wade. (2009). A multimodel assessment of future climatological droughts in the United Kingdom.

Wang, L., Chen, W., and Zhou, W. (2014). Assessment of future drought in Southwest China based on CMIP5 multimodal projections. Advances in Atmospheric Sciences, 31(5), 1035-1050.

Wang, L. Ranasinghe, R. Maskey, S. van Gelder, P. and Vrijling, J. (2016b). Comparison of empirical statistical methods for downscaling daily climate projections from CMIP5 GCMs: a case study of the Huai River Basin, China. International Journal of Climatology, 36(1), pp.145-164.

Wang, X.-j, Zhang, J.y. Shahid, S., Guan, E.-h., Wu, Y.-x., Gao, J., et al. (2016b). Adaptation to climate change impacts on water demand.

Warrick, R. A. (1975). Drought Hazard in the United States: A Research Assessment, National Technical Information Service, Springfield, Virginia.

Wilhite, D., Easterling, W., and Wood, D. (eds). (2007). Planning for Drought: Toward a Reduction of Societal Vulnerability, Westview Press, Boulder, Colorado.

Wilhite DA, Glantz MH. (1985). Understanding the drought phenomenon, the role of definitions. Water Int 1985, 10:111–120.

Wilhite DA, ed. (2005). Drought: A Global Assessment. Routledge Hazards and Disasters Series, vol. I & II. London.

WMO. (World Meteorological Organization). (2006). Drought monitoring and early warning: concepts, progress and future challenges, Tech. Rep. 1006, WMO-No. 1006.

World Bank Group. (2021) 'Ethiopia Climate Risk Country Profile'. Available at: www.worldbank.org.

WMO (World Meteorological Organization). (1987). Standardized Precipitation Index User Guide Journal of Applied Bacteriology, 63(3), pp. 197–200.

Yacoub, E. and Tayfur, G. (2017). Evaluation and Assessment of Meteorological Drought by Different Methods in Trarza Region, Mauritania Water Resources Management, 31(3), pp. 825–845. doi: 10.1007/s11269-016-1510-8.

Yadav, R. et al. (2014). Trend analysis by Mann-Kendall test for precipitation and temperature for thirteen districts of Uttarakhand', Journal of Agrometeorology, 16(2), pp. 164–171.

Yevjevich, V. and Karplus, A. K. (1973). Area-time structure of the monthly precipitation process, Colorado State University, Fort Collins, Colorado, Hydrology.

Yevjevich, V., Hall, J. D., and Salas, W. (eds). (1978). Drought Research Needs, Water Resources Publications, Littleton, Colorado.

Yevjevich, V., Da Cunha, L., and Vlachos E. (eds). (1983). Coping with Droughts, Water Resources Publications. Littleton, Colorado.

Yue, S. and Wang, C. Y. (2004). The Mann-Kendall test modified by effective sample size to detect trend in serially correlated hydrological series, Water Resources Management, 18(3), pp. 201–218. doi: 10.1023/B: WARM.0000043140.61082.60.

Zaiontz C (2020). Mann-Kendall test, real statistics using excel. Proudly powered by WordPress. Real Statistics Using Excel: © 2012–2019.

Zampieri, M. et al. (2009). Hot European summers and the role of soil moisture in the propagation of Mediterranean drought', Journal of Climate, 22(18), pp. 4747–4758. doi: 10.1175/2009JCLI2568.1.

Zhang, Q.; Qi, T.; Singh, V.P.; Chen, Y.D.; Xiao, M. (2015). Regional frequency analysis of droughts in China.

Zhou, Y.; Li, N.; Ji, Z.; Gu, X.; Fan, B. (2013). Temporal and Spatial Patterns of Droughts Based on Standard Precipitation Index (SPI) in Inner Mongolia during 1981–2010.

APPENDICES

Appendices 1. Tables

Table I: - Long-term mean monthly historical precipitation and temperature (Tmax. and Tmin.) data of study area for (1985-2019)

Station	Jan	Feb	Mar	Apr	May	Jun	Jul	Aug	Sep	Oct	Nov	Dec
Arsi Negele	14	29	52	62.8	86.6	92.1	120	99	109	40	5	9.4
Assela	16	38	87	117	109	119	174	177	141	59.8	25	18
Bulbua	15	48	39	63.1	72.5	81.5	128	97	79.9	38.0	14	7.6
Ziway	12	29	47	73.9	75.2	86.1	167	117	84.7	38.9	15	9.9
Koshe	21	40	65	83.2	73.2	78.2	151	123	91.1	43.8	16	15
Tora	22	37	77	102	89.7	81.3	122	108	102	50.8	12	9.8
Kulma	16	37	75	91.3	94	93.5	122	124	110	42.2	10	8.7
Degaa	15	37	63	97.6	101	126	178	169	153	78.0	24	14
Langano	9.2	32	56	79.3	94.6	102	163	124	91.0	42.7	13	5.4

station	Jan	Feb	Mar	Apr	May	Jun	Jul	Aug	Sep	Oct	Nov	Dec
Arsi Negele	26.6021	27.38	27.6043	27.2528	26.8757	25.6923	23.9542	23.8656	24.7111	25.6402	26.1084	26.7057
Assela	22.	23.3	23.9	23.4	23.3	22.4	20.8	20.3	20.5	21.5	21.6	21.5
Degaga	25.4	26.2	26.4	25.5	25.2	23.6	22	22.1	22.5	24	24.5	24.4
Ziway	27.25	28.53	29.57	29.24	27.25	27.25	25.47	25.67	26.85	27.77	27.34	27.30
Langano	28.60	29.70	30.99	30.65	30.05	29.19	26.72	27.35	27.99	28.67	28.67	28.92
Kulmsa	23.27	24.56	25.48	24.84	24.65	23.49	21.37	21.20	21.60	22.82	22.82	22.42

Station	Jan	Feb	Mar	Apr	May	Jun	Jul	Aug	Sep	Oct	Nov	Dec
Arsi Negele	10.41	11.66	12.91	13.02	12.54	13.12	12.98	12.95	12.57	11.69	10.36	10.62
Assela	7.86	8.84	9.88	10.86	10.82	10.68	10.77	10.77	10.32	9.92	8.24	7.26
Degaga	7.06	8.27	9.74	11.51	11.31	11.51	10.92	11.67	11.03	9.83	7.97	7.03
Ziway	12.31	13.64	15.02	15.73	15.93	15.66	15.09	15.06	14.54	13.09	12.04	11.59
Langano	13.03	13.22	13.03	13.03	13.03	13.03	13.03	13.03	13.03	13.80	12.86	13.03
Kulmsa	9.13	10.52	11.85	12.87	12.44	11.92	11.75	9.13	11.34	9.13	10.45	9.55

Source: Ethiopian National Meteorological Agency.

Table II: - Long-term future precipitation data (2020-2100) mean monthly precipitation data of study area

Station	Jan	Feb	Mar	Apr	May	Jun	Jul	Aug	Sep	Oct	Nov	Dec
GP113212	8.1	3.7	5.10	29.5	77.7	108	275	396	354	363	129	29.9
GP114211	2.53	0.95	2.80	9.98	14.2	27.2	61	80.5	76.3	51.9	29.3	11.4
GP114212	3.8	4.8	0.62	3.28	5.76	6.32	18.6	33.0	43.7	33.3	23.7	15
GP115211	18	19	76.3	177	204	414.7	656.5	659.9	631.8	315.9	97.1	36.3
GP115212	6.7	6.7	32	*70*	68	248	461	452	360	134	51	11.7

Source: - Coordinated Regional Climate Downscaling Experiment (CORDEX) under Africa

Table III: - Standardized precipitation index for historical data (SPI1, SPI3, SPI6 and SPI12)

Station	Period (Months)	Wettest condition			Driest condition		
		Date	SPI		Date	SPI	
			Value	Category		Value	Category
Arsi Negele	1	Apr/2003	2.64	EW	Jun/2017	-2.81	ED
	3	Sep/2004	2.19	EW	Oct/2015	-3.1	ED
Assela	1	Jun/2018	2.37	EW	Sep/1991	-3.13	ED
	3	Aug/2018	2.19	EW	Nov/1991	-3.32	ED
Bulbua	1	Sep/2012	2.64	EW	Aug/2016	-2.73	ED
	3	Mar/2012	3.54	EW	Jul/2014	-3.42	ED
Ziway	1	Jul/2012	2.67	EW	Sep/2017	-3.53	ED
	3	Oct/2014	3.11	EW	Jul/1989	-3.47	ED
Koshe	1	Feb/1990	2.48	EW	Aug/2019	-3.09	ED
	3	Oct/1993	2.26	EW	Jul/2019	-3.67	ED
Tora	1	May/1987	2.63	EW	Mar/2000	-2.83	ED
	3	Oct/1993	2.44	EW	Mar/2000	-4.49	ED
Kulmasa	1	Sep/2012	3.46	SW	Mar/2008	-2.96	ED
	3	Sep/2012	3.52	EW	Mar/2000	-4.83	ED
Degaga	1	Nov/2016	2.62	EW	Sep/2019	-2.56	ED
	3	Jun/2016	2.49	EW	Sep/2018	-3.3	ED
Langano	1	Mar/2010	2.51	EW	Apr/1991	-3.15	ED
	3	Jan/2009	2.95	EW	Apr/2008	-2.8	ED

Table IV: - Wettest and driest periods SPI for future data from 2020-2100 RCP4.5 (SPI3, SPI6 and SPI12)

Station	Period (Months)	Wettest condition			Driest condition		
		Date	SPI		Date	SPI	
			Value	Category		Value	Category
GP113212	3	Oct/2059	2.84	EW	Dec/2038	-5.29	ED

	1	Nov/2071	3.1	EW	Apr./2027	-3.1	ED
GP114211	3	Sep/2076	3.16	EW	Dec/2037	-4.55	ED
	1	Feb/2066	2.5	EW	Mar/2035	-4.6	ED
GP114212	3	Mar/2083	3.51	EW	Dec/2038	-3.33	ED
	1	Dec/2083	2.16	EW	Mar/2032	-3.23	ED
GP115211	3	Nov/2090	3.2	EW	Apr/2065	-3.67	ED
	1	Feb/2070	3.0	EW	Dec./2037	-3.4	ED
	3	Nov/2090	3.44	EW	Dec/2037	-3.03	ED
	1	Nov./2091	2.3	EW	Nov/2046	-3.6	ED

EW = extremely wet, ED = extremely dry

Table V: - Wettest and driest periods SPI for future data from 2020-2100 RCP8.5 (SPI3, SPI6 and SPI12)

Station	Period (Months)	Wettest condition			Driest condition		
		Date	SPI		Date	SPI	
			Value	Category		Value	Category
GP113212	3	Jul./2038	2.8	EW	Dec./2080	-3.4	ED
	1	Oct./2038	3	EW	Jul./2086	-3.2	ED
GP114211	3	Oct./2035	3.5	EW	Oct./2083	-3.7	ED
	1	Feb./2045	2.7	EW	Oct./2083	-4.3	ED
GP114212	3	Oct./2035	3.3	EW	Oct./2083	-2.4	ED
	6	Jan./2036	2.7	EW	Jun./2082	-2.3	ED
GP115211	3	Feb./2054	2.6	EW	Apr./2070	-4.7	ED
	1	Apr./2055	3.3	EW	Mar. /2072	-4.2	ED
GP115212	3	Jun./2065	2.6	EW	Jun./2094	-4.1	ED
	1	Jul./2062	2.2	EW	Apr./2032	-3.7	ED

EW = extremely wet, ED = extremely dry

Appendix 2. Figure

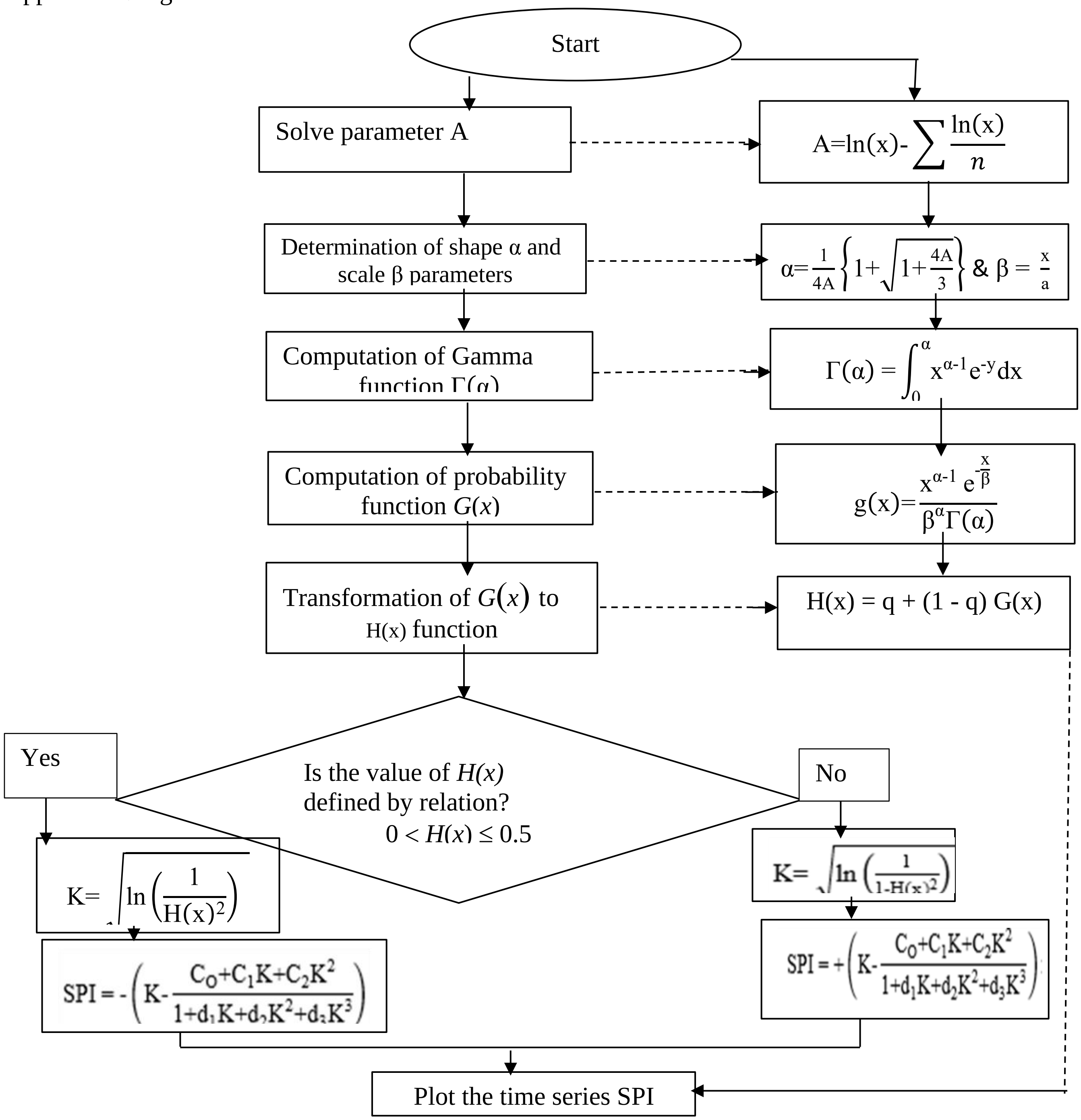

Figure I. Summaries for computation of SPI